Appendix A.35:

Baker St – CPT 14070

Table 1: Site Description for Baker St (CPT 14070).

Attribute	Yes/No			Description/Date	Symbol in Figure 1
	10-m Buffer	20-m Buffer	50-m Buffer		
Near a body of surface water or other free face features?	No	No	No	The center of the site is ~350 m to the NE from the Avon River. The free-face height is ~1.5 m. The swimming pool (~1-m high) is ~53 m to the SW from the center of the site.	NA
Lateral spreading observed during the CES?	No	No	No	Ground cracks <50 mm in width were observed by the mapping team.[1] In the 20- and 50-m buffers. However, they are most likely a local feature (e.g., due to the undulating land or creep toward the lower-elevation ground).	NA
Nearby buildings or structures?	No	Yes	Yes	Building coverage of the 20-m and 50-m buffers is 10% and 23%, respectively. Buildings cover the NE and SE quadrants of the 20-m buffer and all quadrants of the 50-m buffer.	White Fill + Brown Outline
Sloping land?	No	No	Yes	Flat residential area except for the slightly sloping private driveway in the SE quadrant of the 50-m buffer.	NA
Step changes in the ground surface?	No	No	Yes	The residential property in the SE quadrant of the 50-m buffer is ~0.5 m above the street level.	NA
Retaining walls?	No	No	Yes	Approximately 0.5-m high front-lawn retaining lawn in the SE quadrant of the 50-m buffer.	Retaining Wall: Black Line
Vegetation?	Yes	Yes	Yes	Trees and bushes cover 9, 18, and 17% of the 10-, 20-, and 50-m buffers, respectively. They are in all quadrants of the 20- and 50-m buffers and the NE and SE quadrants of the 10-m buffer.	White Fill + Green Outline
Anthropogenic changes to the site between the LiDAR surveys?	No	Yes	Yes	Vegetation removal in the SW quadrant of the 20- and 50-m buffers between Mar 2009 and Sep 3, 2010. Building removal in the SE quadrant of the 50-m buffer between Mar 2013 and Aug 2013. Building removal in the SW quadrant of the 50-m buffer between Jan 2015 and Apr 2015. Building addition at the same property in the SW quadrant of the 50-m buffer in July 2015. Building replacement in the SW quadrant of the 20- and 50-m buffers between July 2015 and Nov 2015.	Vegetation Removal: Green Outline Building Removal/ Addition: Orange Crossline
Other important factors?	Yes	Yes	Yes	Low-motor-vehicle-volume, two-way roadway (Baker St) occupies 44, 29, and 12% of the 10-, 20-, and 50-m buffers, respectively, and runs in the N-S direction.	Road: Gray Fill + Red Outline

Note: Buffer is the area within a circle of a specified radius with CPT investigations done at its center (172.715770°, -43.503609°).

[1] Canterbury Geotechnical Database. (2012). "Observed Ground Crack Locations", Map Layer CGD0400 - 23 July 2012, retrieved July 09, 2018 from https://canterburygeotechnicaldatabase.projectorbit.com/

Figure 1: Site plan with areas where ejecta-induced settlement is considered.

Note 1: Two patches (outlined in red) in the free field were selected for settlement assessment as areas free of vegetation and structures. Other important factors considered in the patch selection process were its proximity to a CPT, a property subjected to addition and/or demolition of a structure, front yard/backyard alterations (e.g., ploughing, rubble, scrap), and aerial distribution of sediment ejecta. In addition, the entire portion of the road within the 50-m buffer was considered for the settlement assessment. The LiDAR-based settlement analyses for the Sep-10 EQ were not conducted due to the evident absence of ejecta from Patches A and B and Road. The Oct 2015 LiDAR survey was not considered for Patches A and B due to the anthropogenic changes.

Table 2: LiDAR flight error adjustments, global adjustments for the difference between average LiDAR point elevations and benchmark survey elevations, and vertical tectonic movement adjustments.

	Adjustments (mm)		
Earthquake Event(s)	LiDAR Flight Error	Global Offset[2]	Tectonic Vertical Movement
Sep-10	-150	-3	0
Feb-11	+100	16	-25
Jun-11	0	38	-50
Dec-11	0	-65	+15
CES	-50	-14	-60
Any LiDAR survey affected by ejecta?			Yes

Notes: The negative sign indicates the subtraction from the ground surface subsidence, while the positive sign indicates the addition to the ground surface subsidence; Ejecta were not removed (at least not entirely) from the road, which affected the Mar 2011 LiDAR survey and potentially the May 2011 LiDAR survey (this requires the addition of ~50 mm to the ground surface subsidence for the Feb-11 EQ and the subtraction of ~50 mm from the ground surface subsidence for the Jun-11 EQ).

Table 3a: LiDAR Measurement Error for Patch A.

Surveys	Buffer	Area Averaged Difference Indicating Repeat Measurement Error (mm)	6*$_{\text{individual LiDAR points}}$ (mm)	%Reduction in 6 due to Area Averaging of LiDAR Points
Post Feb 2011: Mar 2011 and May 2011	10-m	NA	59	[81,81]
	20-m	ND		
	50-m	48		
Post Dec 2011: Feb 2012 and Oct 2015	10-m	NA	70	[ND,ND]
	20-m	ND		
	50-m	ND		

*Standard deviation; NA = Not available.

[2] Russell, J., & van Ballegooy, S. (2015). *Canterbury Earthquake Sequence: Increased liquefaction vulnerability assessment methodology*. New Zealand: Tonkin & Taylor Ltd.

Table 3b: LiDAR Measurement Error for Patch B.

Surveys	Buffer	Area Averaged Difference Indicating Repeat Measurement Error (mm)	$6^*_{\text{individual LiDAR points}}$ (mm)	%Reduction in 6 due to Area Averaging of LiDAR Points
Post Feb 2011: Mar 2011 and May 2011	10-m	NA	59	[80,80]
	20-m	NA		
	50-m	47		
Post Dec 2011: Feb 2012 and Oct 2015	10-m	NA	70	[ND,ND]
	20-m	NA		
	50-m	ND		

*Standard deviation; NA = Not available; ND = Not determined.

Table 3c: LiDAR Measurement Error for Road.

Surveys	Buffer	Area Averaged Difference Indicating Repeat Measurement Error (mm)	$6^*_{\text{individual LiDAR points}}$ (mm)	%Reduction in 6 due to Area Averaging of LiDAR Points
Post Feb 2011: Mar 2011 and May 2011	10-m	97	59	[125,149]
	20-m	88		
	50-m	74		
Post Dec 2011: Feb 2012 and Oct 2015	10-m	56	70	[73,80]
	20-m	51		
	50-m	56		

*Standard deviation.

Table 4a: Ground surface subsidence adjustments due to LiDAR measurement error for Patch A.

Earthquake Event(s)	$6_{\text{pre-EQ LiDAR survey}}$ (mm)	$6_{\text{post-EQ LiDAR survey}}$ (mm)	6_{total} (mm)	Area Average Adjusted 6 (mm) **
Sep-10	158	56	134	±109
Feb-11	56	59	59	±48
Jun-11	59	61	62	±51
Dec-11	61	70	87	±70
CES	158	70	124	±101

**Based on the highest %Reduction in Table 3a.

Table 4b: Ground surface subsidence adjustments due to LiDAR measurement error for Patch B.

Earthquake Event(s)	$\delta_{pre\text{-}EQ\ LiDAR\ survey}$ (mm)	$\delta_{post\text{-}EQ\ LiDAR\ survey}$ (mm)	δ_{total} (mm)	Area Average Adjusted δ (mm) **
Sep-10	158	56	134	$\pm$107
Feb-11	56	59	59	$\pm$47
Jun-11	59	61	62	$\pm$50
Dec-11	61	70	87	$\pm$69
CES	158	70	124	$\pm$99

**Based on the highest %Reduction in Table 3b.

Table 4c: Ground surface subsidence adjustments due to LiDAR measurement error for Road.

Earthquake Event(s)	$\delta_{pre\text{-}EQ\ LiDAR\ survey}$ (mm)	$\delta_{post\text{-}EQ\ LiDAR\ survey}$ (mm)	δ_{total} (mm)	Area Average Adjusted δ (mm) **
Sep-10	158	56	134	$\pm$200
Feb-11	56	59	59	$\pm$88
Jun-11	59	61	62	$\pm$93
Dec-11	61	70	87	$\pm$129
CES	158	70	124	$\pm$186

**Based on the highest %Reduction in Table 3c.

Table 5a: Raw liquefaction-related ground surface subsidence using original LiDAR points for Patch A.

	Average Ground Surface Subsidence (mm)		
Earthquake Event(s)	10-m Buffer	20-m Buffer	50-m Buffer
Sep-10	NA	ND	ND
Feb-11	NA	ND	42
Jun-11	NA	ND	110
Dec-11	NA	ND	112
CES	NA	ND	ND

Table 5b: Raw liquefaction-related ground surface subsidence using original LiDAR points for Patch B.

	Average Ground Surface Subsidence (mm)		
Earthquake Event(s)	10-m Buffer	20-m Buffer	50-m Buffer
Sep-10	NA	NA	ND
Feb-11	NA	NA	17
Jun-11	NA	NA	115
Dec-11	NA	NA	105
CES	NA	NA	ND

Table 5c: Raw liquefaction-related ground surface subsidence using original LiDAR points for Road.

	Average Ground Surface Subsidence (mm)		
Earthquake Event(s)	10-m Buffer	20-m Buffer	50-m Buffer
Sep-10	ND	ND	ND
Feb-11	51	28	0
Jun-11	79	84	83
Dec-11	100	101	99
CES	ND	ND	ND

Table 6a: Corrected liquefaction-related ground surface subsidence using original LiDAR points for Patch A with the calculated adjustments in Table 2.

	Average Calculated Ground Surface Subsidence (mm)		
Earthquake Event(s)	10-m Buffer	20-m Buffer	50-m Buffer
Sep-10	NA	ND	ND
Feb-11	NA	ND	133±50
Jun-11	NA	ND	98±50
Dec-11	NA	ND	62±75
CES	NA	ND	ND

Notes: Plus/minus values are same as those in Table 4a, but rounded to the nearest 25 mm; Positive overall values indicate ground surface subsidence, while negative overall values indicate ground surface uplift.

Table 6b: Corrected liquefaction-related ground surface subsidence using original LiDAR points for Patch B with the calculated adjustments in Table 2.

	Average Calculated Ground Surface Subsidence (mm)		
Earthquake Event(s)	10-m Buffer	20-m Buffer	50-m Buffer
Sep-10	NA	NA	ND
Feb-11	NA	NA	109±50
Jun-11	NA	NA	103±50
Dec-11	NA	NA	55±75
CES	NA	NA	ND

Notes: Plus/minus values are same as those in Table 4b, but rounded to the nearest 25 mm; Positive overall values indicate ground surface subsidence, while negative overall values indicate ground surface uplift.

Table 6c: Corrected liquefaction-related ground surface subsidence using original LiDAR points for Road with the calculated adjustments in Table 2.

	Average Calculated Ground Surface Subsidence (mm)		
Earthquake Event(s)	10-m Buffer	20-m Buffer	50-m Buffer
Sep-10	ND	ND	ND
Feb-11	192±100	169±100	141±100
Jun-11	17±100	22±100	21±100
Dec-11	50±125	50±125	49±125
CES	ND	ND	ND

Notes: Plus/minus values are same as those in Table 4c, but rounded to the nearest 25 mm; Positive overall values indicate ground surface subsidence, while negative overall values indicate ground surface uplift.

Table 7a: Corrected liquefaction-related ground surface subsidence for Patch A using LiDAR DEMs.

	Estimated Ground Surface Subsidence (mm)								
	10-m Buffer			20-m Buffer			50-m Buffer		
Earthquake Event(s)	16th %ile	50th %ile	84th %ile	16th %ile	50th %ile	84th %ile	16th %ile	50th %ile	84th %ile
Sep-10	NA	NA	NA	<50	<50	<50	<50	<50	<50
Feb-11	NA	NA	NA	200	200	200	150	200	250
Jun-11	NA	NA	NA	<50	50	50	<50	50	50
Dec-11	NA	NA	NA	150	150	150	150	150	150
CES	NA	NA	NA	450	450	450	450	450	450

Note: These percentiles are not the exact statistical measures; they indicate the spatial variability of ground surface subsidence.

Table 7b: Corrected liquefaction-related ground surface subsidence for Patch B using LiDAR DEMs.

	Estimated Ground Surface Subsidence (mm)								
	10-m Buffer			20-m Buffer			50-m Buffer		
Earthquake Event(s)	16th %ile	50th %ile	84th %ile	16th %ile	50th %ile	84th %ile	16th %ile	50th %ile	84th %ile
Sep-10	NA	NA	NA	NA	NA	NA	<50	<50	<50
Feb-11	NA	NA	NA	NA	NA	NA	150	150	200
Jun-11	NA	NA	NA	NA	NA	NA	<50	50	50
Dec-11	NA	NA	NA	NA	NA	NA	150	150	150
CES	NA	NA	NA	NA	NA	NA	350	400	450

Note: These percentiles are not the exact statistical measures; they indicate the spatial variability of ground surface subsidence.

Table 7c: Corrected liquefaction-related ground surface subsidence for Road using LiDAR DEMs.

	Estimated Ground Surface Subsidence (mm)								
	10-m Buffer			20-m Buffer			50-m Buffer		
Earthquake Event(s)	16th %ile	50th %ile	84th %ile	16th %ile	50th %ile	84th %ile	16th %ile	50th %ile	84th %ile
Sep-10	50	100	150	50	100	150	100	150	200
Feb-11	150	200	200	150	200	200	150	200	250
Jun-11	<50	<50	50	<50	<50	50	<50	<50	50
Dec-11	150	150	150	150	150	150	150	150	250
CES	400	400	450	400	450	450	400	450	700

Note: These percentiles are not the exact statistical measures; they indicate the spatial variability of ground surface subsidence.

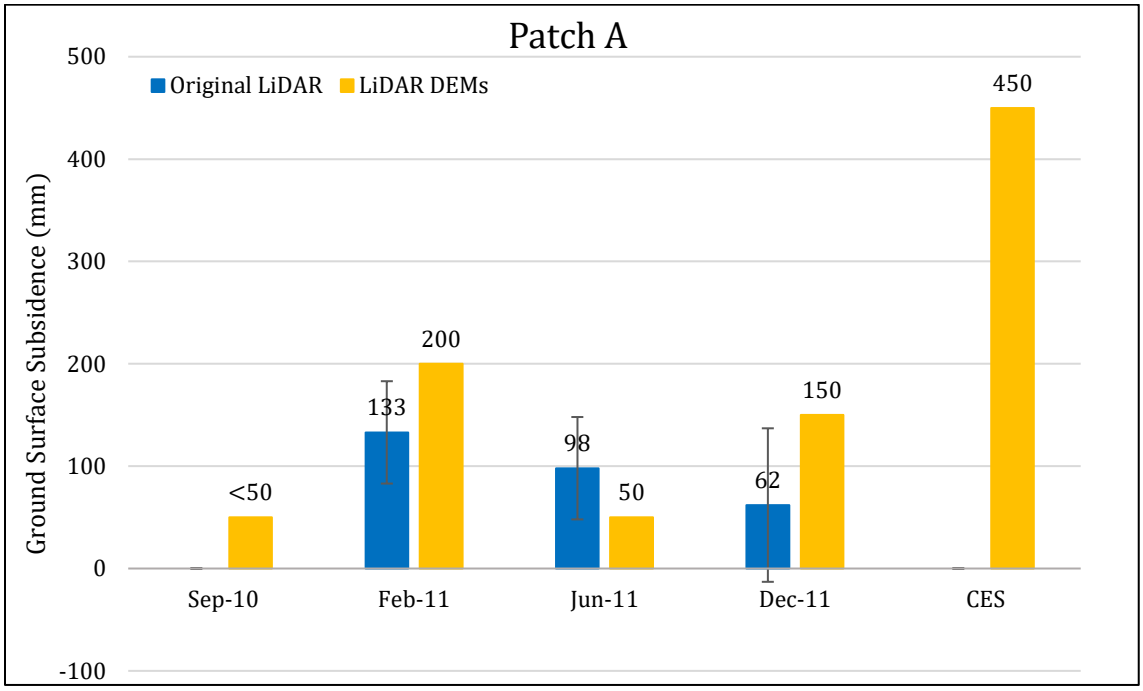

Figure 2: Comparison between ground surface subsidence determined from original LiDAR survey points and ground surface subsidence (50th %ile) estimated using LiDAR DEMs for Patch A (50-m buffer).

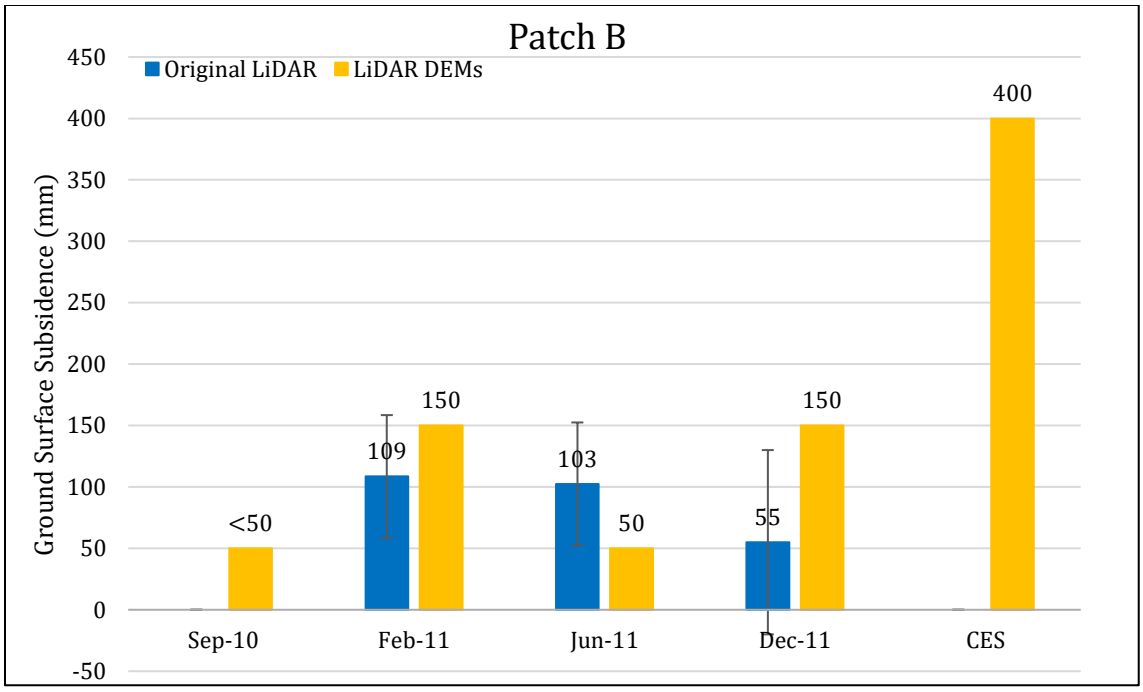

Figure 3: Comparison between ground surface subsidence determined from original LiDAR survey points and ground surface subsidence (50th %ile) estimated using LiDAR DEMs for Patch B (50-m buffer).

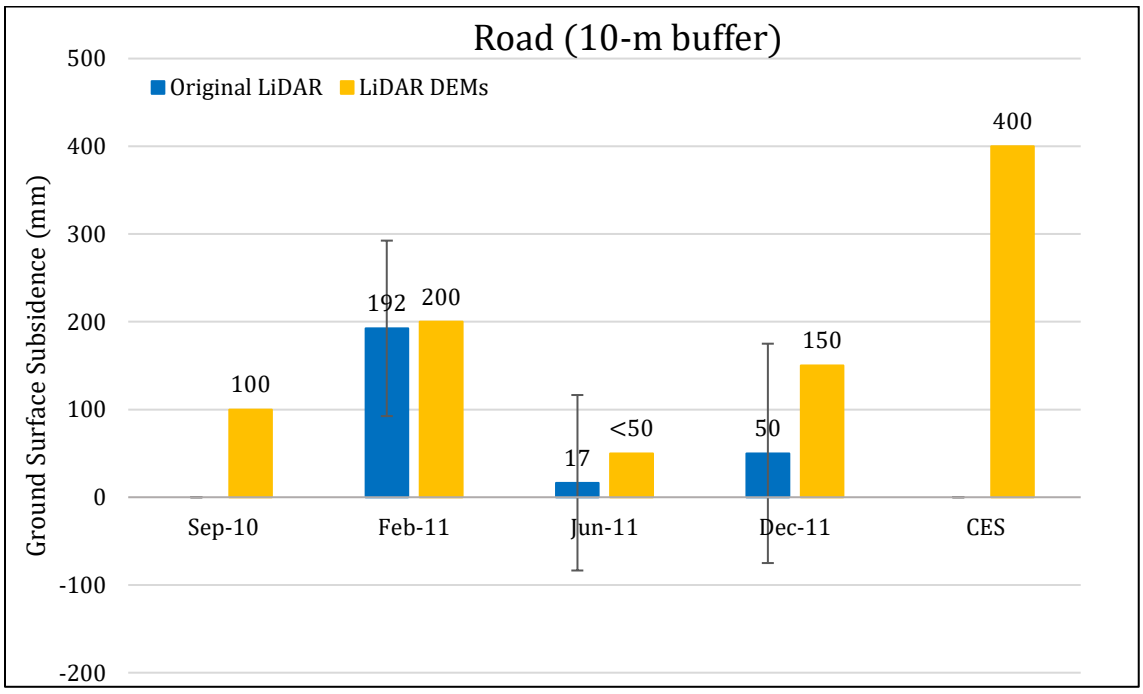

Figure 4: Comparison between ground surface subsidence determined from original LiDAR survey points and ground surface subsidence (50th %ile) estimated using LiDAR DEMs for Road (10-m buffer).

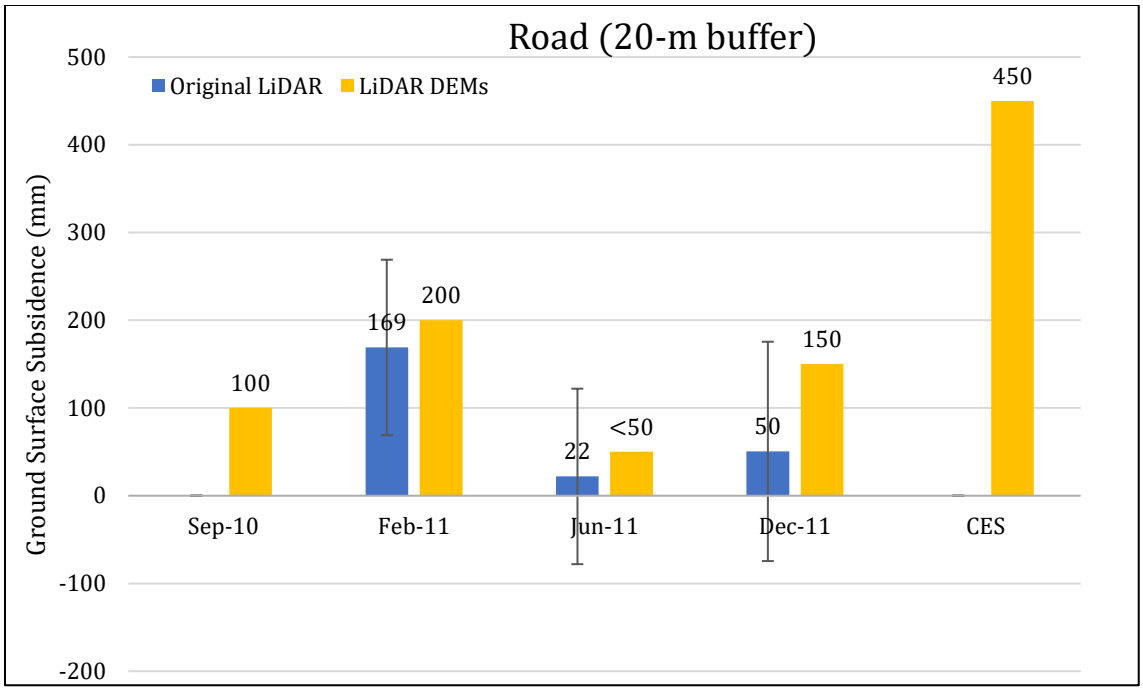

Figure 5: Comparison between ground surface subsidence determined from original LiDAR survey points and ground surface subsidence (50th %ile) estimated using LiDAR DEMs for Road (20-m buffer).

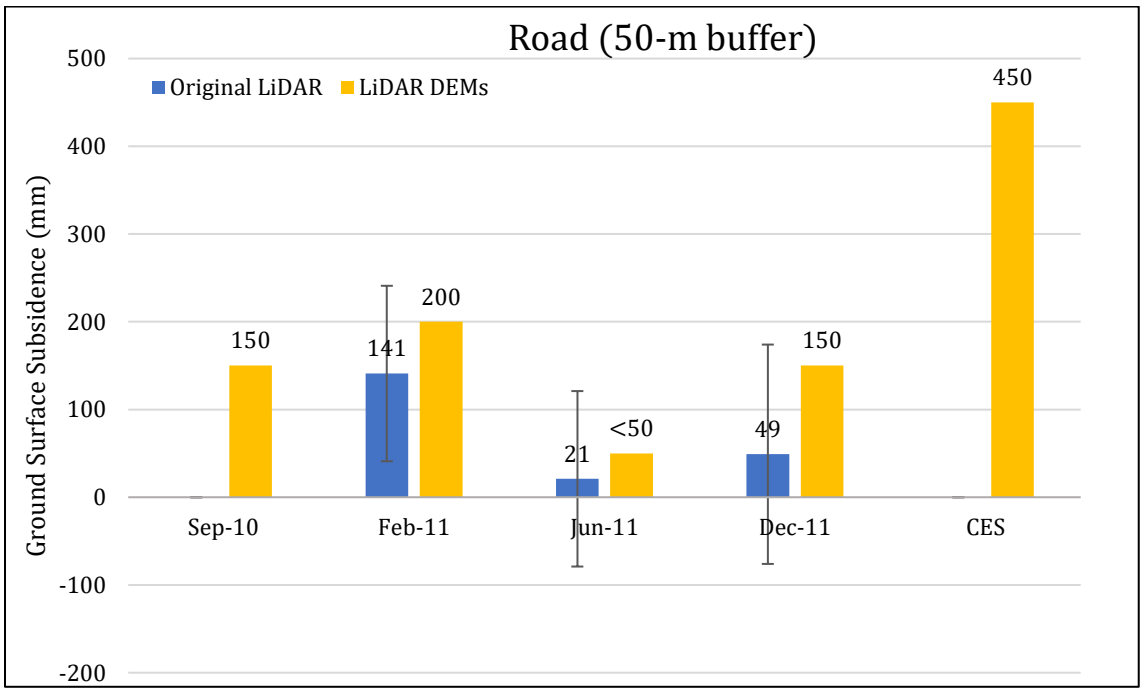

Figure 6: Comparison between ground surface subsidence determined from original LiDAR survey points and ground surface subsidence (50th %ile) estimated using LiDAR DEMs for Road (50-m buffer).

Note 2:

- Patches A and B: The ground surface subsidence computed using the original LiDAR survey points is ~50 mm lower for the Feb-11 EQ and ~50 mm higher for the Jun-11 EQ than the ground surface subsidence estimated using the LiDAR DEMs. The subsidence determined from the original LiDAR survey points is roughly three times lower than the ground surface subsidence estimated using the LiDAR DEM for the Dec-11 EQ.
- Road (10-m and 20-m buffers): The ground surface subsidence values determined from the original LiDAR survey points are similar to the ground surface subsidence values estimated using the LiDAR DEMs for the Feb-11 and Jun-11 EQs. For the Dec-11 EQ, the subsidence computed using the original LiDAR survey points is roughly three times lower than the subsidence estimated using the LiDAR DEM.
- Road (50-m buffer): The ground surface subsidence determined from the original LiDAR survey points is similar to the ground surface subsidence estimated using the LiDAR DEM for the Jun-11 EQ. The subsidence computed using the original LiDAR survey points is lower by ~60 mm for the Feb-11 EQ and three times lower for the Dec-11 EQ than the subsidence estimated using the LiDAR DEMs.

Table 8a: Ejecta-Induced settlement for the top 20 m of the soil profile for Patch A (50-m buffer) for the 50th %ile PGA, P_L=50%, and C_{FC}=0.13 using BI-2014, ZRB-2002, and I_c cutoff of 2.6.

Earthquake Event(s)	M_W	PGA (g)	Depth to Groundwater (m)	S_T (mm)	S_{V1D} (mm)	$S_{E,L}$ (mm)
Sep-10	7.1	0.18	1.7	ND	25±20	ND
Feb-11	6.2	0.49	2.0	133±50	122±50	11±71
Jun-11	6.2	0.25	1.3	98±50	55±25	43±56
Dec-11	6.1	0.37	1.5	62±75	102±50	-39±90

Notes: S_T = Total settlement (Table 6); S_{V1D} = Average vertical settlement due to volumetric compression using Boulanger and Idriss (2014) (BI-2014), Zhang et al. (2002) (ZRB-2002) procedures and de Greef and Lengkeek (2018) thin-layer correction; $S_{E,L}$ = Ejecta-induced settlement as the difference between the LiDAR-based S_T and S_{V1D}.

Table 8b: Ejecta-Induced settlement for the top 20 m of the soil profile for Patch B (50-m buffer) for the 50th %ile PGA, P_L=50%, and C_{FC}=0.13 using BI-2014, ZRB-2002, and I_c cutoff of 2.6.

Earthquake Event(s)	M_W	PGA (g)	Depth to Groundwater (m)	S_T (mm)	S_{V1D} (mm)	$S_{E,L}$ (mm)
Sep-10	7.1	0.18	1.7	ND	36±20	ND
Feb-11	6.2	0.49	2.0	109±50	159±50	-50±71
Jun-11	6.2	0.25	1.3	103±50	80±25	23±56
Dec-11	6.1	0.37	1.5	55±75	137±50	-82±90

Notes: S_T = Total settlement (Table 6); S_{V1D} = Average vertical settlement due to volumetric compression using Boulanger and Idriss (2014) (BI-2014), Zhang et al. (2002) (ZRB-2002) procedures and de Greef and Lengkeek (2018) thin-layer correction; $S_{E,L}$ = Ejecta-induced settlement as the difference between the LiDAR-based S_T and S_{V1D}.

Table 8c: Ejecta-Induced settlement for the top 20 m of the soil profile for Road (10-m buffer) for the 50th %ile PGA, P_L=50%, and C_{FC}=0.13 using BI-2014, ZRB-2002, and I_c cutoff of 2.6.

Earthquake Event(s)	M_W	PGA (g)	Depth to Groundwater (m)	S_T (mm)	S_{V1D} (mm)	$S_{E,L}$ (mm)
Sep-10	7.1	0.18	1.7	ND	12±20	ND
Feb-11	6.2	0.49	2.0	192±100	99±50	93±112
Jun-11	6.2	0.25	1.3	17±100	37±25	-20±103
Dec-11	6.1	0.37	1.5	50±125	76±50	-26±135

Notes: S_T = Total settlement (Table 6); S_{V1D} = Average vertical settlement due to volumetric compression using Boulanger and Idriss (2014) (BI-2014), Zhang et al. (2002) (ZRB-2002) procedures and de Greef and Lengkeek (2018) thin-layer correction; $S_{E,L}$ = Ejecta-induced settlement as the difference between the LiDAR-based S_T and S_{V1D}.

Table 8d: Ejecta-Induced settlement for the top 20 m of the soil profile for Road (20-m buffer) within the 20-m buffer for the 50th %ile PGA, P_L=50%, and C_{FC}=0.13 using BI-2014, ZRB-2002, and I_c cutoff of 2.6.

Earthquake Event(s)	M_W	PGA (g)	Depth to Groundwater (m)	S_T (mm)	S_{V1D} (mm)	$S_{E,L}$ (mm)
Sep-10	7.1	0.18	1.7	ND	12±20	ND
Feb-11	6.2	0.49	2.0	169±100	99±50	70±112
Jun-11	6.2	0.25	1.3	22±100	37±25	-15±103
Dec-11	6.1	0.37	1.5	50±125	76±50	-26±135

Notes: S_T = Total settlement (Table 6); S_{V1D} = Average vertical settlement due to volumetric compression using Boulanger and Idriss (2014) (BI-2014), Zhang et al. (2002) (ZRB-2002) procedures and de Greef and Lengkeek (2018) thin-layer correction; $S_{E,L}$ = Ejecta-induced settlement as the difference between the LiDAR-based S_T and S_{V1D}.

Table 8e: Ejecta-Induced settlement for the top 20 m of the soil profile for Road (50-m buffer) for the 50th %ile PGA, P_L=50%, and C_{FC}=0.13 using BI-2014, ZRB-2002, and I_C cutoff of 2.6.

Earthquake Event(s)	M_W	PGA (g)	Depth to Groundwater (m)	S_T (mm)	S_{V1D} (mm)	$S_{E,L}$ (mm)
Sep-10	7.1	0.18	1.7	ND	37±20	ND
Feb-11	6.2	0.49	2.0	141±100	162±50	-21±112
Jun-11	6.2	0.25	1.3	21±100	74±25	-53±103
Dec-11	6.1	0.37	1.5	49±125	135±50	-86±135

Notes: S_T = Total settlement (Table 6); S_{V1D} = Average vertical settlement due to volumetric compression using Boulanger and Idriss (2014) (BI-2014), Zhang et al. (2002) (ZRB-2002) procedures and de Greef and Lengkeek (2018) thin-layer correction; $S_{E,L}$ = Ejecta-induced settlement as the difference between the LiDAR-based S_T and S_{V1D}.

Note 3: The uncertainty for volumetric settlement was derived based on the sensitivity of volumetric settlement to PGA, C_{FC}, and P_L for each earthquake event for VsVp 57203 *Shirley Intermediate School* and CC LIQ 1 – CPT 5586 – *Vivian St* sites. Taking the 50th percentile as the baseline case, the minimum and maximum values corresponding to the difference between the 25th percentile and the 50th percentile and the 75th percentile and the 50th percentile were determined. The arithmetic mean of the range of the minimum and maximum difference was evaluated for each patch at the two sites. The maximum arithmetic mean for each earthquake event was rounded to the nearest five and used as the uncertainty value. Accordingly, the 1-D volumetric settlement uncertainties of ±20, ±50, ±25, and ±50 mm for the Sep-10, Feb-11, Jun-11, and Dec-11 earthquake events, respectively, were used for all sites in this study.

Table 9a: Coverage area and height of ejecta estimates for Patch A (20- and 50-m buffers) using photographs.

Earthquake Event	$A_{E,thick}$ (m^2)	$H_{E,thick}$ (mm)	$A_{E,thin}$ (m^2)	$H_{E,thin}$ (mm)	A_T (m^2)
Sep-10	0	0	0	0	81.9
Feb-11	57.8	40-60	23.1	20-40	81.9
Jun-11	0	0	4.6	30-50	81.9
Dec-11	12.2	40-60	0	0	81.9

Notes: $A_{E,thick/thin}$ = Coverage area of thick/thin ejecta layers; $H_{E,thick/thin}$ = Lower-upper estimate of height of thick/thin ejecta layers; A_T = Total assessment area of a buffer being considered; Thin and thick layers correspond to light gray and dark gray colors of ejecta observed in aerial photographs.

Table 9b: Coverage area and height of ejecta estimates for Patch B (50-m buffer) using photographs.

Earthquake Event	$A_{E,thick}$ (m^2)	$H_{E,thick}$ (mm)	$A_{E,thin}$ (m^2)	$H_{E,thin}$ (mm)	A_T (m^2)
Sep-10	0	0	0	0	68.5
Feb-11	34.2	60-80	6.8	40-60	68.5
Jun-11	0	0	2.8	30-50	68.5
Dec-11	20.9	30-50	3.7	20-40	59.6*

Notes: $A_{E,thick/thin}$ = Coverage area of thick/thin ejecta layers; $H_{E,thick/thin}$ = Lower-upper estimate of height of thick/thin ejecta layers; A_T = Total assessment area of a buffer being considered; Thin and thick layers correspond to light gray and dark gray colors of ejecta observed in aerial photographs; * indicates reduction in A_T due to the presence of the car (unable to see below it).

Table 9c: Coverage area and height of ejecta estimates for Road (20-m buffer) using photographs.

EQ Event	$H_{E,trap.\ prism1}$ (mm)	$H_{E,trap.\ prism2}$ (mm)	$V_{E,trap.prism}$ (m^3)	$H_{E,prism/pyr}$ (mm)	$V_{E,prism+pyr}$ (m^3)	$H_{E,thin}$ (mm)	$A_{E,thin}$ (m^2)	A_T (m^2)
Sep-10	0	0	0	0	0	0	0	363
Feb-11	200-300	50-150	39.5-71.0	30-300	3.22-4.02	0	0	363
Jun-11	180-200	30-50	32.9-39.1	30-200	2.08-2.66	10-20	9.1	363
Dec-11	160-220	30-70	35.2-48.3	30-220	0.97-1.34	3-6	2.4	363

Notes: $H_{E,trap.\ prism1/2}$ = Lower-upper estimate of ejecta height at the curb/centerline based on 2-4% cross slope of normal crown and the maximum curb height of 150 mm; $V_{E,trap.\ prism}$ = Lower-upper estimate of total volume of ejecta shaped as a trapezoidal prism; $H_{E,prism/pyr}$ = Lower-upper estimate of ejecta height near the curb based on 2-4% cross slope of normal crown; $V_{E,prism+pyr}$ = Lower-upper estimate of total volume of prismatic- and pyramidal-shape ejecta; $A_{E,thin}$ =Coverage area of thin ejecta layers; $H_{E,\ thin}$ = Lower-upper estimate of height of thin ejecta layers; A_T= Total assessment area of a buffer being considered.

Table 9d: Coverage area and height of ejecta estimates for Road (50-m buffer) using photographs.

EQ Event	$H_{E,trap.\ prism1}$ (mm)	$H_{E,trap.\ prism2}$ (mm)	$V_{E,trap.prism}$ (m^3)	$H_{E,prism/pyr}$ (mm)	$V_{E,prism+pyr}$ (m^3)	$H_{E,thin}$ $H_{E,thick}$ (mm)	$A_{E,thin}$ $A_{E,thick}$ (m^2)	$H_{E,cc}$ (mm)	$V_{E,cc}$ (m^3)	A_T (m^2)
Sep-10	0	0	0	0	0	0	0	0	0	937
Feb-11	180-300	30-150	94.2-151	30-300	9.74-12.4	0	0	0	0	937
Jun-11	170-200	20-50	53.9-64.3	20-200	17.6-24.2	10-20	98.8	508-537	1.33	937
Dec-11	160-220	10-70	61.8-82.0	22-220	12.9-18.1	3-6 20-40	53.2 9.9	202-779*	4.29*	937

Notes: $H_{E,trap.\ prism1/2}$ = Lower-upper estimate of ejecta height at the curb/centerline based on 2-4% cross slope of normal crown and the maximum curb height of 150 mm; $V_{E,trap.\ prism}$ = Lower-upper estimate of total volume of ejecta shaped as a trapezoidal prism; $H_{E,prism/pyr}$ = Lower-upper estimate of ejecta height near the curb based on 2-4% cross slope of normal crown; $V_{E,prism+pyr}$ = Lower-upper estimate of total volume of prismatic- and pyramidal-shape ejecta; $A_{E,thin}$ =Coverage area of thin ejecta layers; $H_{E,\ thin}$ = Lower-upper estimate of height of thin ejecta layers; A_T= Total assessment area of a buffer being considered; * Ejecta may originate from the adjacent driveway.

Note 4: The values in Table 9 correspond to the coverage area of ejecta outlined in aerial photographs (Figures 27, 29, and 81-83) and the lower and upper estimates of ejecta height based on geometrical approximations, ground photographs (Figures 85, 87, 88, and 89), and EQC LDAT property inspection reports (Figures 84 and 86). The ejecta-induced settlement using photographs and engineering judgment, $S_{E,P}$, is estimated as

$$
\begin{aligned}
S_{E,P} = & \frac{\sum_{i=1}^{a} A_{E,thick,i} * H_{E,thick,i} + \sum_{j=1}^{b} A_{E,thin,j} * H_{E,thin,j} + \frac{1}{3}\sum_{k=1}^{c} A_{E,pile,k} * R_{E,pile,k} * tan30°}{A_T} \\
& + \frac{\sum_{l=1}^{d} \left(\frac{1}{2}(H_{E,trap.\ prism\ 1,l} + H_{E,trap.\ prism\ 2,l}) * W_{E,trap.\ prism,l}\right) * L_{E,trap.\ prism,l}}{A_T} \\
& + \frac{\frac{1}{2}\sum_{n=1}^{f} W_{E,prism,n} * H_{E,prism,n} * L_{E,prism,n}}{A_T} \\
& + \frac{\frac{1}{3}\sum_{p=1}^{g} W_{E,r.pyramid,p} * H_{E,r.pyramid,p} * L_{E,r.pyramid,p}}{A_T} \\
& + \frac{\frac{1}{6}\sum_{r=1}^{h} W_{E,t.pyramid,r} * H_{E,t.pyramid,r} * L_{E,t.pyramid,r}}{A_T} \\
& = \frac{\sum_{i=1}^{a} V_{E,thick,i} + \sum_{j=1}^{b} V_{E,thin,j} + \sum_{k=1}^{c} V_{E,conical\ component,k} + \sum_{l=1}^{d} V_{E,trap.\ prism,l}}{A_T} \\
& + \frac{\sum_{n=1}^{f} V_{E,prism,n} + \sum_{p=1}^{g} V_{E,r.pyramid,p} + \sum_{r=1}^{h} V_{E,t.pyramid,r}}{A_T}
\end{aligned}
$$

where

- $A_{E,thick,i}$ and $H_{E,thick,i}$ are the area and the height of a thick ejecta layer, respectively;
- $A_{E,thin,j}$ and $H_{E,thin,j}$ are the area and the height of a thin ejecta layer, respectively;
- $A_{E,pile,k}$ and $R_{E,pile,k}$ are the area and the radius of an ejecta pile component, respectively, shaped as a cone with the repose angle of 30°;
- $W_{E,trap.\ prism,l}$ and $L_{E,trap.\ prism,l}$ are the width and the length, respectively, of the coverage area of an ejecta layer shaped as a trapezoidal prism, while $H_{E,trap.\ prism\ 1,l}$ and $H_{E,trap.\ prism\ 2,l}$ are the heights of the trapezoidal prism-like ejecta layer;
- $W_{E,prism,n}$ and $L_{E,prism,n}$ are the width and the length of the coverage area of a prismatically shaped ejecta layer, respectively, and $H_{E,prism,n}$ is the height of a prism-like ejecta layer;
- $W_{E,pyr,p}$ and $L_{E,pyr,p}$ are the width and the length of the coverage area of a rectangular-base pyramid-like ejecta layer, respectively, and $H_{E,pyr,p}$ is the height of a pyramid-like ejecta layer;
- $W_{E,pyr,r}$ and $L_{E,pyr,r}$ are the width and the length of the coverage area of a triangular-base pyramid-like ejecta layer, respectively, and $H_{E,pyr,r}$ is the height of a triangular-base pyramid-like ejecta layer;
- A_T is the total assessment area for a buffer being considered (Figure 1).

Table 10a: Ejecta-induced settlement estimates for Patches A and B based on photographs.

Earthquake Event	Patch A (50-m buffer)		Patch B (50-m buffer)	
	$S_{E,P,lower}$ (mm)	$S_{E,P,upper}$ (mm)	$S_{E,P,lower}$ (mm)	$S_{E,P,upper}$ (mm)
Sep-10	0	0	0	0
Feb-11	34	54	34	46
Jun-11	2	3	1	2
Dec-11	6	9	12	20

Note: $S_{E,P,lower}$ and $S_{E,P,upper}$ correspond to lower and upper estimates of $S_{E,P}$, respectively.

Table 10b: Ejecta-induced settlement estimates for Road based on photographs.

Earthquake Event	Road (20-m buffer)		Road (50-m buffer)	
	$S_{E,P,lower}$ (mm)	$S_{E,P,upper}$ (mm)	$S_{E,P,lower}$ (mm)	$S_{E,P,upper}$ (mm)
Sep-10	0	0	0	0
Feb-11	118	207	111	174
Jun-11	97	116	79	98
Dec-11	100	137	85	112

Note: $S_{E,P,lower}$ and $S_{E,P,upper}$ correspond to lower and upper estimates of $S_{E,P}$, respectively.

Table 11a: Best final estimates of ejecta-induced settlement for Patches A and B.

Earthquake Event	Patch A (50-m buffer)			Patch B (50-m buffer)		
	$S_{E,L}$ (mm)	$S_{E,P}$ (mm)	$S_{E,final}$ (mm)	$S_{E,L}$ (mm)	$S_{E,P}$ (mm)	$S_{E,final}$ (mm)
Sep-10	ND	0	0	ND	0	0
Feb-11	11±71	44±10	40±10	-50±71	40±6	40±5
Jun-11	43±56	2.5±0.5	5±5	23±56	1.5±0.5	5±5
Dec-11	-39±90	7.5±1.5	10±5	-82±90	16±4	15±5

Notes: $S_{E,L}$ = Ejecta-induced settlement based on LiDAR data reported in Table 8; $S_{E,P}$ = Median ejecta-induced settlement for the range of values reported in Table 10; $S_{E,final}$ = Best final estimate of ejecta-induced settlement rounded to the nearest 5 mm; Final plus/minus values are also rounded to the nearest 5 mm; ND = Not determined.

Table 11b: Best final estimates of ejecta-induced settlement for Road.

EQ Event	Road (20-m buffer)			Road (50-m buffer)		
	$S_{E,L}$ (mm)	$S_{E,P}$ (mm)	$S_{E,final}$ (mm)	$S_{E,L}$ (mm)	$S_{E,P}$ (mm)	$S_{E,final}$ (mm)
Sep-10	ND	0	0	ND	0	0
Feb-11	70±112	163±44	155±40	-21±112	143±31	145±30
Jun-11	-15±103	107±9	105±10	-53±103	89±9	90±10
Dec-11	-26±135	119±18	120±20	-86±135	99±13	100±15

Notes: $S_{E,L}$ = Ejecta-induced settlement based on LiDAR data reported in Table 8; $S_{E,P}$ = Median ejecta-induced settlement for the range of values reported in Table 10; $S_{E,final}$ = Best final estimate of ejecta-induced settlement rounded to the nearest 5 mm; Final plus/minus values are also rounded to the nearest 5 mm; ND = Not determined.

Note 5:

- Patch A: $S_{E,final}$ for the Sep-10 and Dec-11 EQs is based solely on $S_{E,P}$ due to the evident absence of ejecta for the Sep-10 EQ and the negative $S_{E,L}$ value for the Dec-11 EQ. $S_{E,final}$ for the Feb-11 and Jun-11 EQs is a weighted average of $S_{E,L}$ and $S_{E,P}$ with the weight coefficients of 0.1 and 0.9, respectively. The uncertainty associated with $S_{E,final}$ is also a weighted average of uncertainties associated with $S_{E,L}$ and $S_{E,P}$ with the same weights of 0.1 and 0.9, respectively.
- Patch B: $S_{E,final}$ for the Sep-10 and Dec-11 EQs is based solely on $S_{E,P}$ due to the evident absence of ejecta for the Sep-10 EQ and the negative $S_{E,L}$ values for the Feb-11 and Dec-11 EQs. $S_{E,final}$ for the Jun-11 EQs is a weighted average of $S_{E,L}$ and $S_{E,P}$ with the weight coefficients of 0.1 and 0.9, respectively. The uncertainty associated with $S_{E,final}$ is also a weighted average of uncertainties associated with $S_{E,L}$ and $S_{E,P}$ with the same weights of 0.1 and 0.9, respectively.
- Road (20-m buffer): $S_{E,final}$ for the Sep-10, Jun-11, and Dec-11 EQs is based solely on $S_{E,P}$ due to the evident absence of ejecta for the Sep-10 EQ and the negative $S_{E,L}$ value for the Jun-11 and Dec-11 EQs. $S_{E,final}$ for the Feb-11 EQ is a weighted average of $S_{E,L}$ and $S_{E,P}$ with the weight coefficients of 0.1 and 0.9, respectively. The uncertainty associated with $S_{E,final}$ is also the weighted average of uncertainties associated with $S_{E,L}$ and $S_{E,P}$ with the same weights of 0.1 and 0.9, respectively.
- Road (50-m buffer): $S_{E,final}$ for the Sep-10 and Dec-11 EQs is based solely on $S_{E,P}$ due to the evident absence of ejecta for the Sep-10 EQ and the negative $S_{E,L}$ values for the Feb-11, Jun-11, and Dec-11 EQs.
- The weight coefficients are based on the LiDAR error bands, LPI prediction error (Maurer et al. 2014[3]), presence of ejecta at the time of LiDAR surveys, completeness of visual evidence (i.e., ground and aerial photographs and EQC LDAT property inspection reports for the site), notable discrepancy between the LiDAR-based estimates of ejecta-induced settlement and the observed quantum of ejecta, and Note 2. The Baker St site is in the apparent zone of higher ground surface subsidence for the Sep-10 EQ (i.e., the overestimate of the ground surface elevation by the Jul-03 LiDAR survey and the underestimate of the ground surface elevation by the Sep-10 LiDAR survey) and the apparent zone of lower ground surface subsidence for

[3] Maurer, B. W., Green, R. A., Cubrinovski, M., & Bradley, B. A. (2014). Evaluation of the Liquefaction Potential Index for Assessing Liquefaction Hazard in Christchurch, New Zealand. *Journal of Geotechnical and Geoenvironmental Engineering*, 140(7), 04014032-1-11. doi:10.1061/(asce)gt.1943-5606.0001117

the Feb-11 EQ (i.e., the underestimate of the ground surface elevation by the Sep-10 LiDAR survey). The site is also in the zone of slight to moderate LPI overprediction of liquefaction severity for the Sep-10 EQ and accurate LPI prediction of liquefaction severity for the Feb-11 EQ. The LDAT property inspection reports are available for both Patch A and Patch B (Figures 97 and 99). Ground photographs showing the remnants of ejecta for Patches A and B are available. Ground photographs showing the remnants of ejecta at properties within the 50-m buffer are also available. The maximum height of ejecta in the backyard that is just outside the NW quadrant of the 50-m buffer was measured as 200 mm; however, this yard had more ejecta than the yards within the 50-m buffer based on visual inspection of the aerial photograph for the Feb-11 EQ.

- Ejecta occurred predominantly on the road; however, the $S_{E,L}$ values for the road are negative and differ significantly from the $S_{E,P}$ values for the road which are typically greater than 100 mm. The significant discrepancy between the two sets of values might be due to the shear displacement driven by gently sloping land from the properties toward the road, which could have pushed the road up; this mechanism could not be captured by LiDAR and 1-D volumetric settlement.

<u>Summary 1</u>:

- **The best estimate of the ejecta-induced free-field ground settlement at the Baker St site for the SEP 2010, FEB 2011, JUN 2011, and DEC 2011 earthquake is 0 mm, 40±10 mm, 5±5 mm, and 10±5 mm, respectively.**
- **The best estimate of the ejecta-induced settlement of the road at the Baker St site for the SEP 2010, FEB 2011, JUN 2011, and DEC 2011 earthquake is 0 mm, 155±40 mm, 105±10 mm, and 120±20 mm, respectively.**
- **The ejecta-induced settlement of the road is more representative of the site.**

Figure 7: Location of the site.

Figure 8: Position of the site relative to nearby buildings, vegetation, and free-face features.

Figure 9: Street view of the flat land.

Figure 10: Street view of the retaining wall (the property on the left side of the image).

Figure 11: Satellite image of the site taken in Dec 2004.

Figure 12: Satellite image of the site taken in Mar 2009.

Figure 13: Satellite image of the site taken on Sep 3, 2010.

Figure 14: Satellite image of the site taken on Sep 5, 2010.

Figure 15: Satellite image of the site taken on Feb 7, 2011.

Figure 16: Satellite image of the site taken on Feb 23, 2011.

Figure 17: Satellite image of the site taken on Feb 26, 2011.

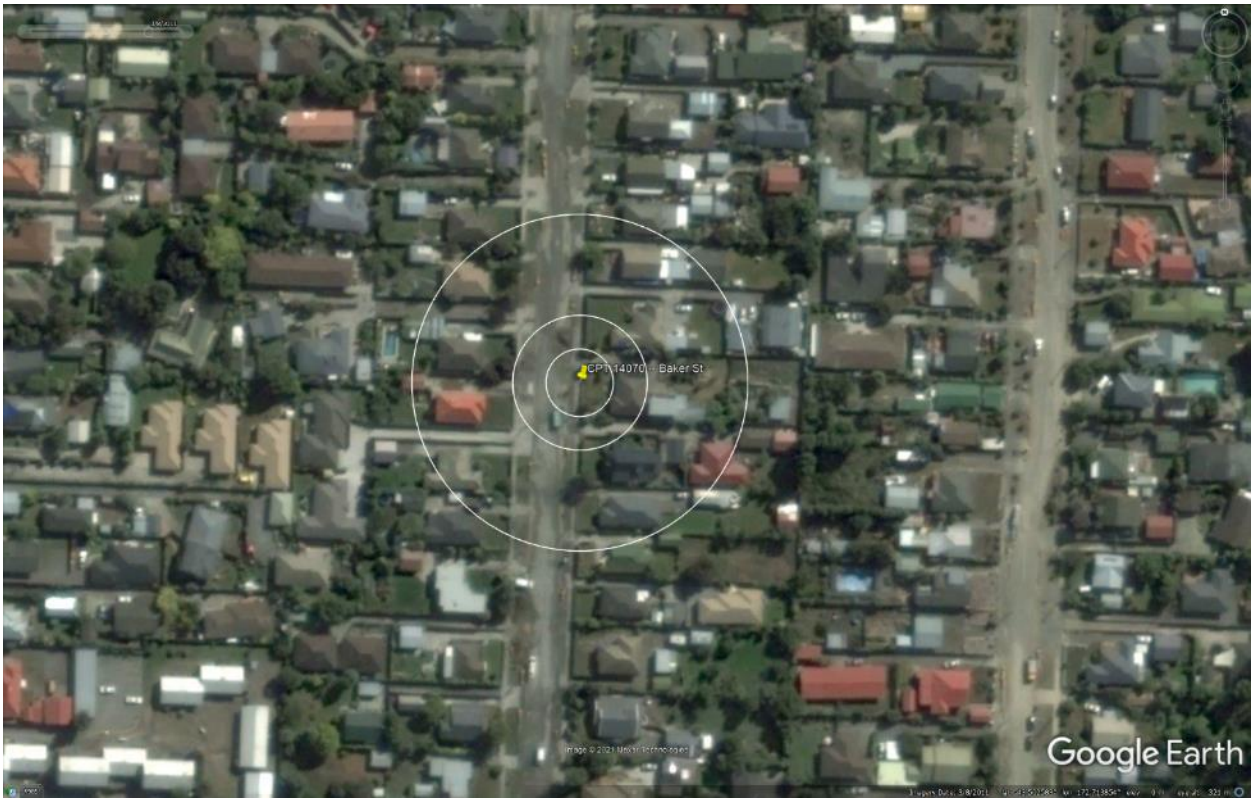

Figure 18: Satellite image of the site taken on Mar 8, 2011.

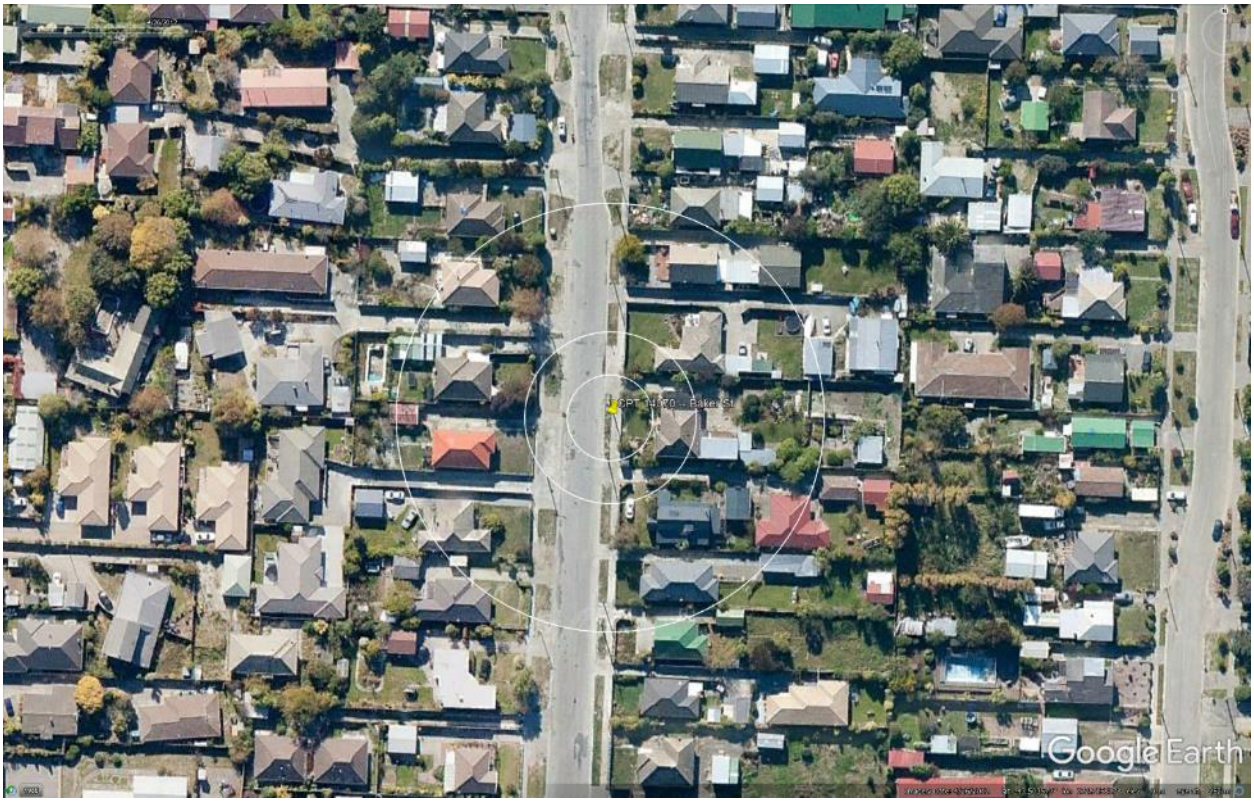

Figure 19: Satellite image of the site taken in Apr 2012.

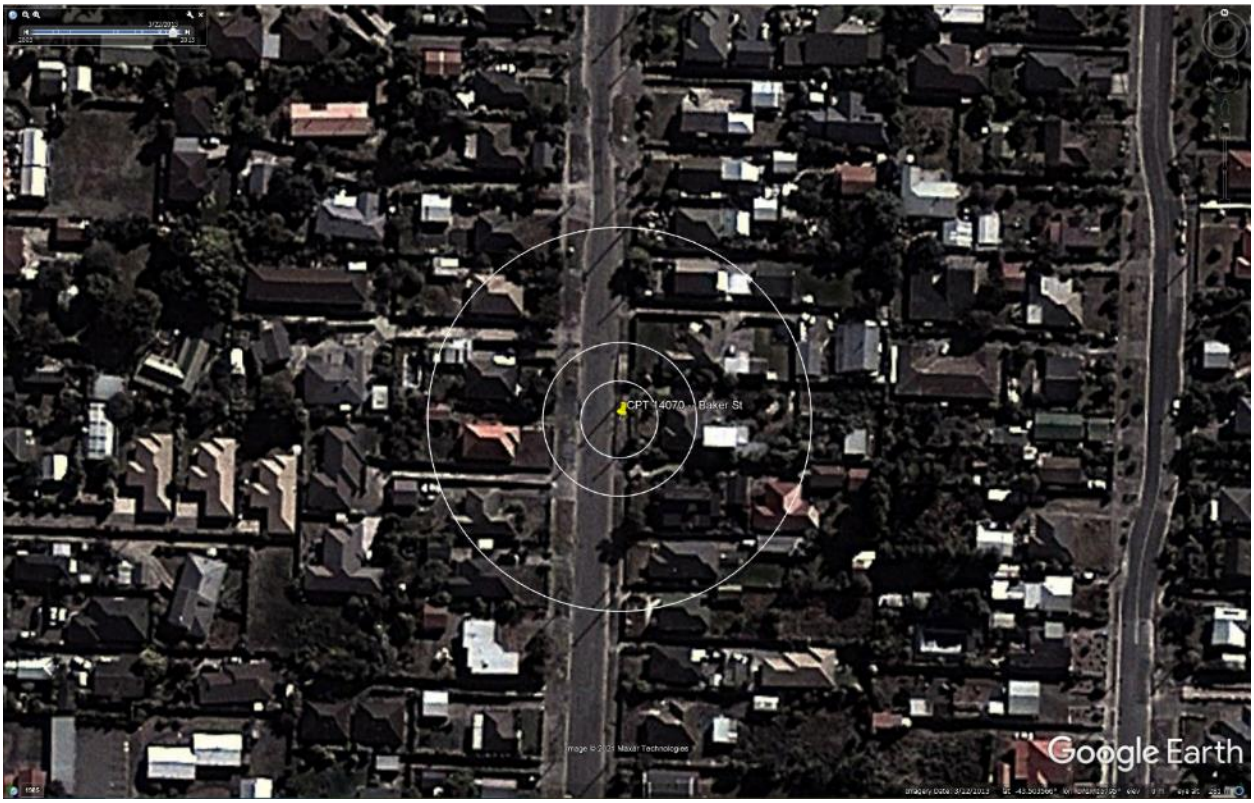

Figure 20: Satellite image of the site taken in Mar 2013.

Figure 21: Satellite image of the site taken in Aug 2013.

Figure 22: Satellite image of the site taken in Jan 2015.

Figure 23: Satellite image of the site taken in Apr 2015.

Figure 24: Satellite image of the site taken in July 12, 2015.

Figure 25: Satellite image of the site taken in July 22, 2015.

Figure 26: Satellite image of the site taken in Nov 2015.

Figure 27: Aerial photograph of the site taken on Sep 4, 2010.

Figure 28: Aerial photograph of the site taken on Feb 24, 2011.

Figure 29: Aerial photograph of the site taken on June 14-15, 2011.

Figure 30: Aerial photograph of the site taken on June 16, 2011.

Figure 31: Aerial photograph of the site taken on Dec 24, 2011.

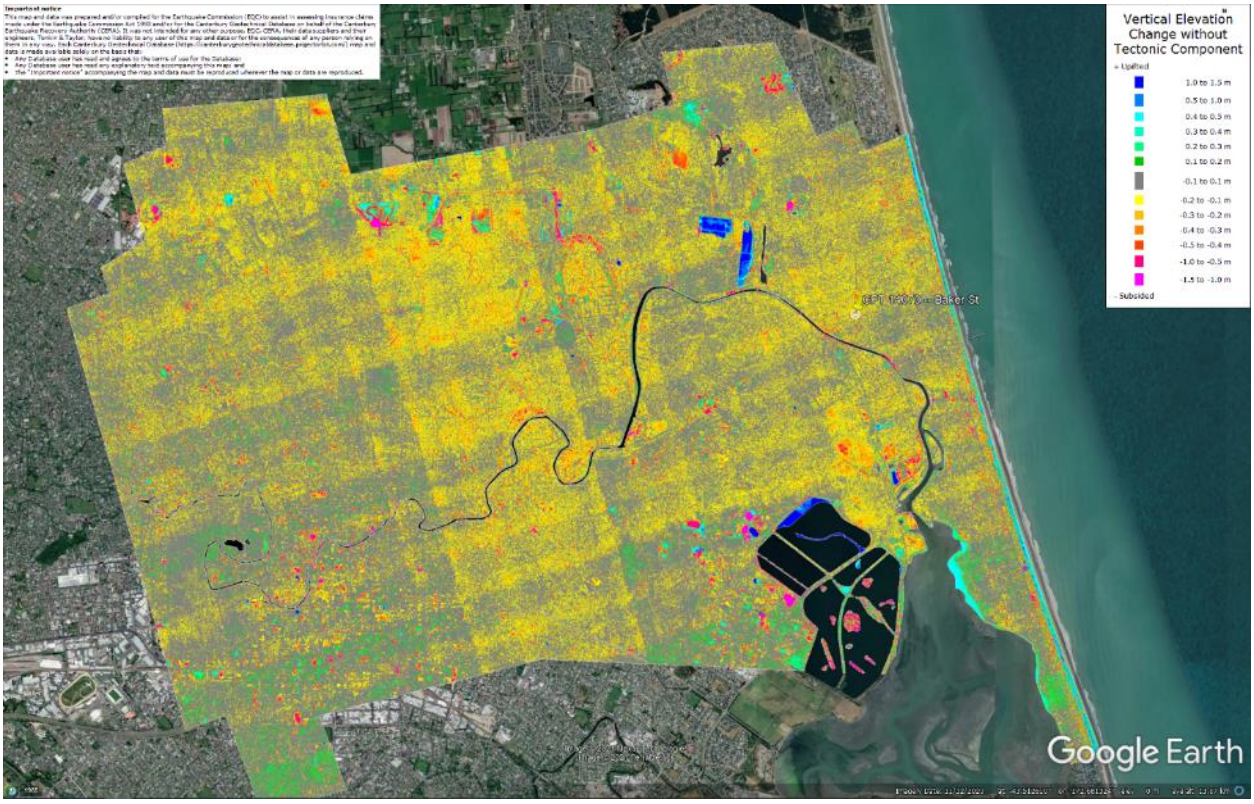

Figure 32: Vertical Ground Movements (Surface – Tectonic) for Sep 2010 Earthquake – the site is in the apparent zone of overestimated ground surface subsidence (i.e., July 2003 and Sep 2010 LiDAR flight error bands).

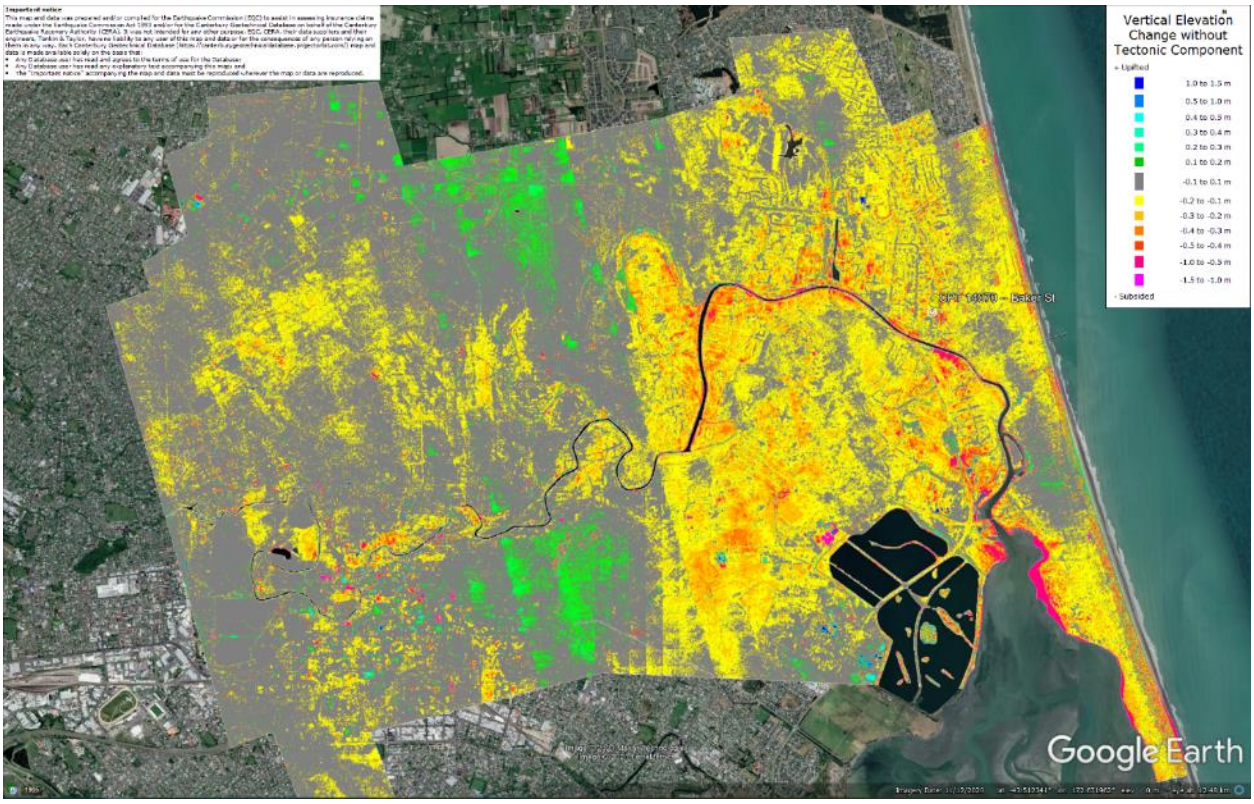

Figure 33: Vertical Ground Movements (Surface – Tectonic) for Feb 2011 Earthquake – the site is in the apparent zone of underestimated ground surface subsidence (i.e., Sep 2010 LiDAR flight error band).

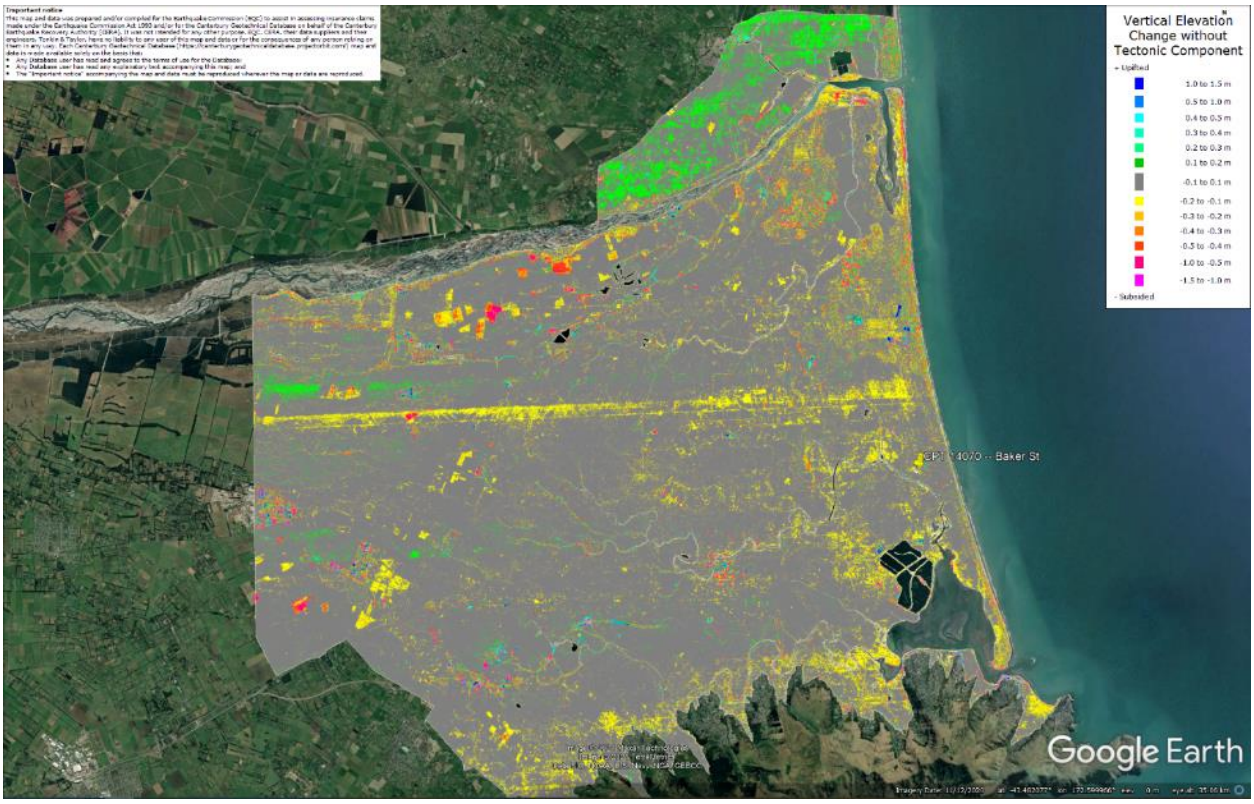

Figure 34: Vertical Ground Movements (Surface – Tectonic) for June 2011 Earthquake – the site is not in the apparent zone of overestimated/underestimated ground surface subsidence.

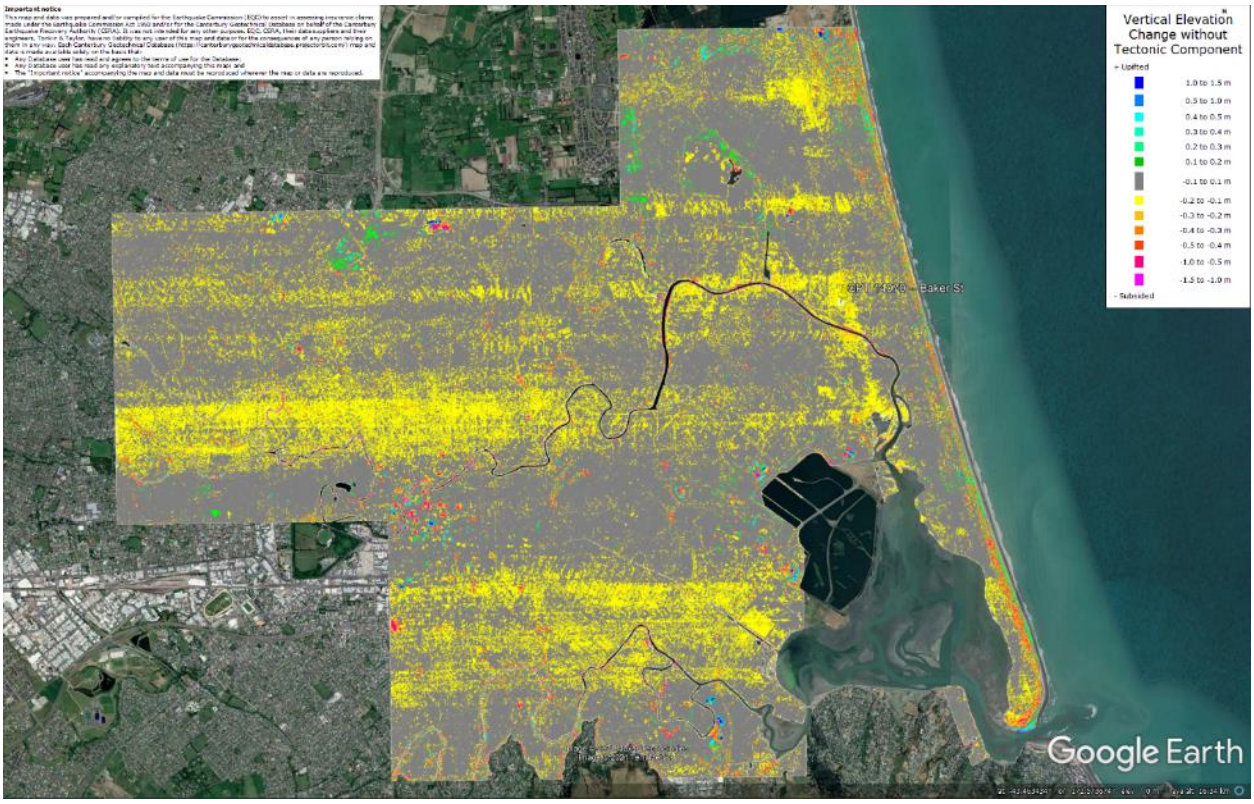

Figure 35: Vertical Ground Movements (Surface – Tectonic) for Dec 2011 Earthquake – the site is not in the apparent zone of overestimated/underestimated ground surface subsidence.

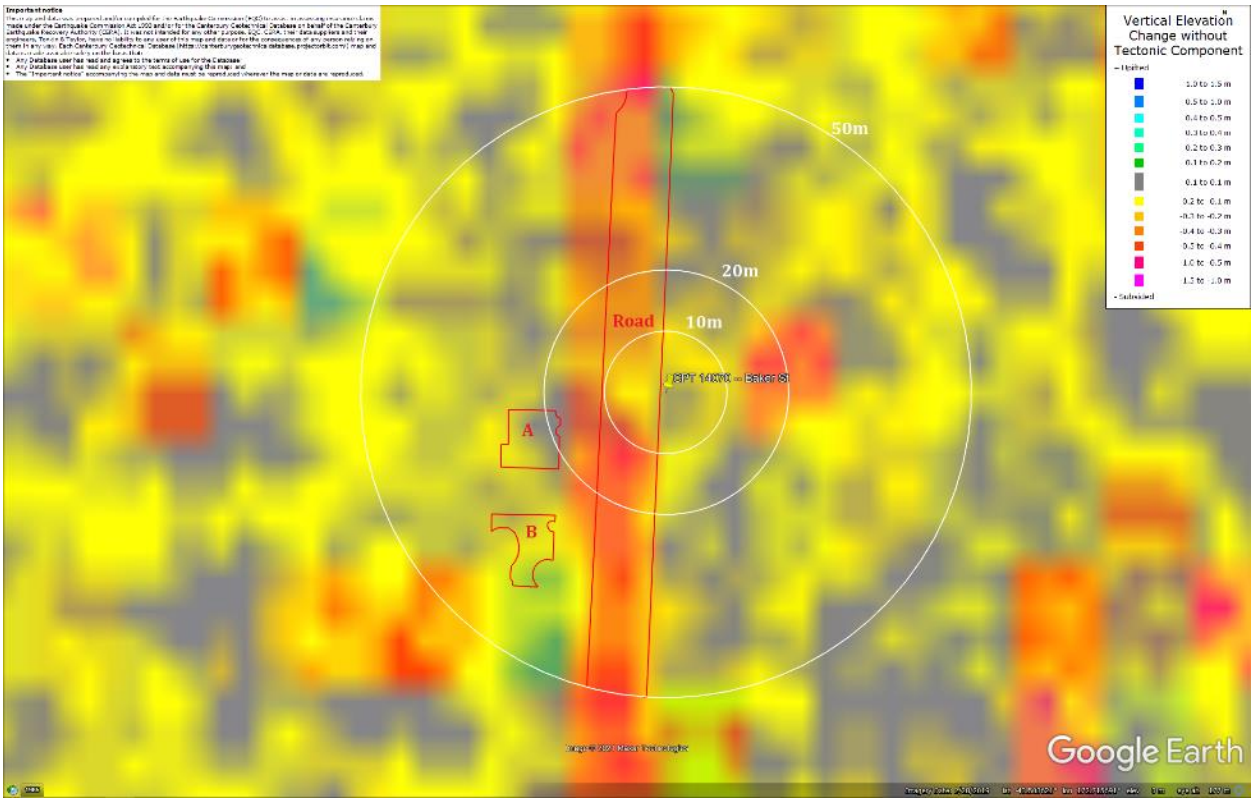

Figure 36: Ground surface subsidence without tectonic component for Sep 2010 Earthquake according to the LiDAR DEM.

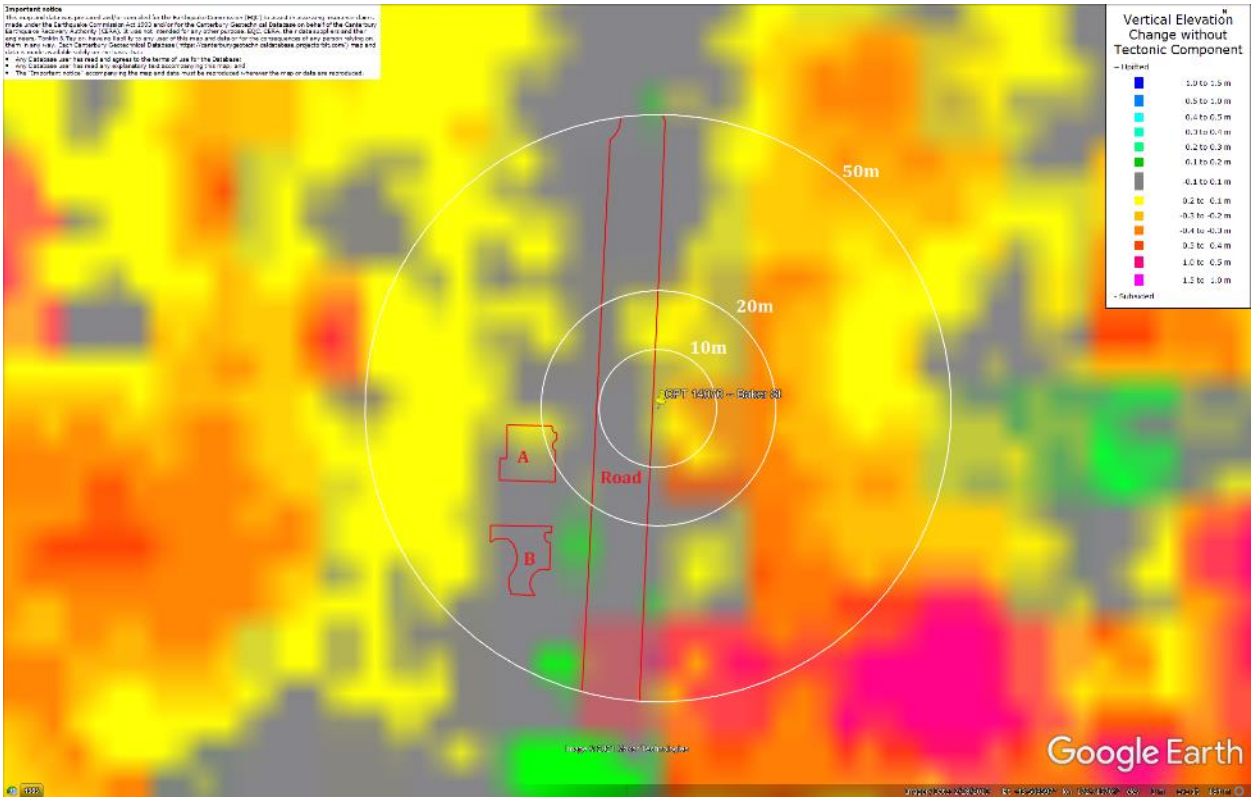

Figure 37: Ground surface subsidence without tectonic component for Feb 2011 Earthquake according to the LiDAR DEM.

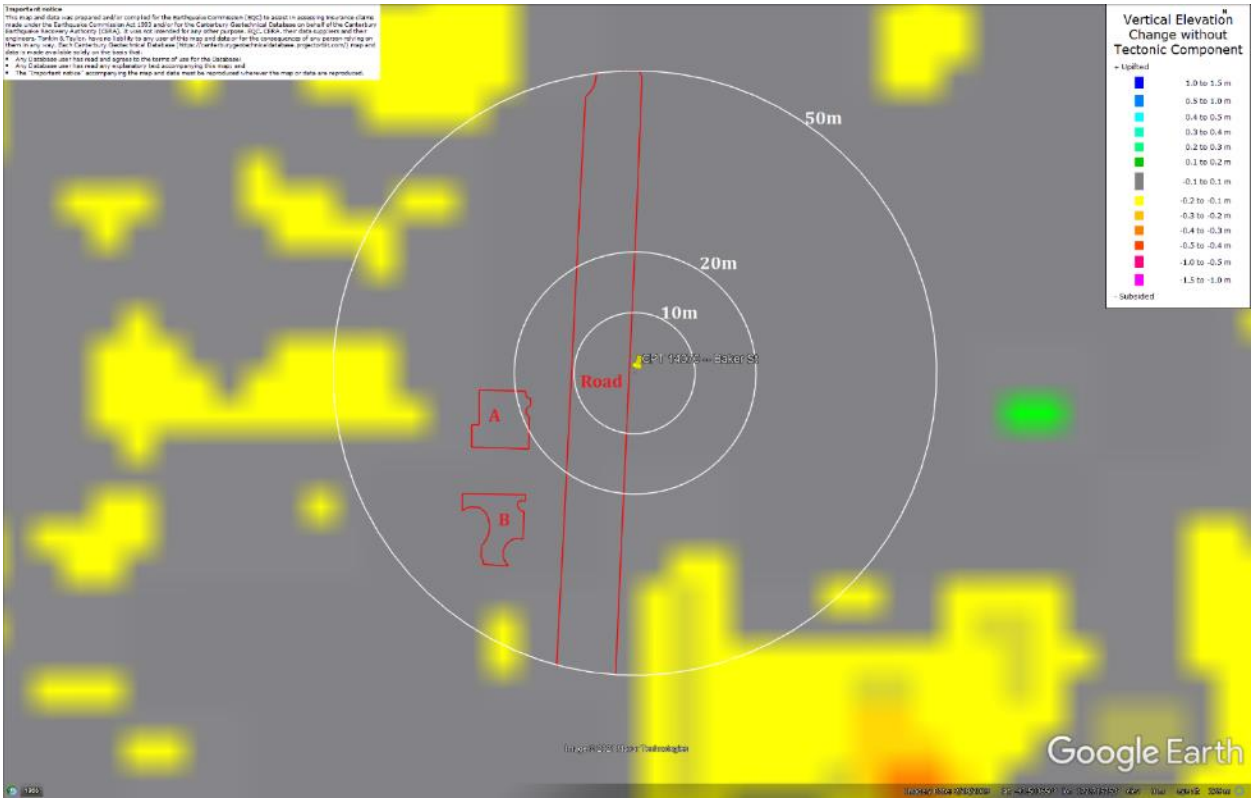

Figure 38: Ground surface subsidence without tectonic component for June 2011 Earthquake according to the LiDAR DEM.

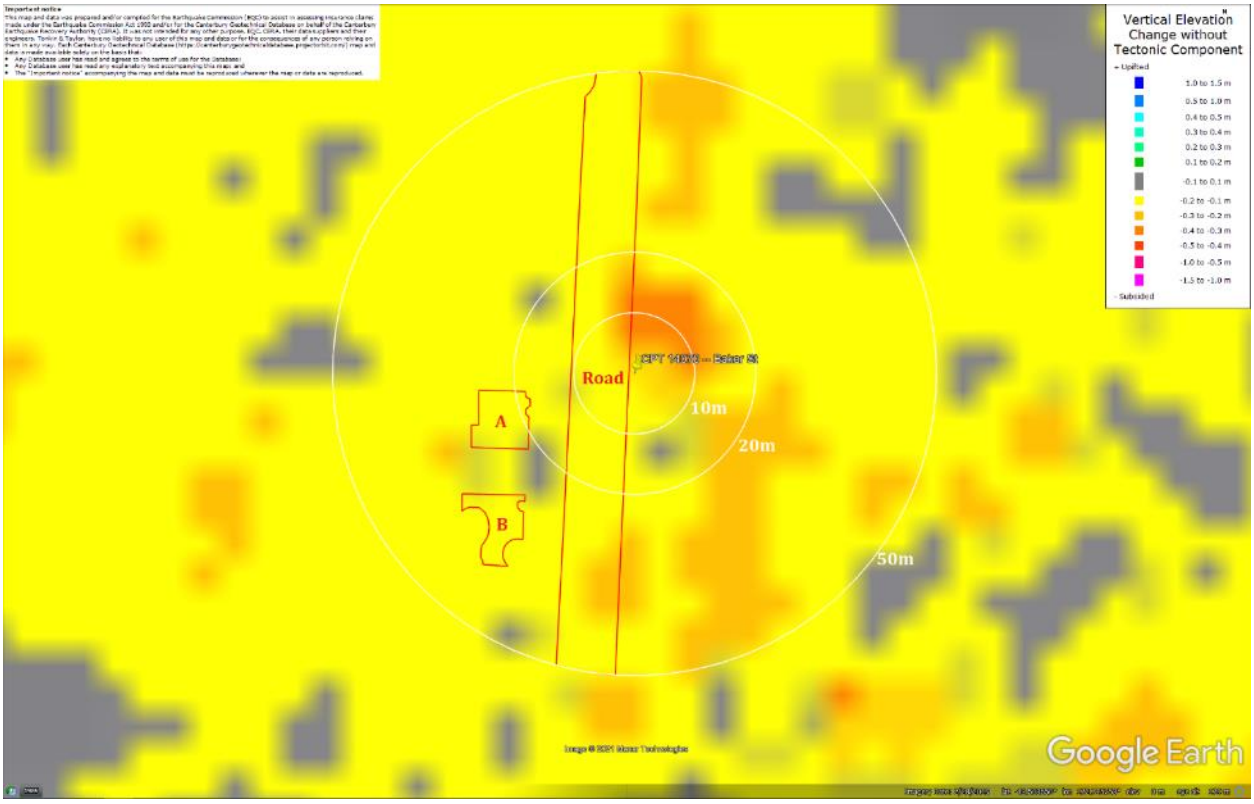

Figure 39: Ground surface subsidence without tectonic component for Dec 2011 Earthquake according to the LiDAR DEM.

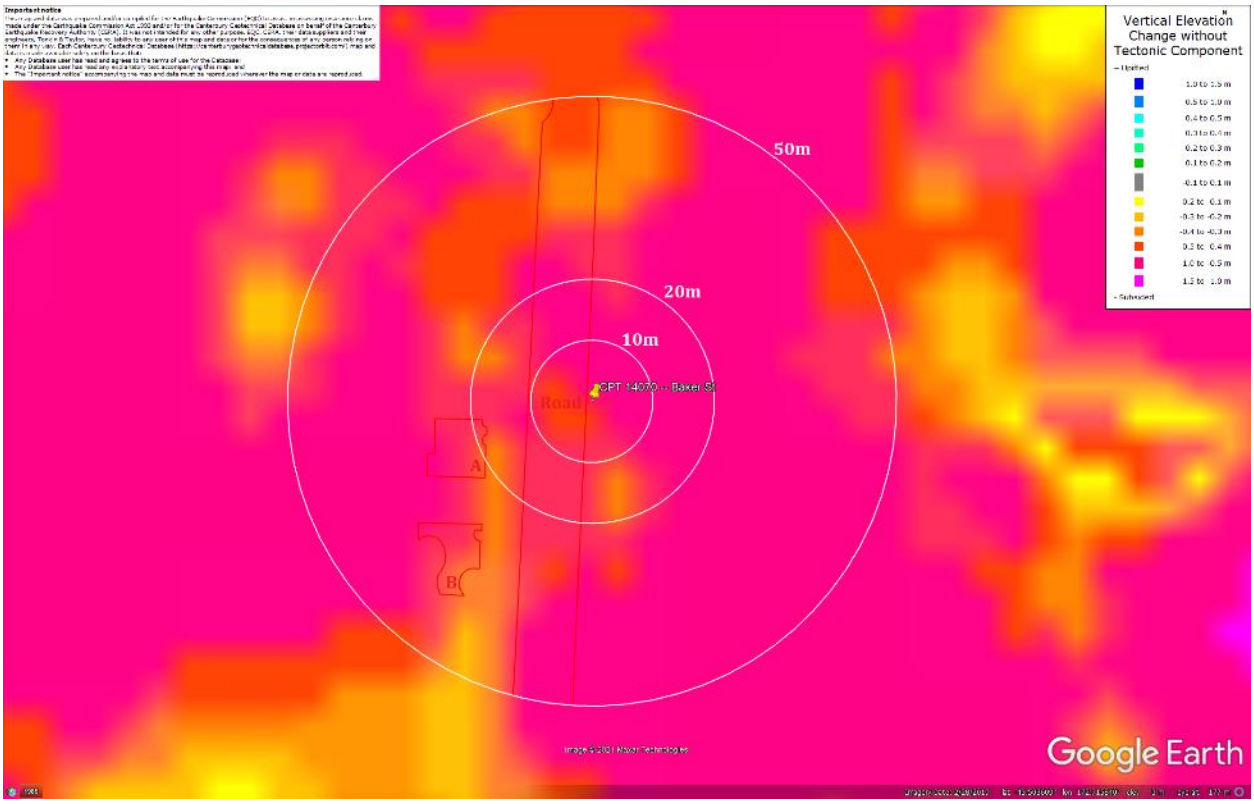

Figure 40: Ground surface subsidence without tectonic component for Canterbury Earthquake Sequence according to the LiDAR DEM.

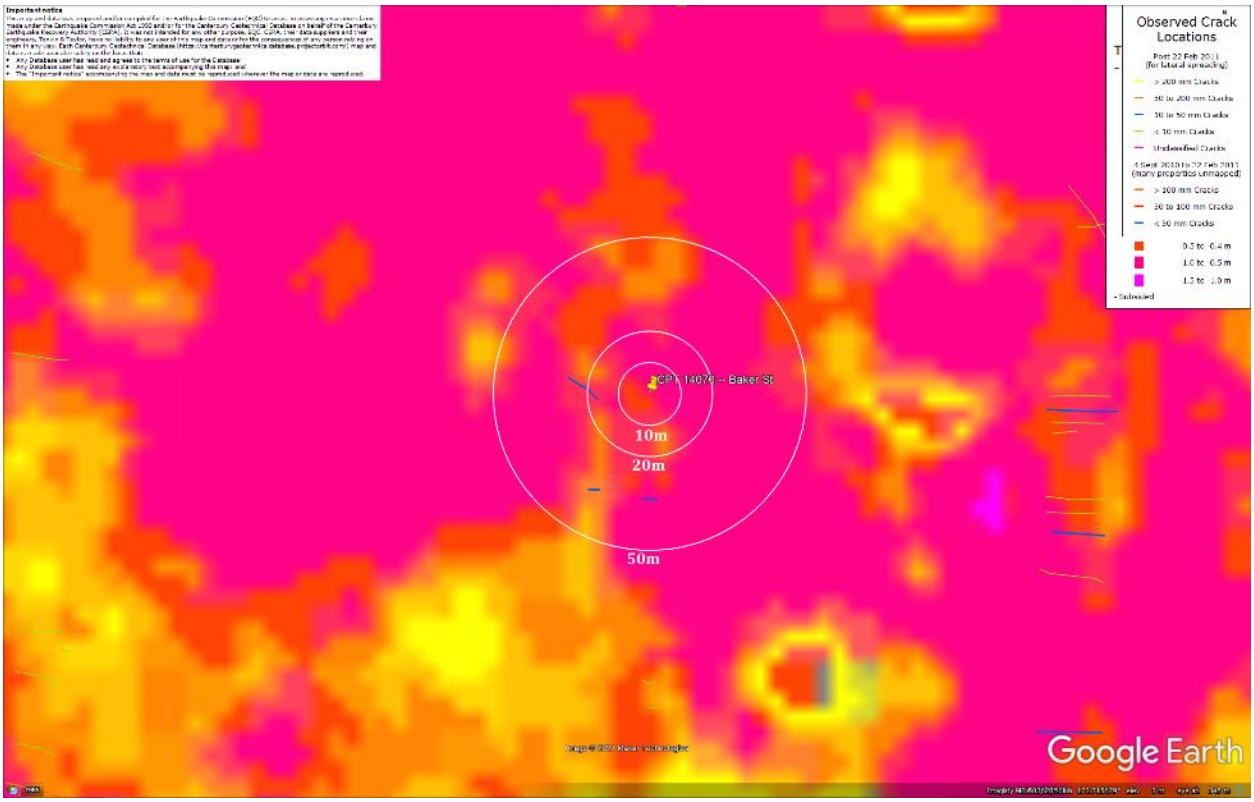

Figure 41: No lateral spreading for Canterbury Earthquake Sequence.

Figure 42: Vertical tectonic movements for Sep 2010 Earthquake.

Figure 43: Vertical tectonic movements for Feb 2011 Earthquake.

Figure 44: Vertical tectonic movements for June 2011 Earthquake.

Figure 45: Vertical tectonic movements for Dec 2011 Earthquake.

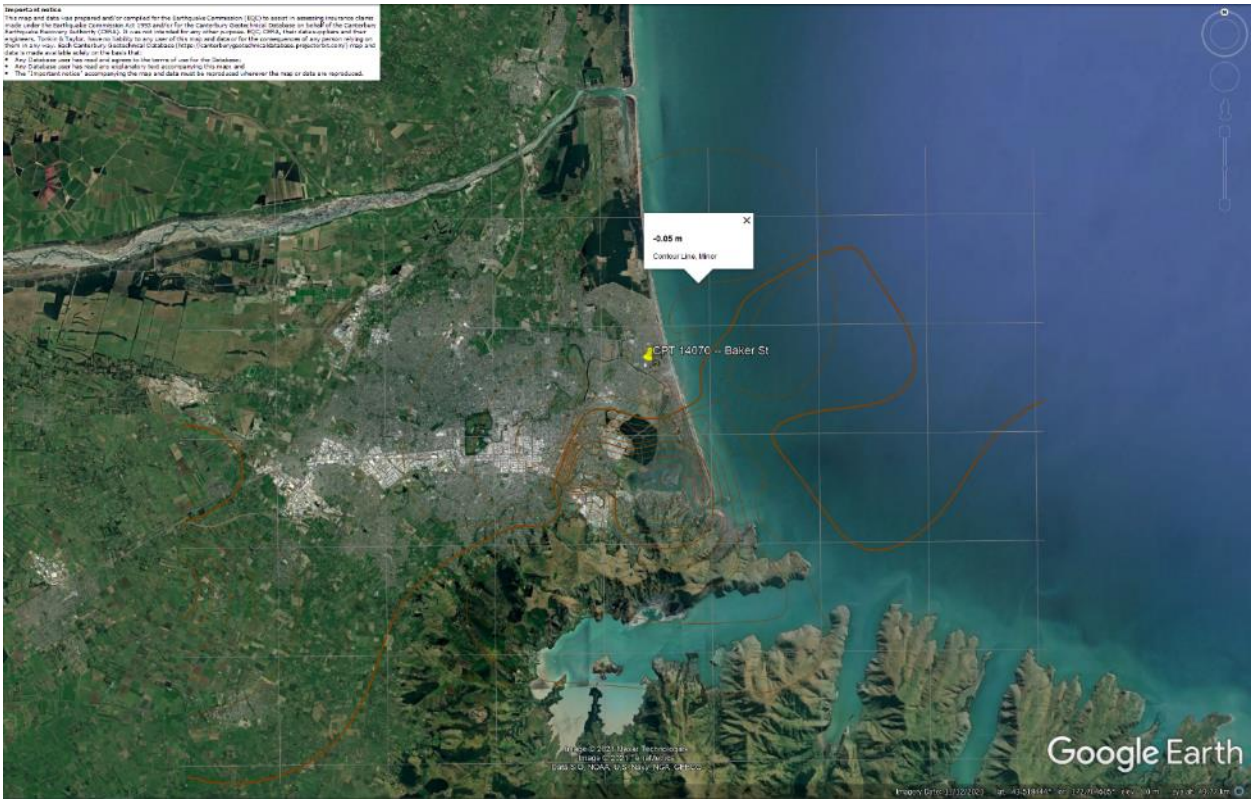

Figure 46: Vertical tectonic movements for Canterbury Earthquake Sequence.

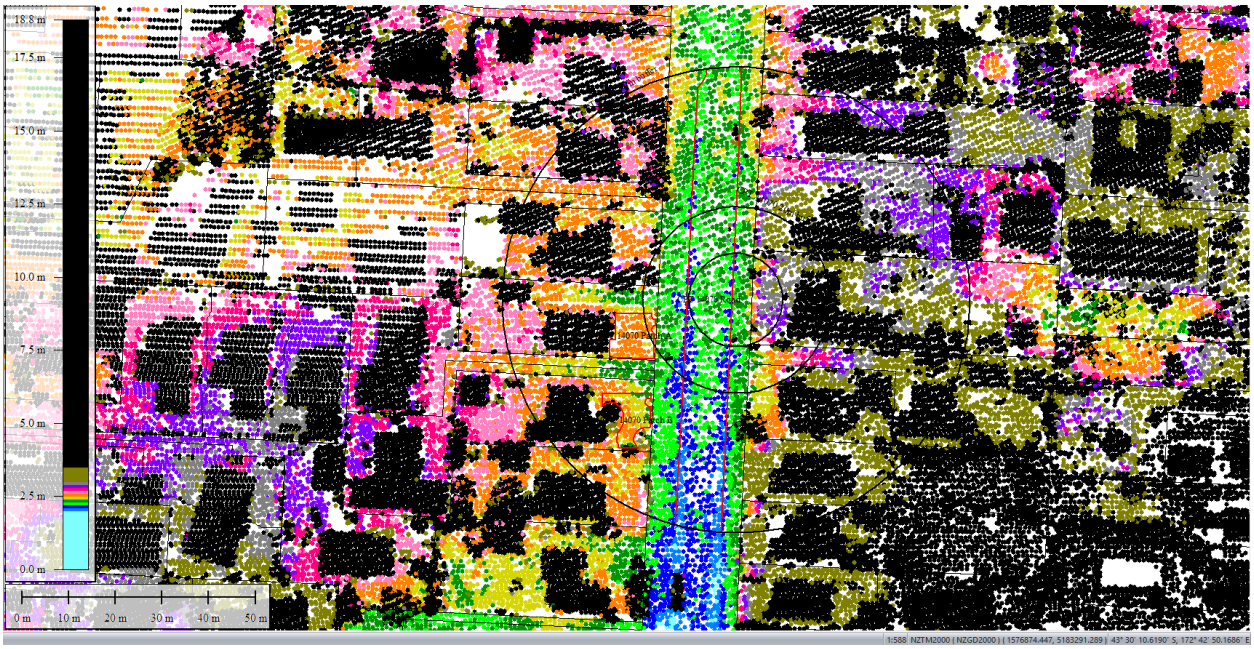

Figure 47: Sep 5, 2010 LiDAR survey.

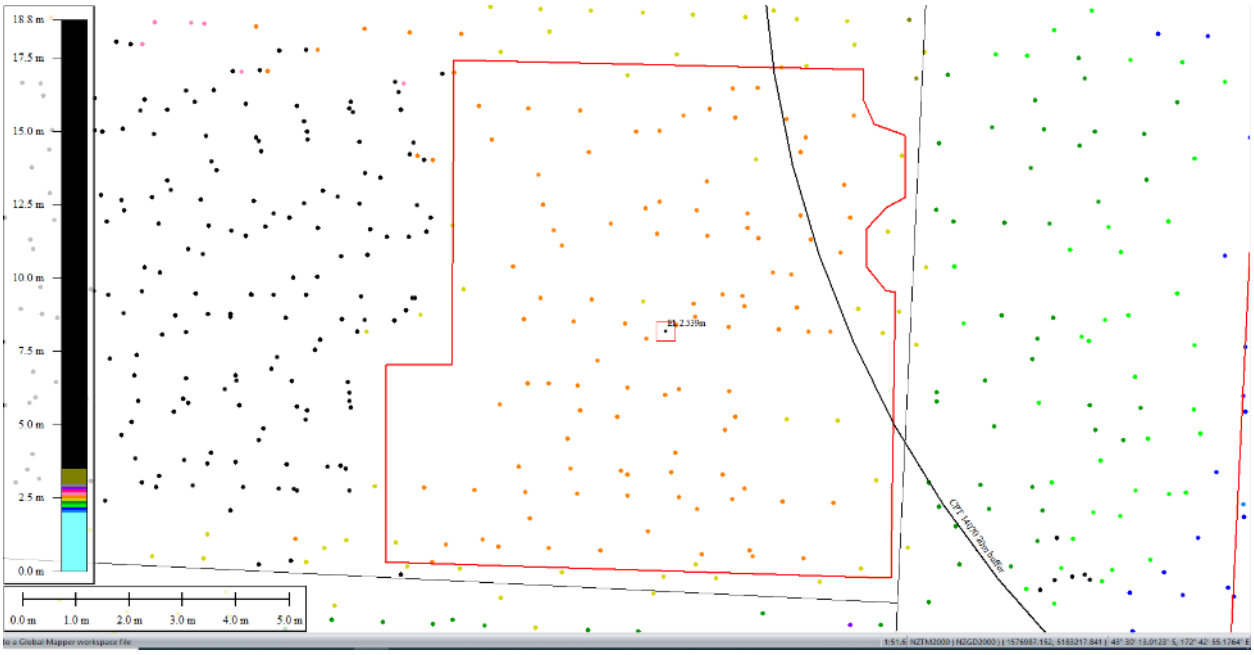

Figure 48: Ground surface elevation averaged over 50-m buffer for Patch A for Sep 5, 2010 LiDAR survey.

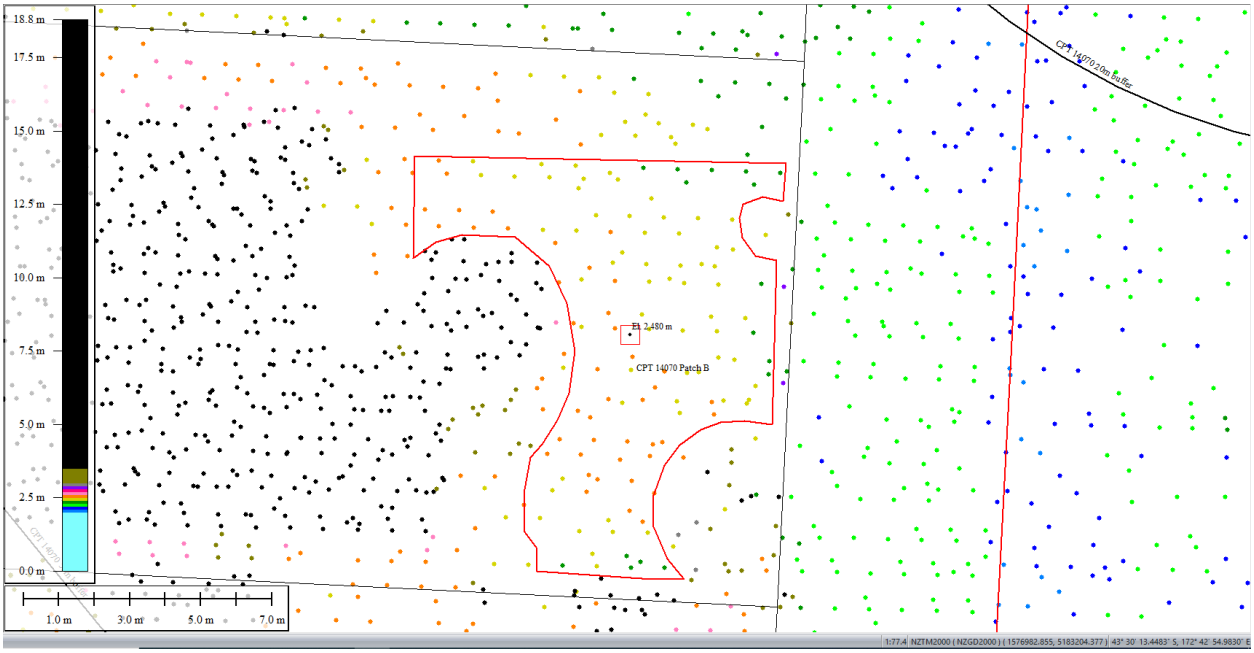

Figure 49: Ground surface elevation averaged over 50-m buffer for Patch B for Sep 5, 2010 LiDAR survey.

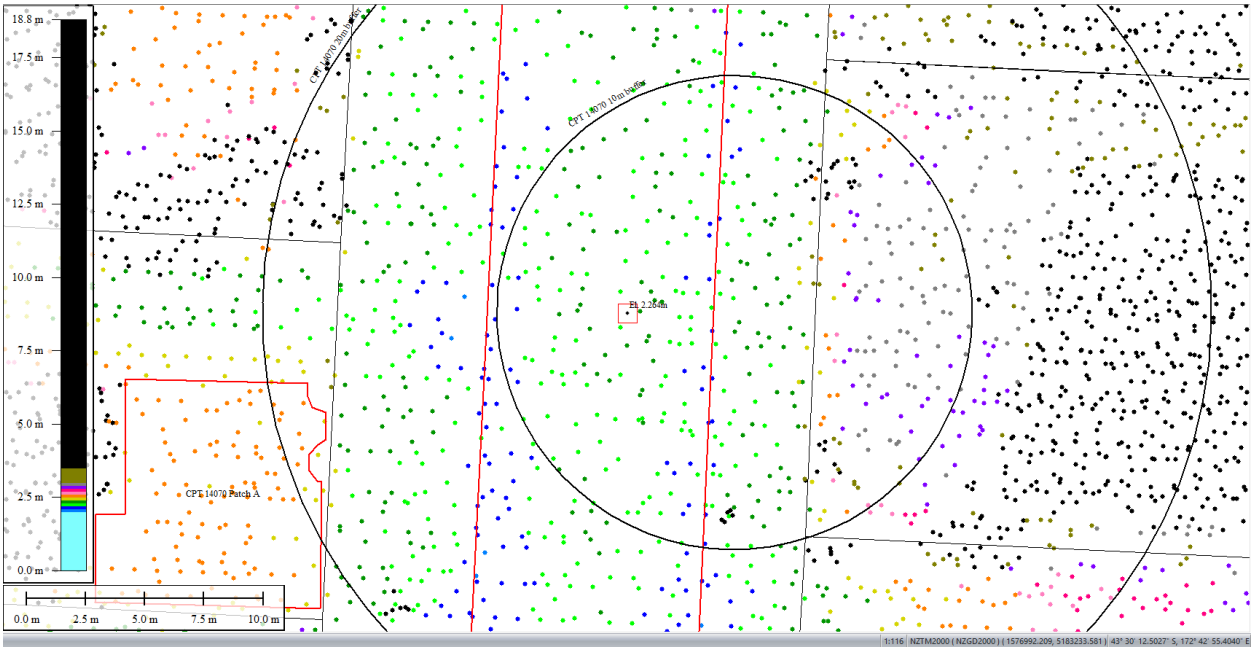

Figure 50: Ground surface elevation averaged over 10-m buffer for Road for Sep 5, 2010 LiDAR survey.

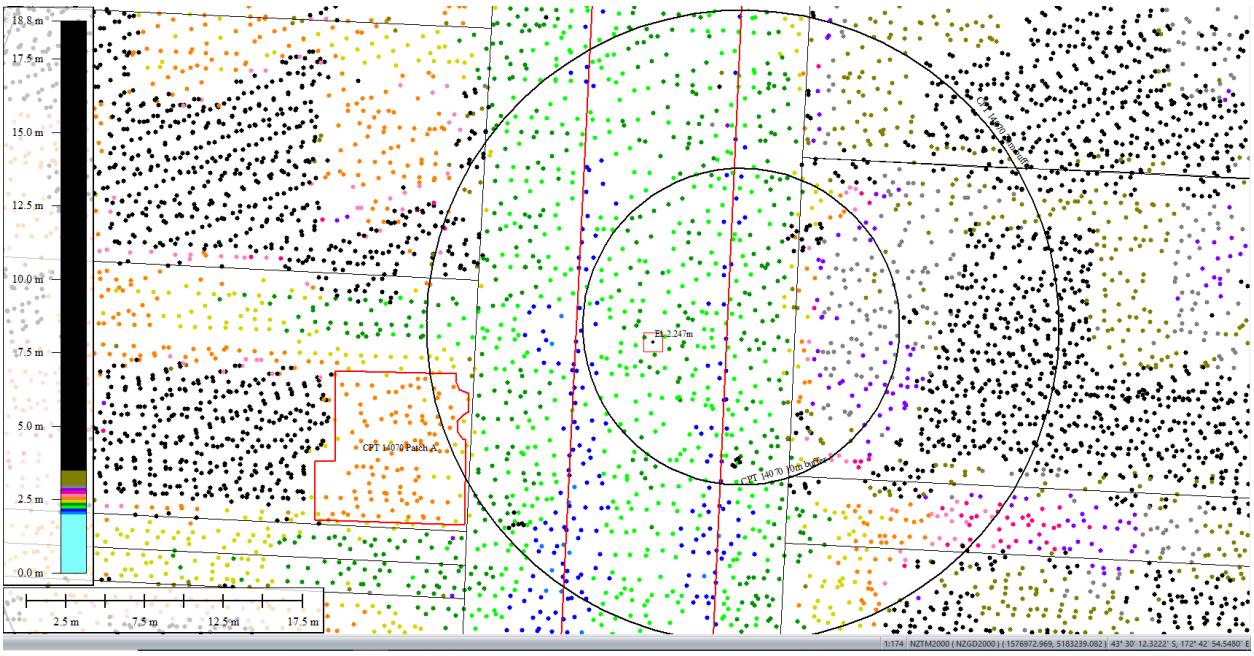

Figure 51: Ground surface elevation averaged over 20-m buffer for Road for Sep 5, 2010 LiDAR survey.

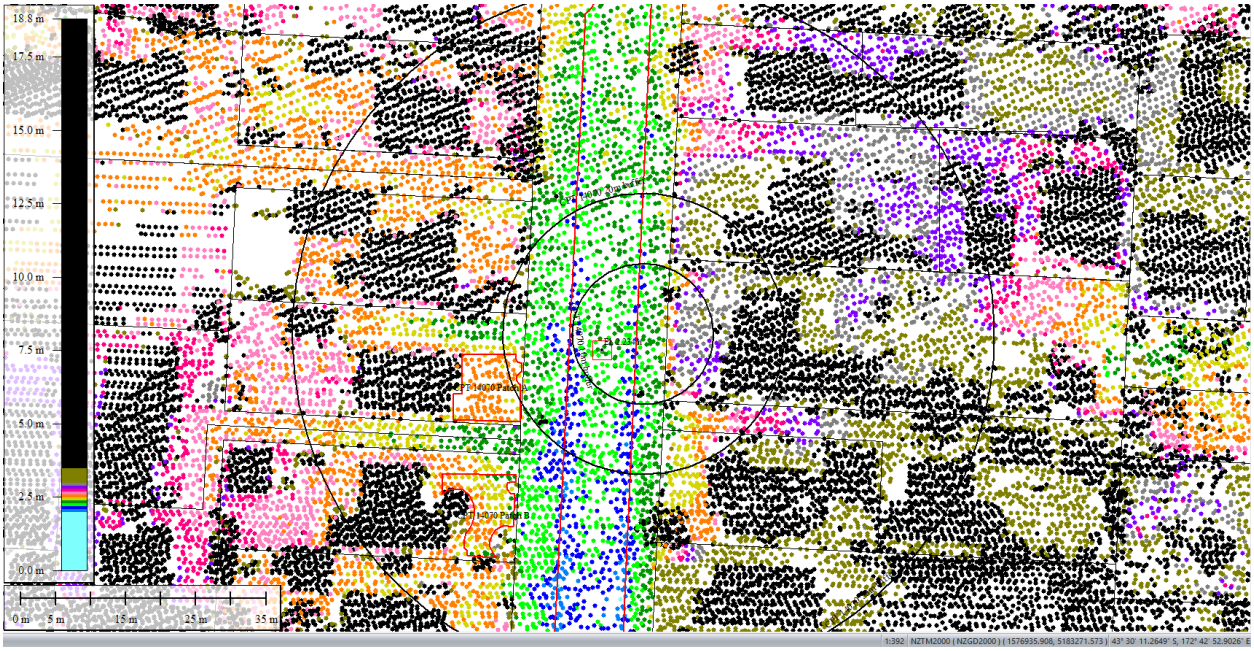

Figure 52: Ground surface elevation averaged over 50-m buffer for Road for Sep 5, 2010 LiDAR survey.

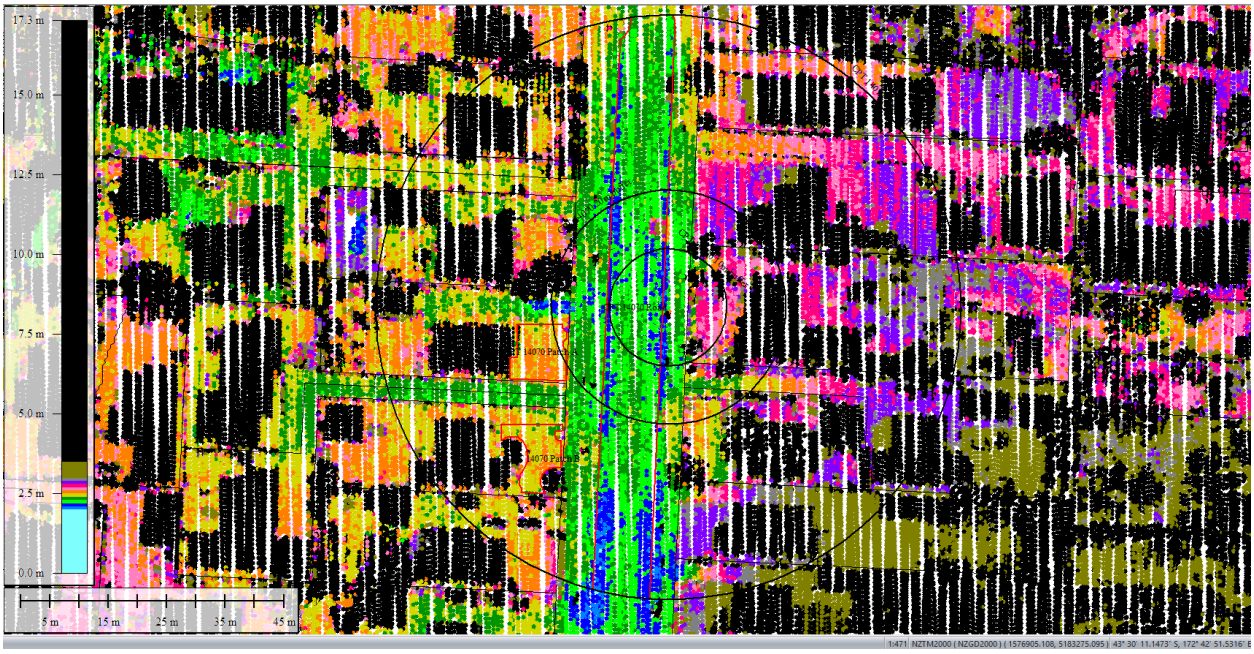

Figure 53: Mar 2011 LiDAR survey.

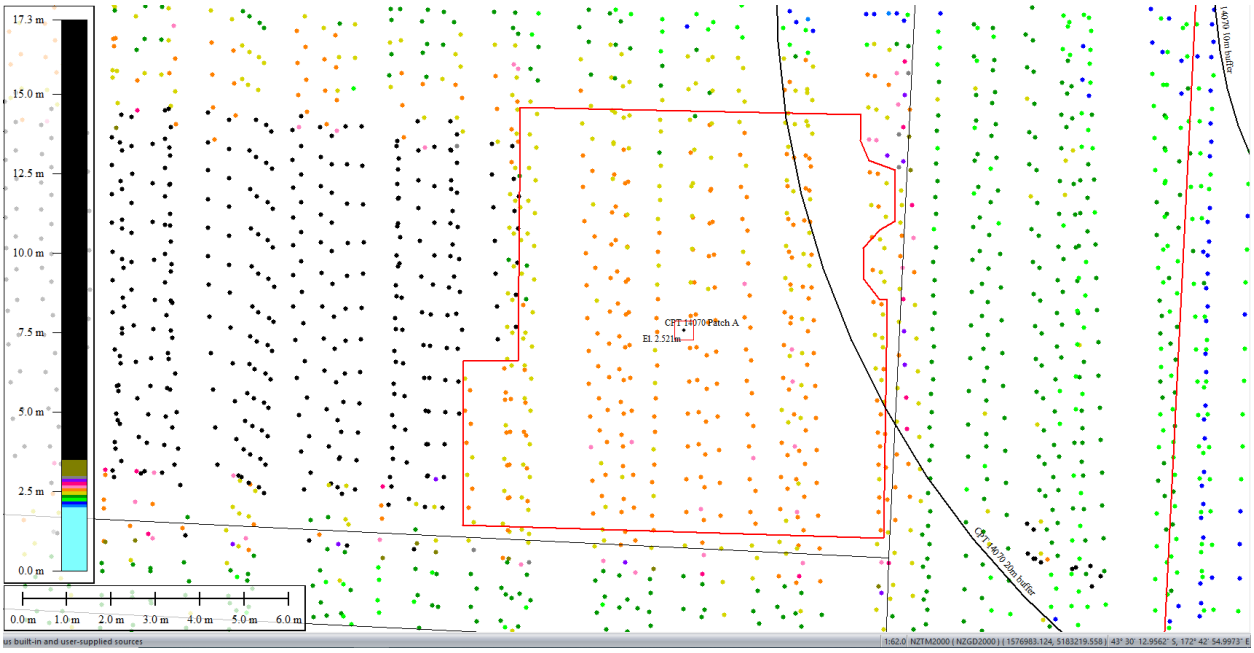

Figure 54: Ground surface elevation averaged over 50-m buffer for Patch A for Mar 2011 LiDAR survey.

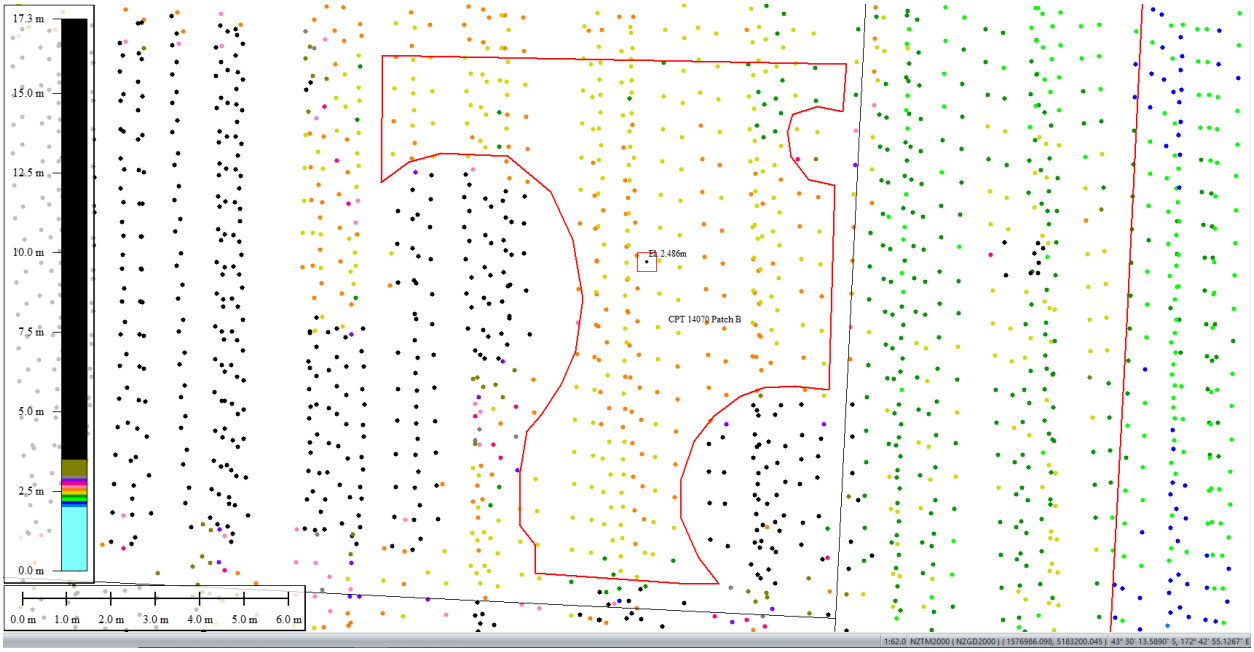

Figure 55: Ground surface elevation averaged over 50-m buffer for Patch B for Mar 2011 LiDAR survey.

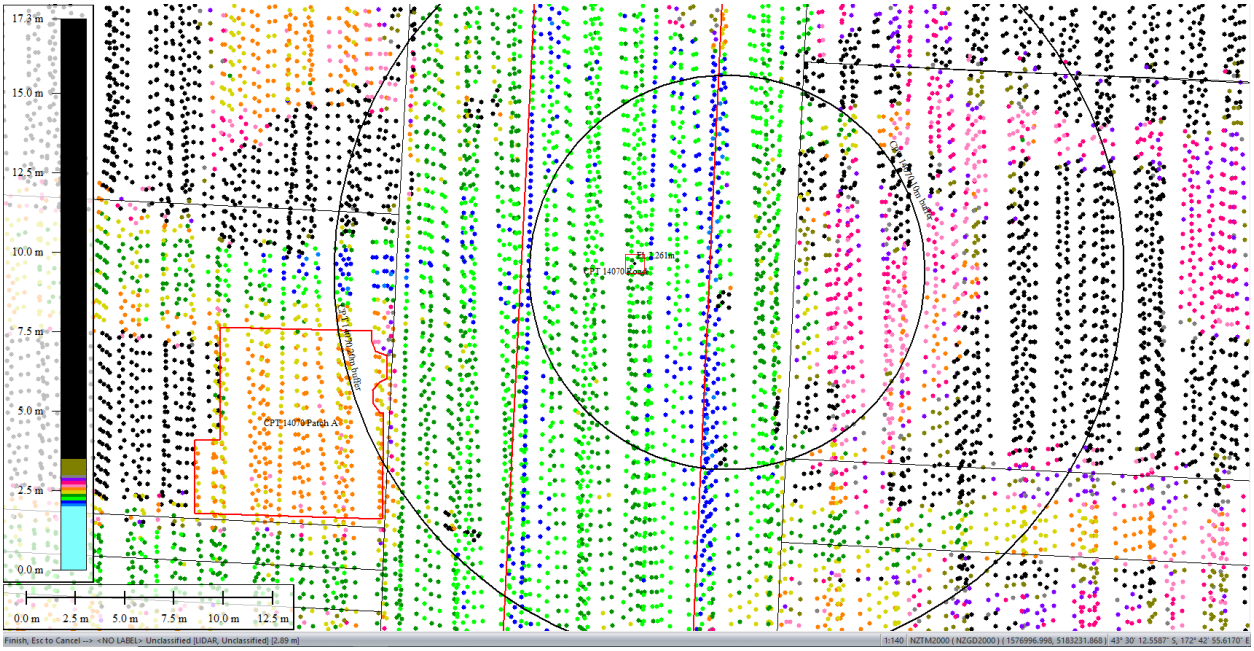

Figure 56: Ground surface elevation averaged over 10-m buffer for Road for Mar 2011 LiDAR survey.

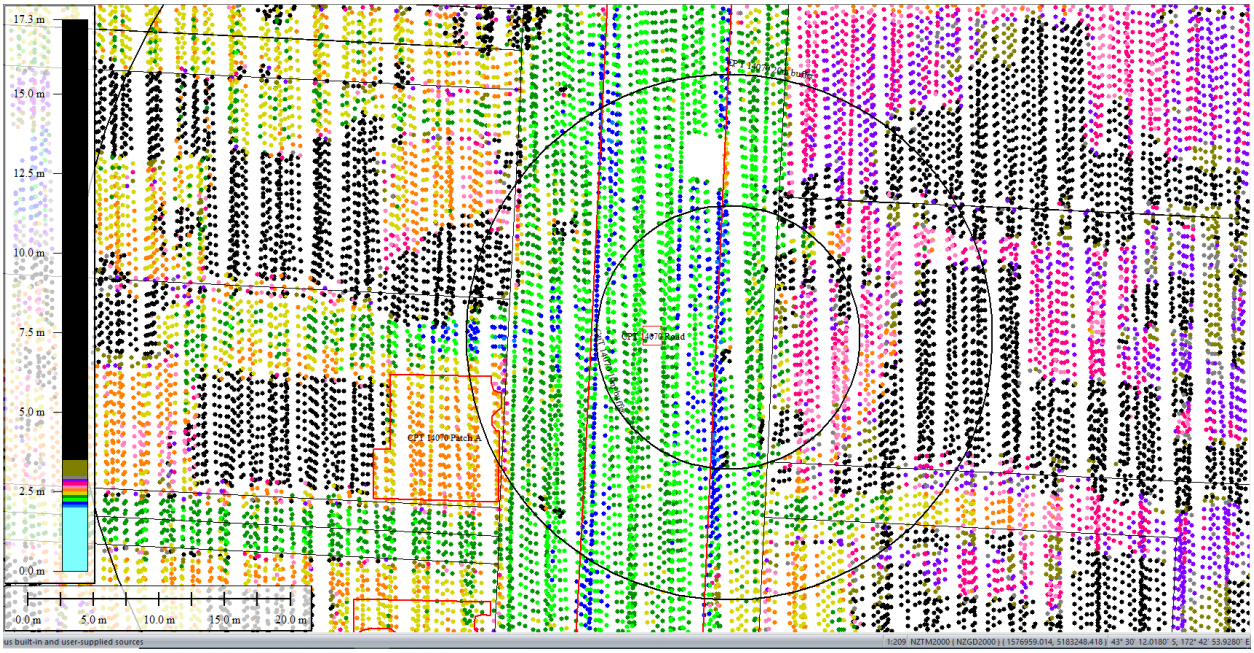

Figure 57: Ground surface elevation averaged over 20-m buffer for Road for Mar 2011 LiDAR survey (el. 2.263m).

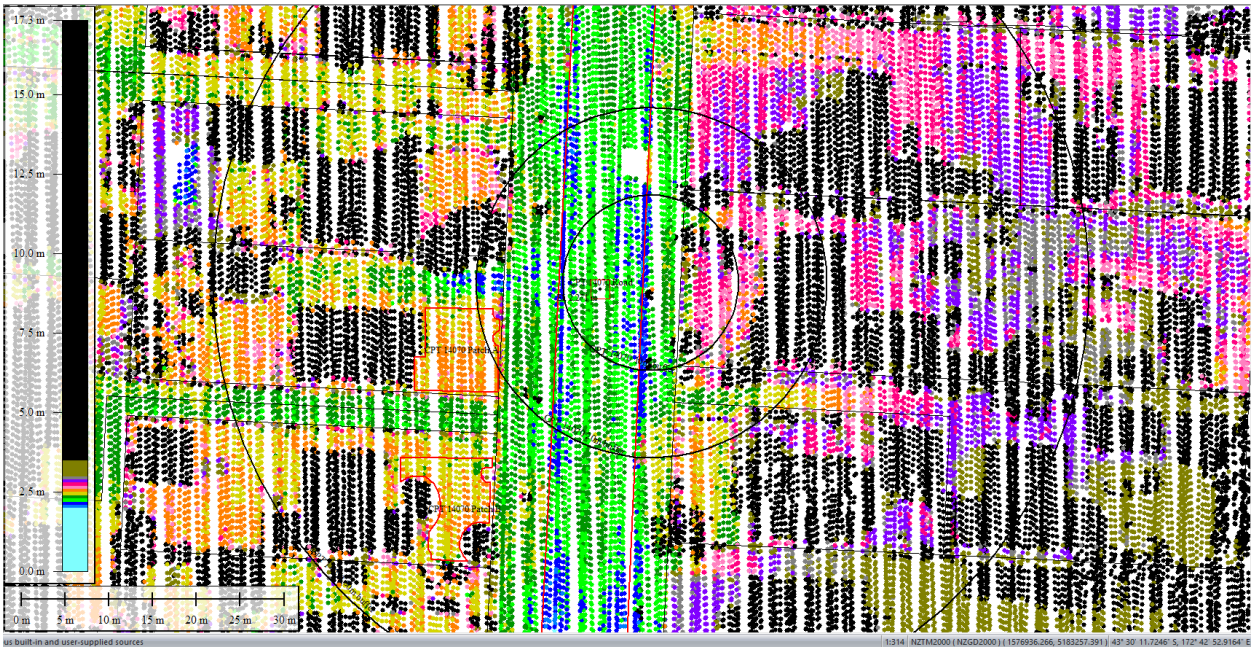

Figure 58: Ground surface elevation averaged over 50-m buffer for Road for Mar 2011 LiDAR survey.

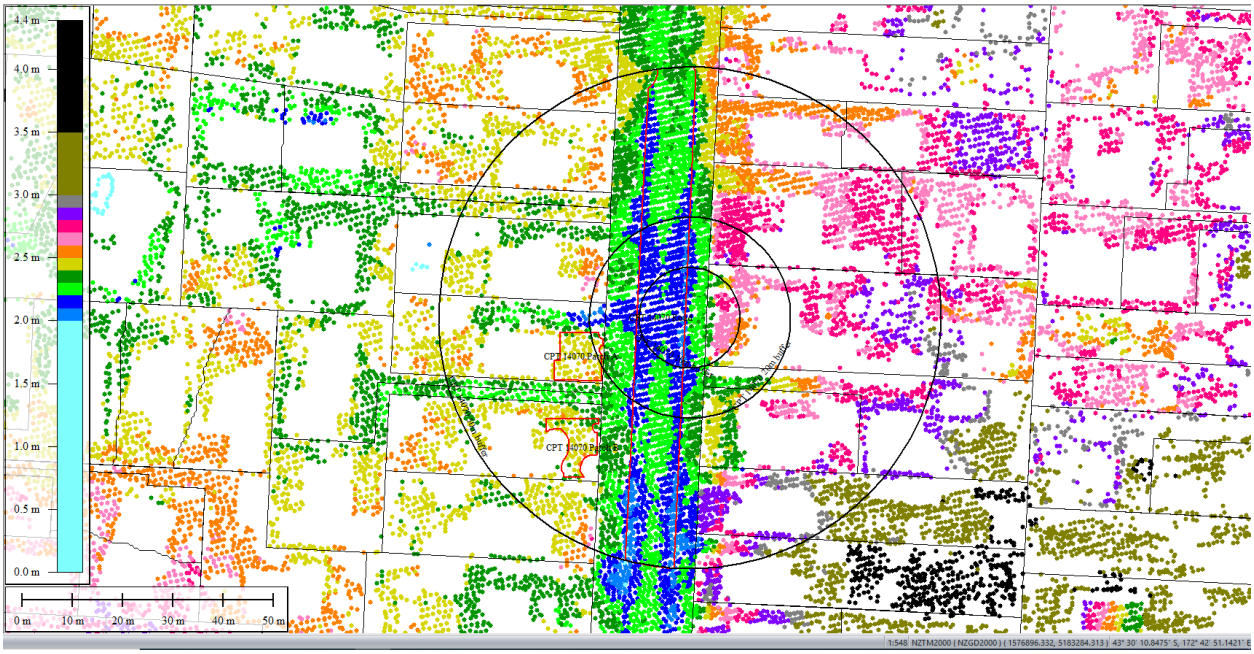

Figure 59: May 2011 LiDAR survey.

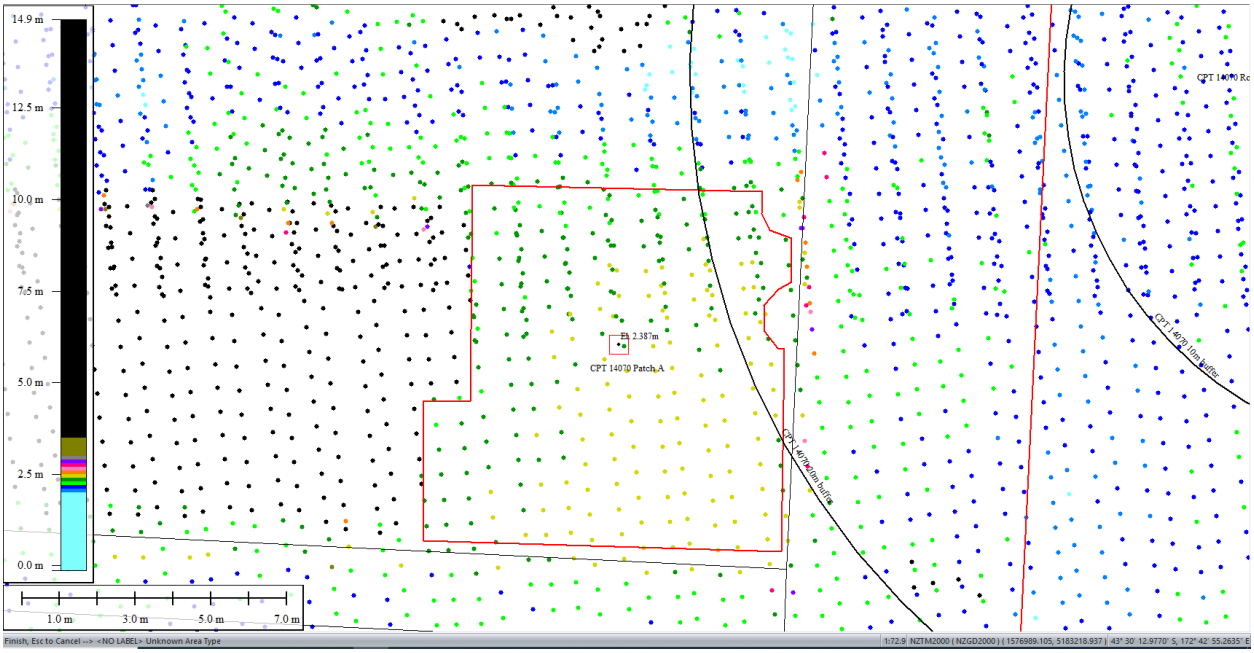

Figure 60: Ground surface elevation averaged over 50-m buffer for Patch A for May 2011 LiDAR survey.

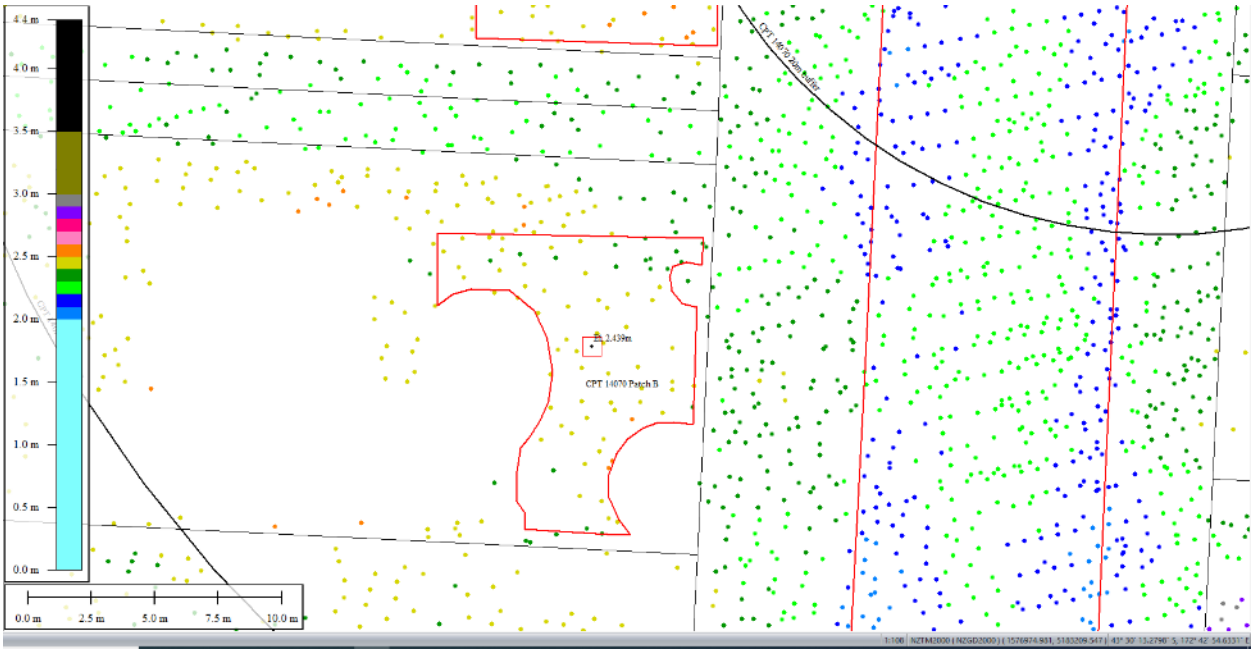

Figure 61: Ground surface elevation averaged over 50-m buffer for Patch B for May 2011 LiDAR survey.

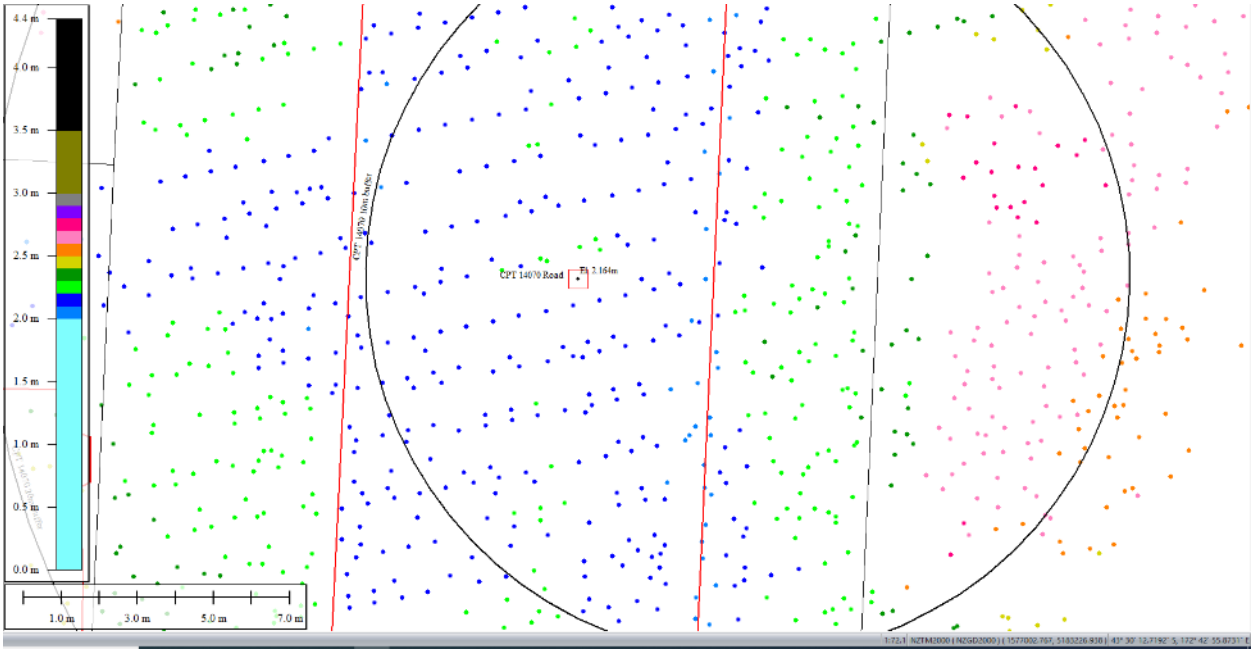

Figure 62: Ground surface elevation averaged over 10-m buffer for Road for May 2011 LiDAR survey.

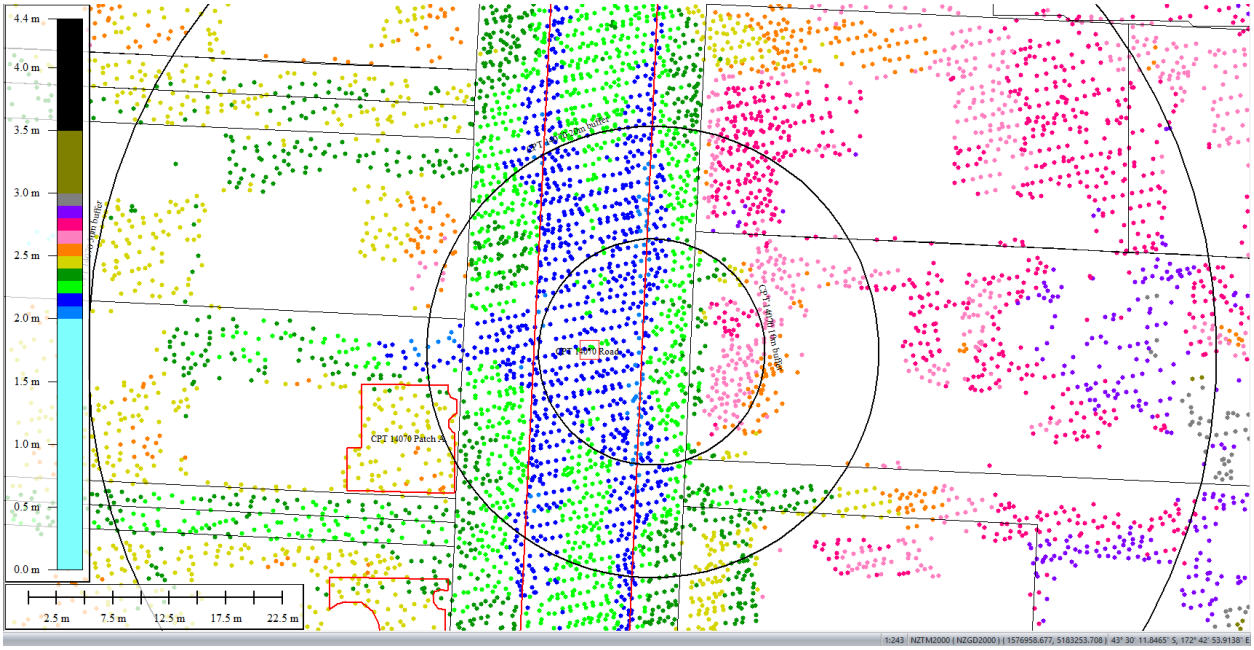

Figure 63: Ground surface elevation averaged over 20-m buffer for Road for May 2011 LiDAR survey (el. 2.175m).

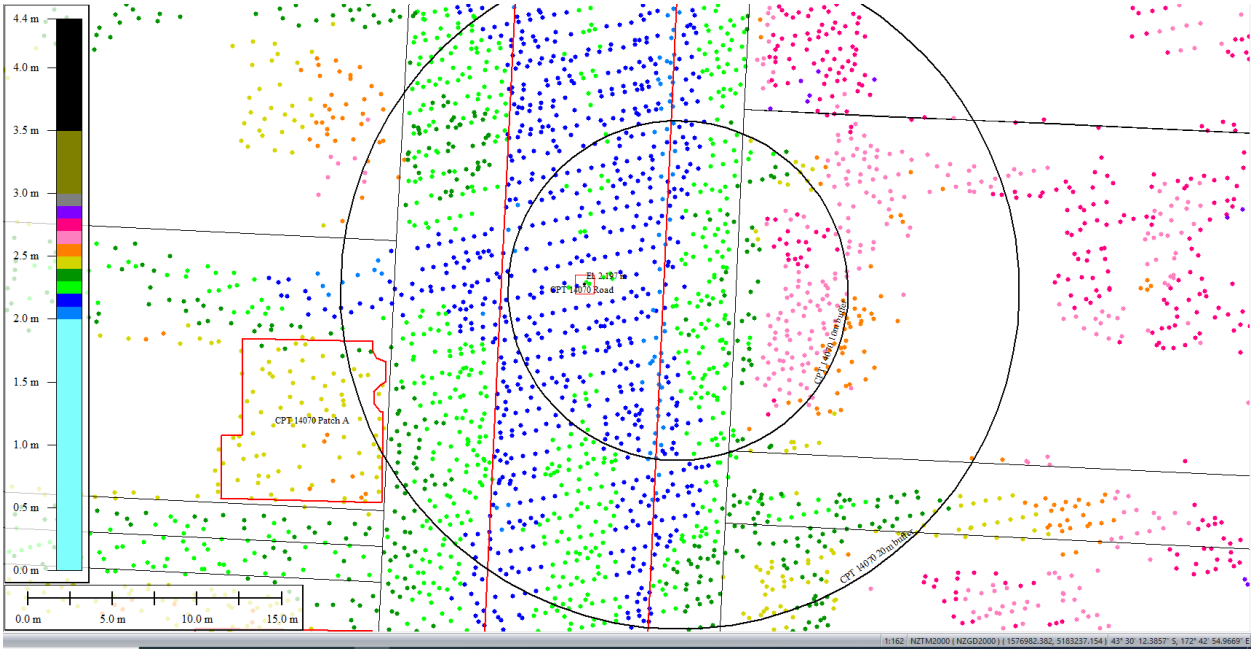

Figure 64: Ground surface elevation averaged over 50-m buffer for Road for May 2011 LiDAR survey.

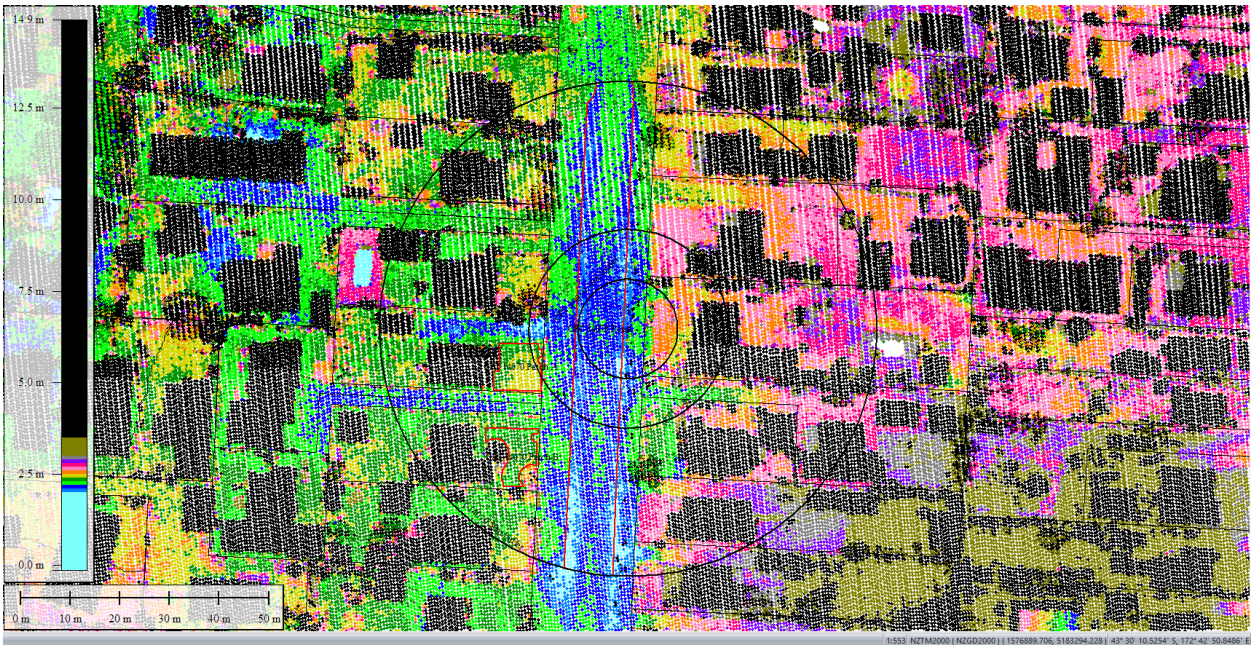

Figure 65: Sep 2011 LiDAR survey.

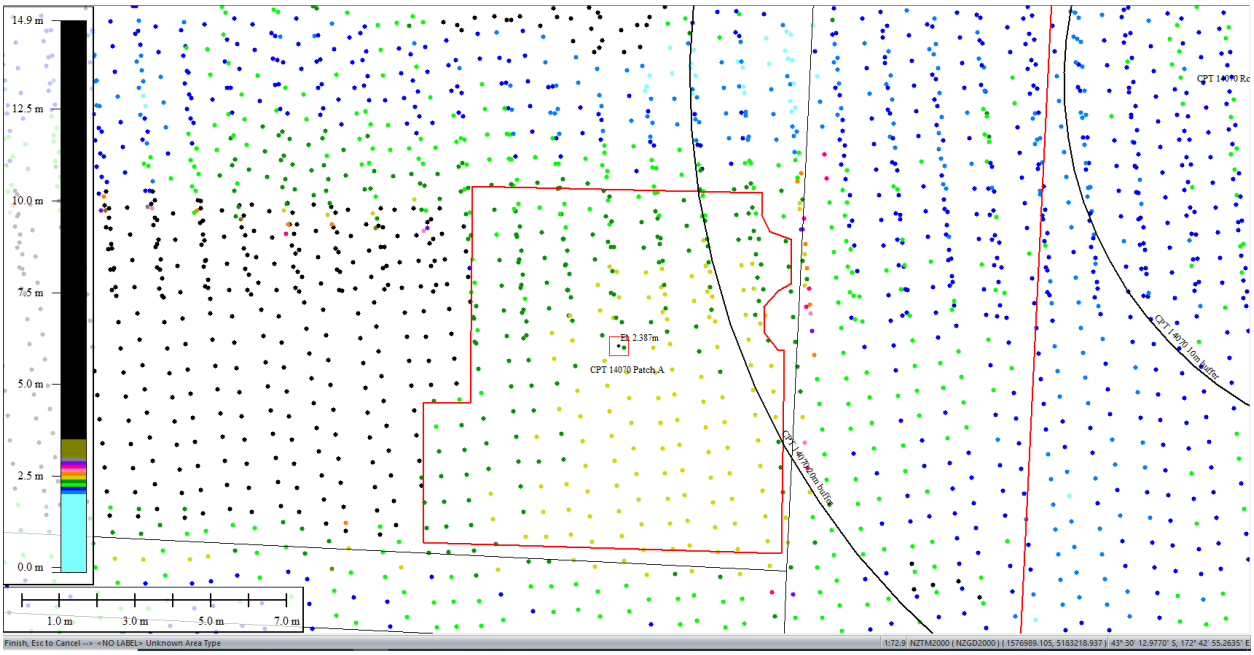

Figure 66: Ground surface elevation averaged over 50-m buffer for Patch A for Sep 2011 LiDAR survey.

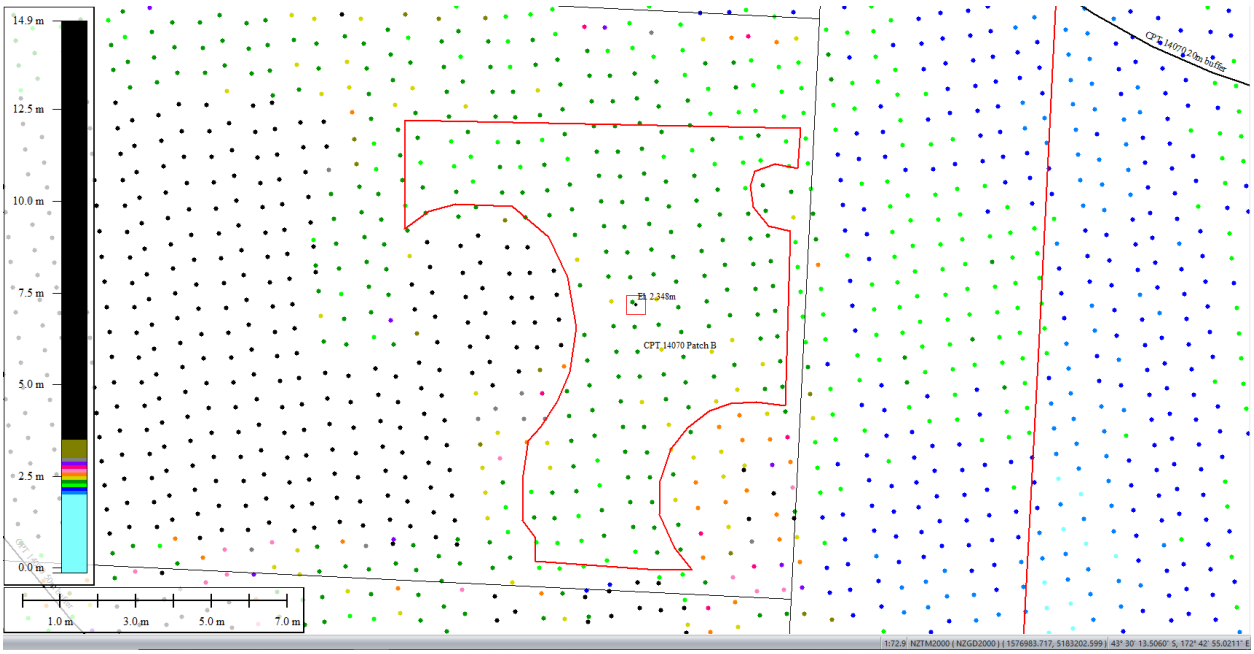

Figure 67: Ground surface elevation averaged over 50-m buffer for Patch B for Sep 2011 LiDAR survey.

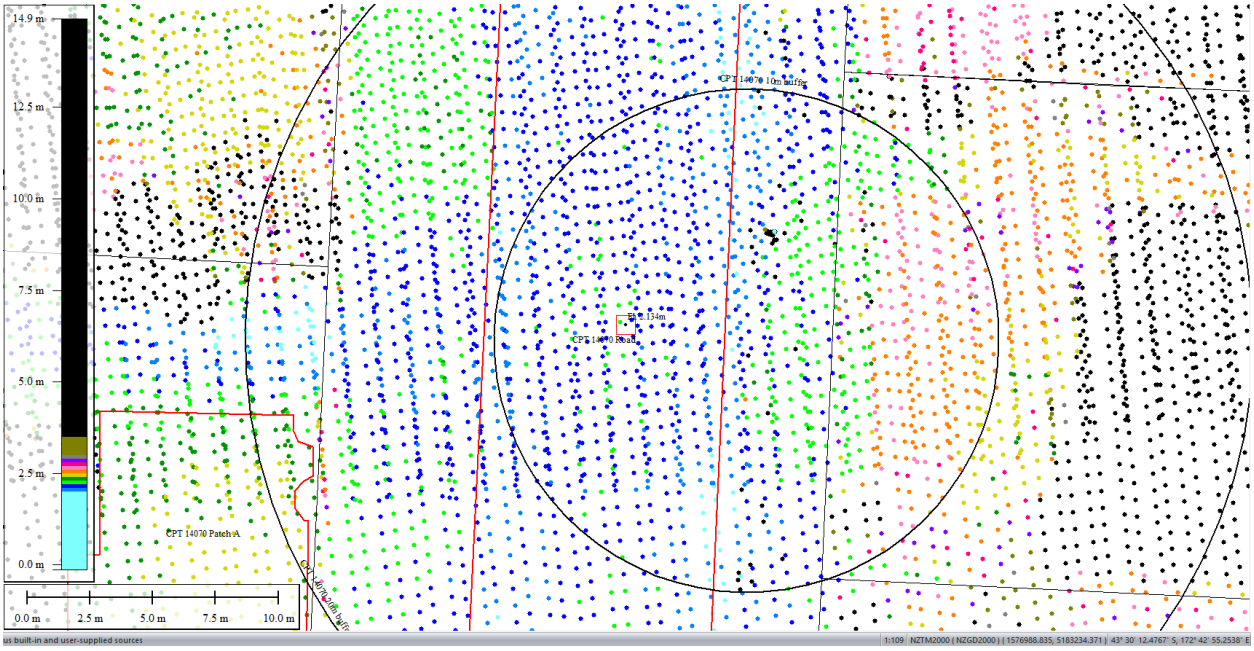

Figure 68: Ground surface elevation averaged over 10-m buffer for Road for Sep 2011 LiDAR survey.

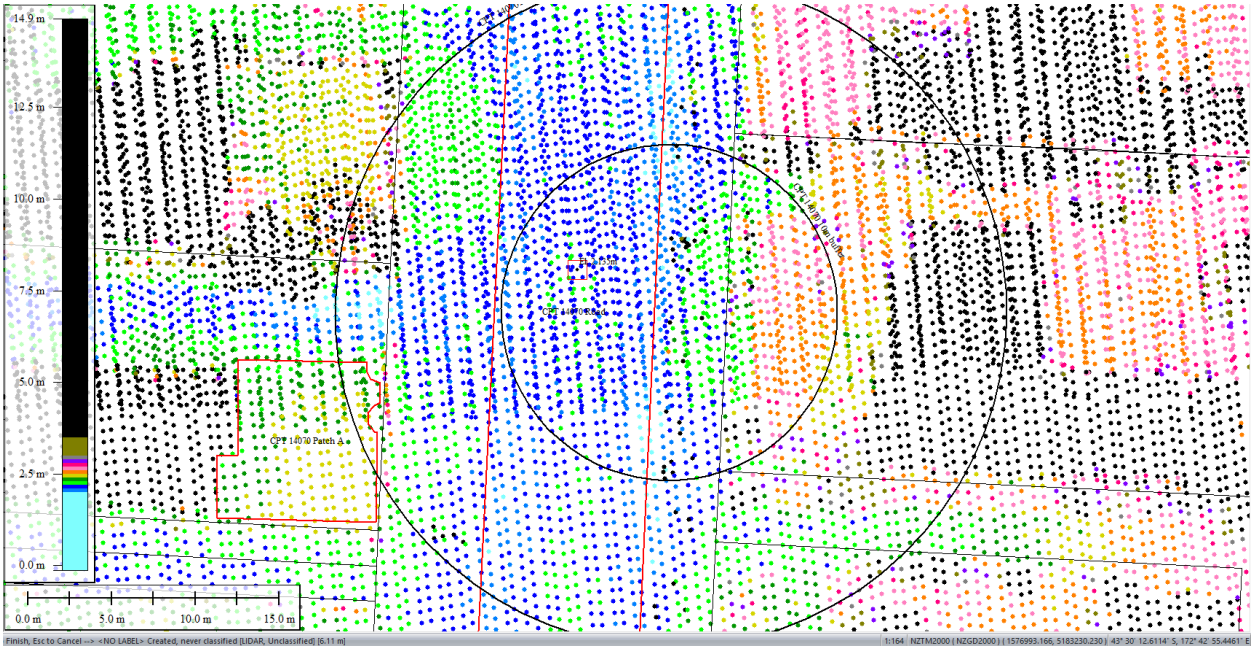

Figure 69: Ground surface elevation averaged over 20-m buffer for Road for Sep 2011 LiDAR survey.

Figure 70: Ground surface elevation averaged over 50-m buffer for Road for Sep 2011 LiDAR survey.

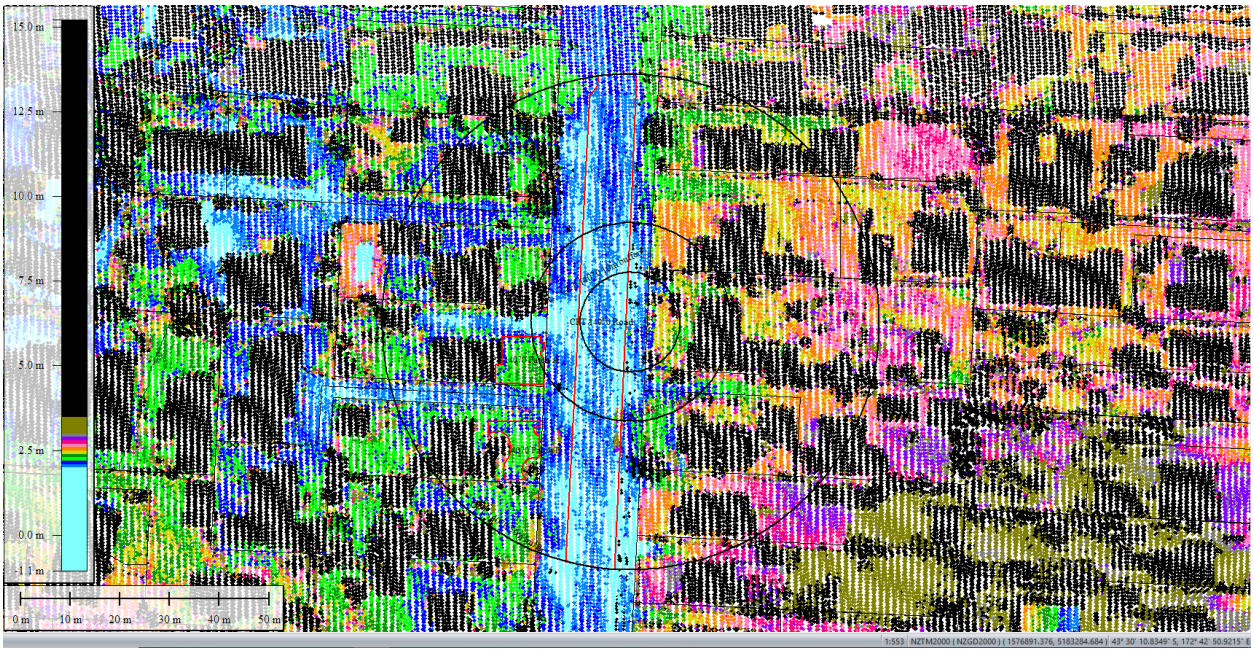

Figure 71: Feb 2012 LiDAR survey.

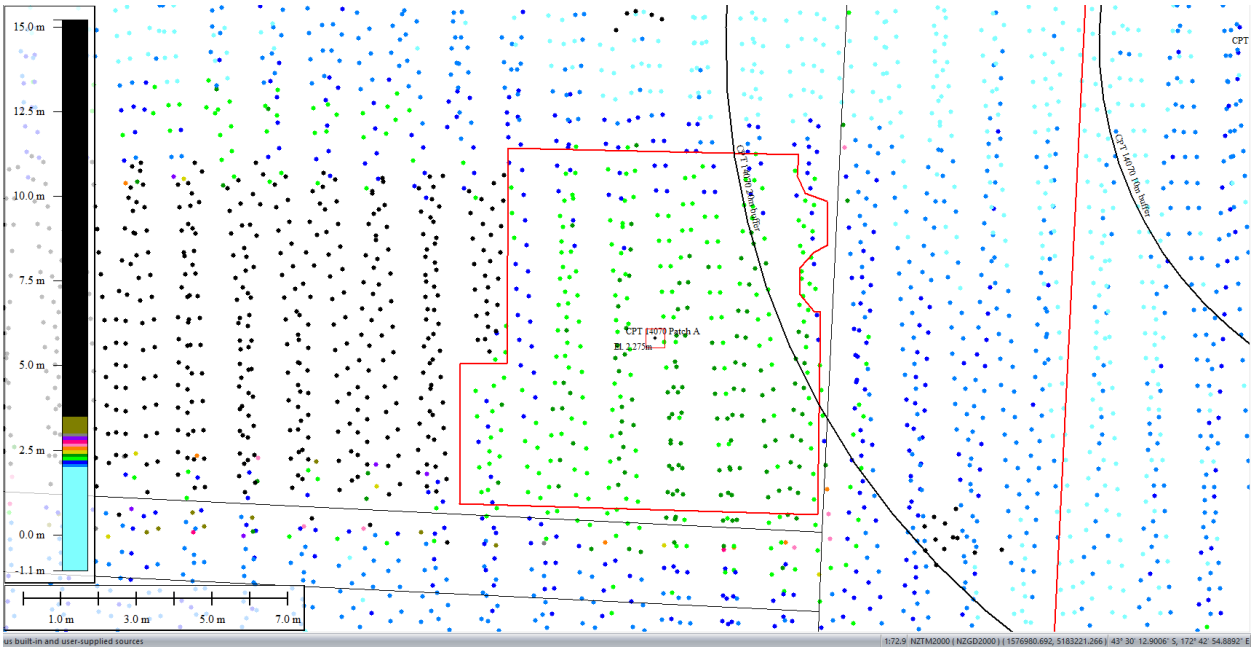

Figure 72: Ground surface elevation averaged over 50-m buffer for Patch A for Feb 2012 LiDAR survey.

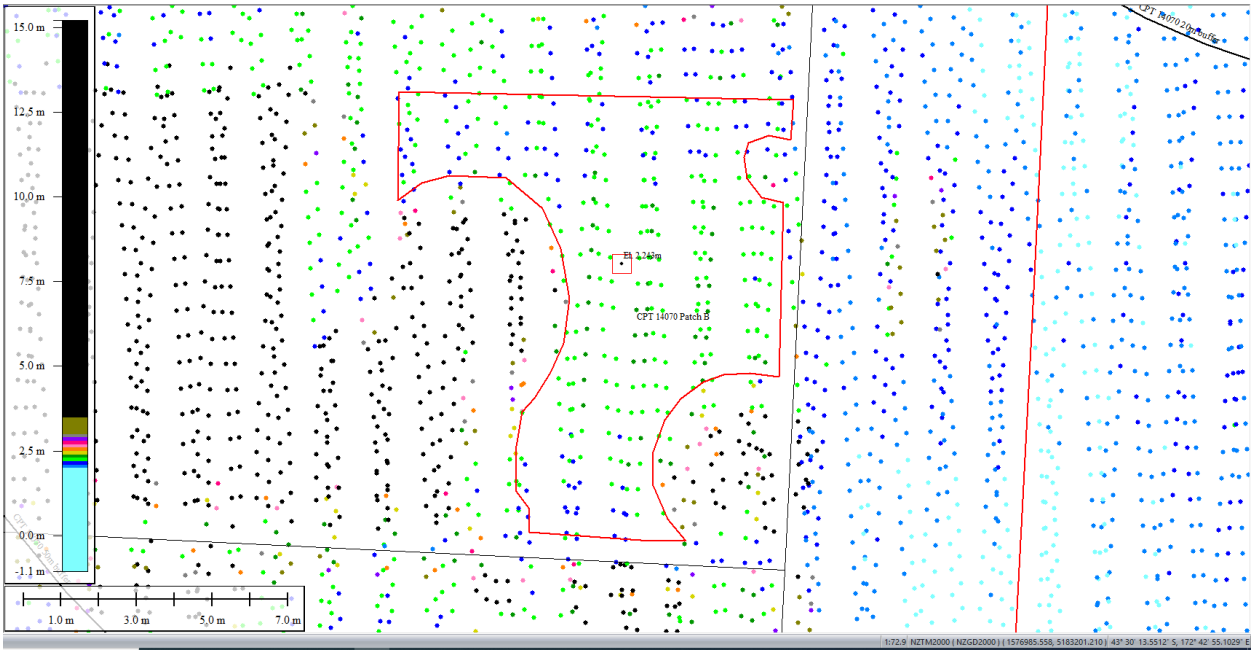

Figure 73: Ground surface elevation averaged over 50-m buffer for Patch B for Feb 2012 LiDAR survey.

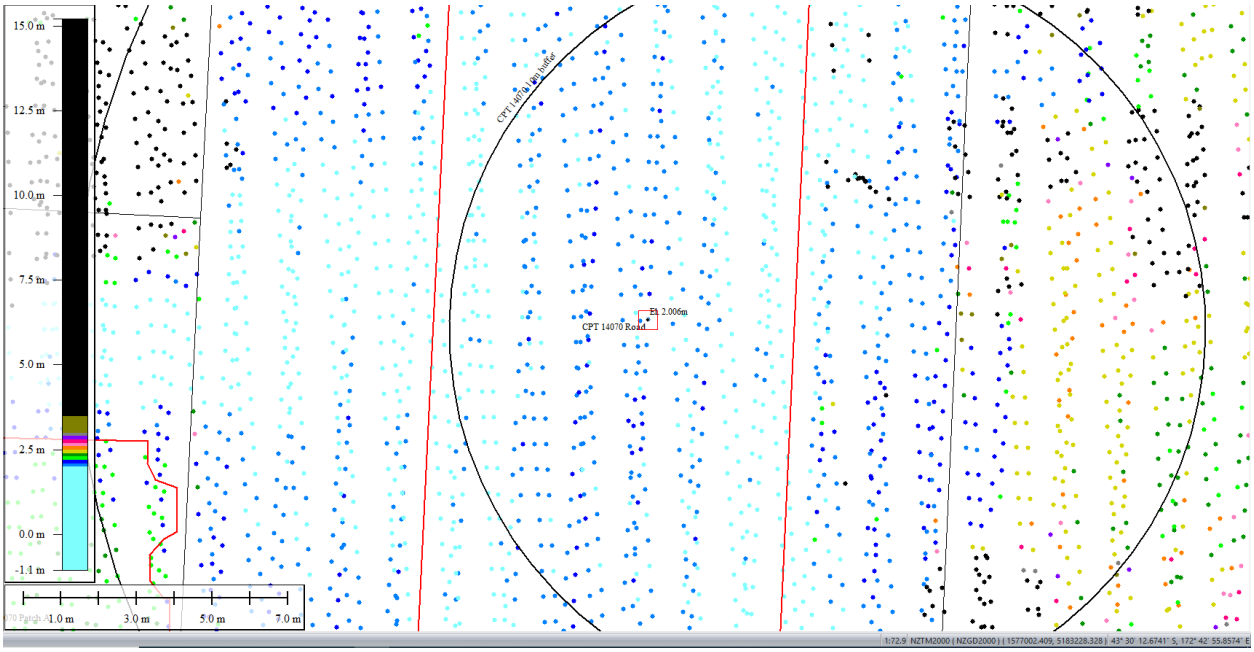

Figure 74: Ground surface elevation averaged over 10-m buffer for Road for Feb 2012 LiDAR survey.

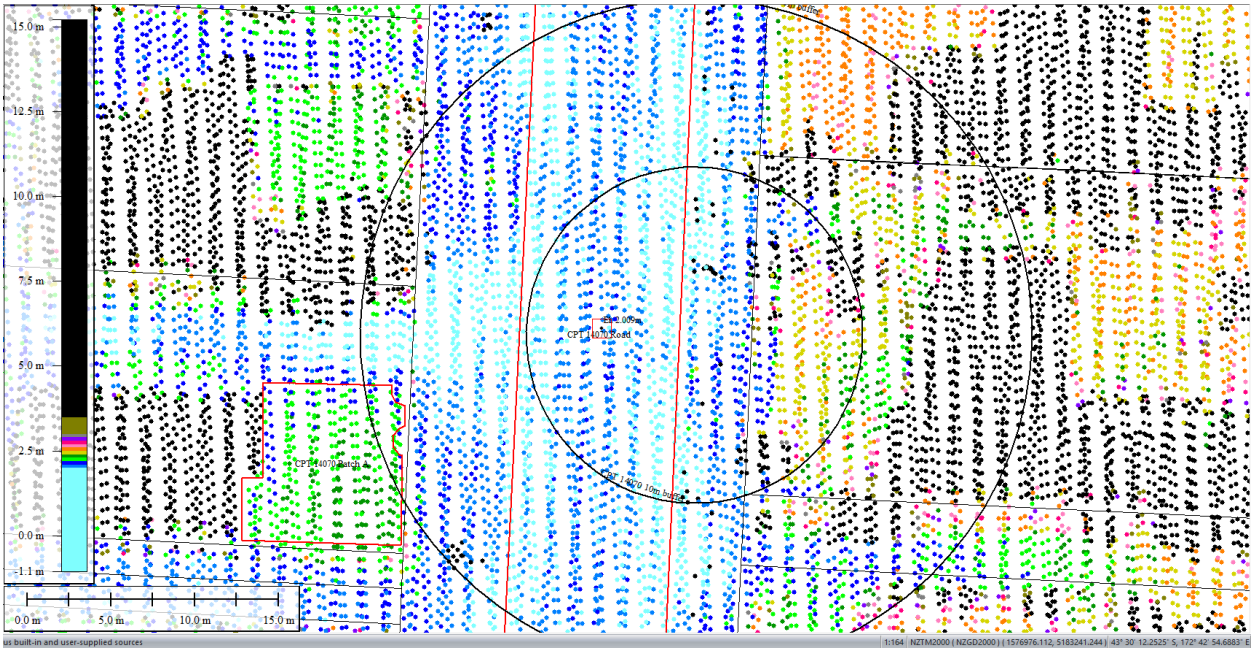

Figure 75: Ground surface elevation averaged over 20-m buffer for Road for Feb 2012 LiDAR survey.

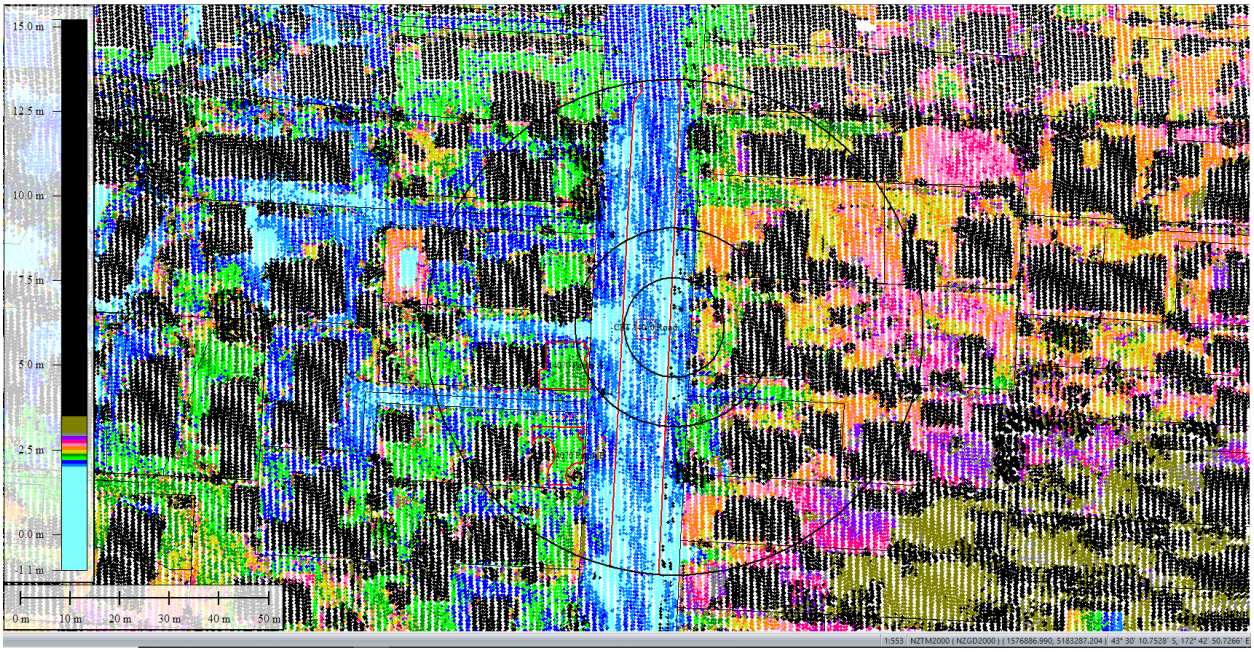

Figure 76: Ground surface elevation averaged over 50-m buffer for Road for Feb 2012 LiDAR survey (el. 2.024m).

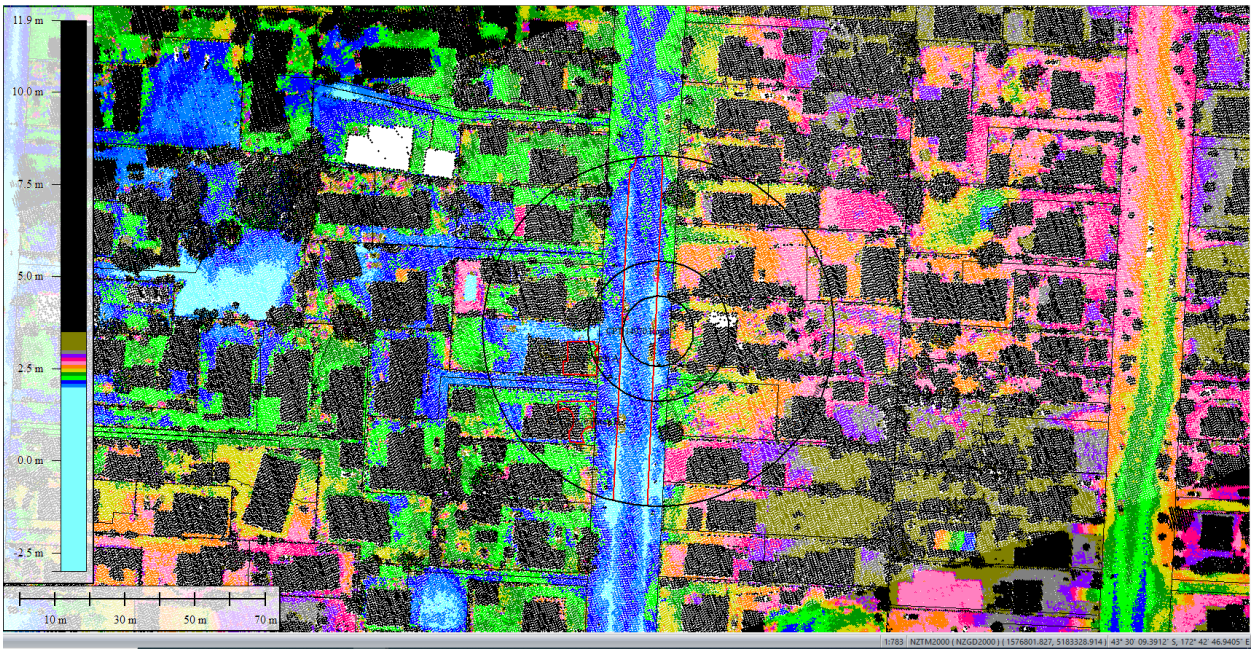

Figure 77: Oct 2015 LiDAR survey.

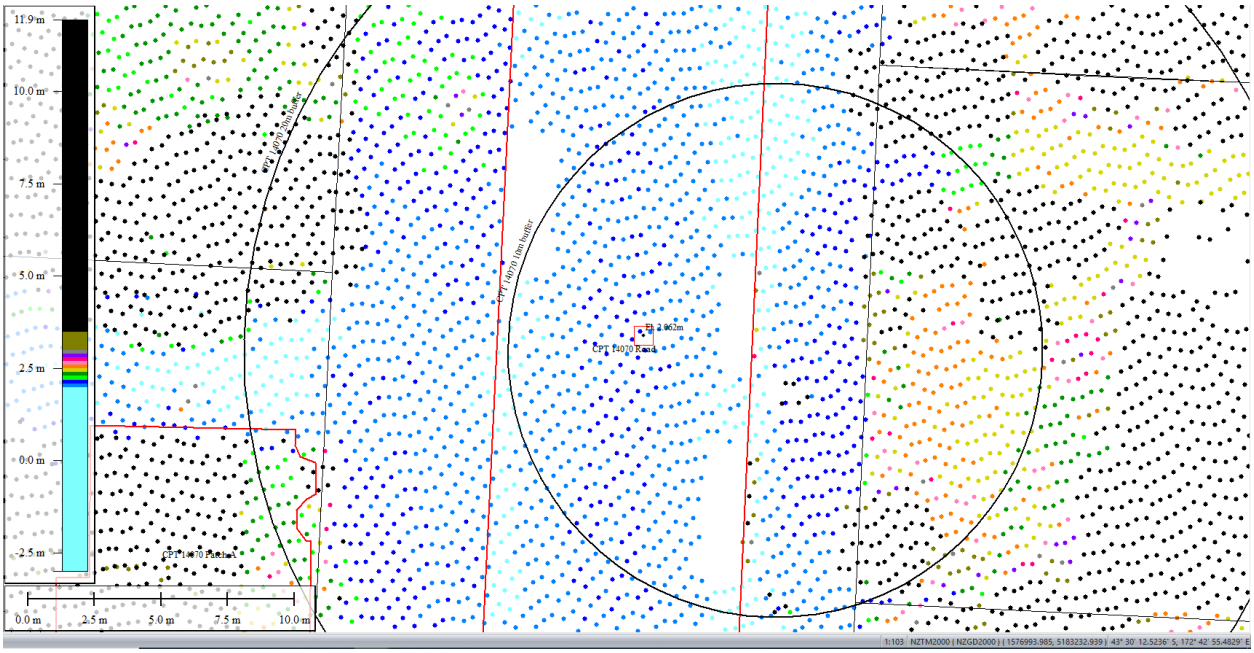

Figure 78: Ground surface elevation averaged over 10-m buffer for Road for Oct 2015 LiDAR survey.

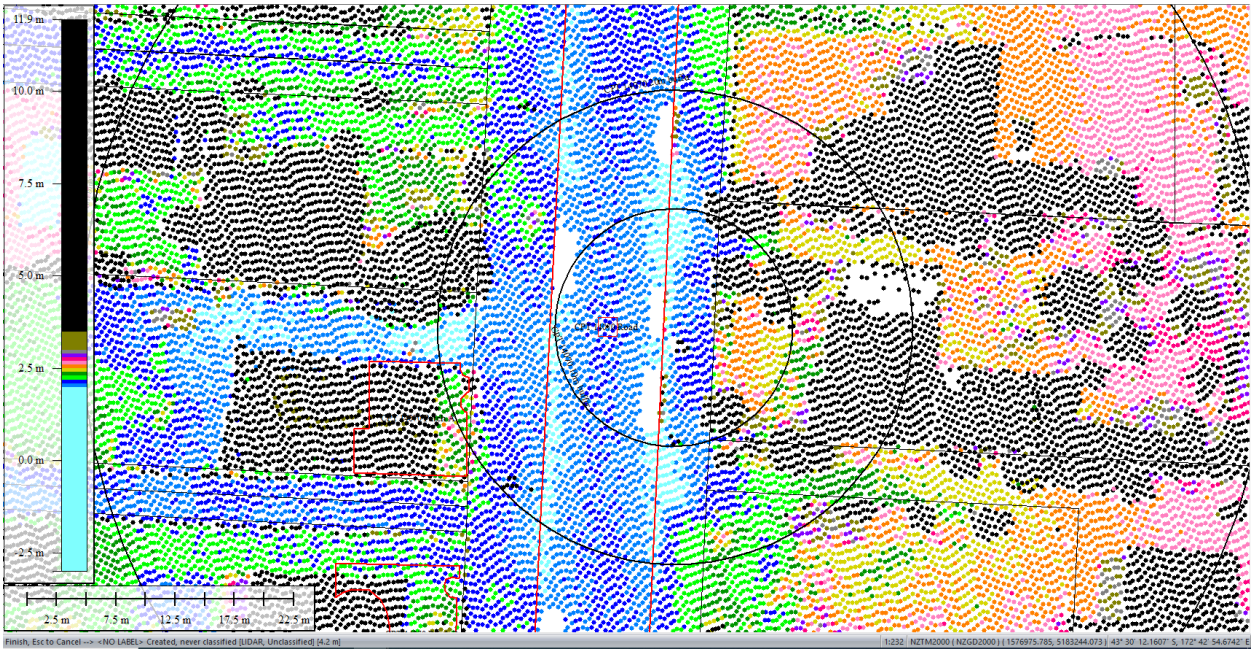

Figure 79: Ground surface elevation averaged over 20-m buffer for Road for Oct 2015 LiDAR survey (el. 2.060m).

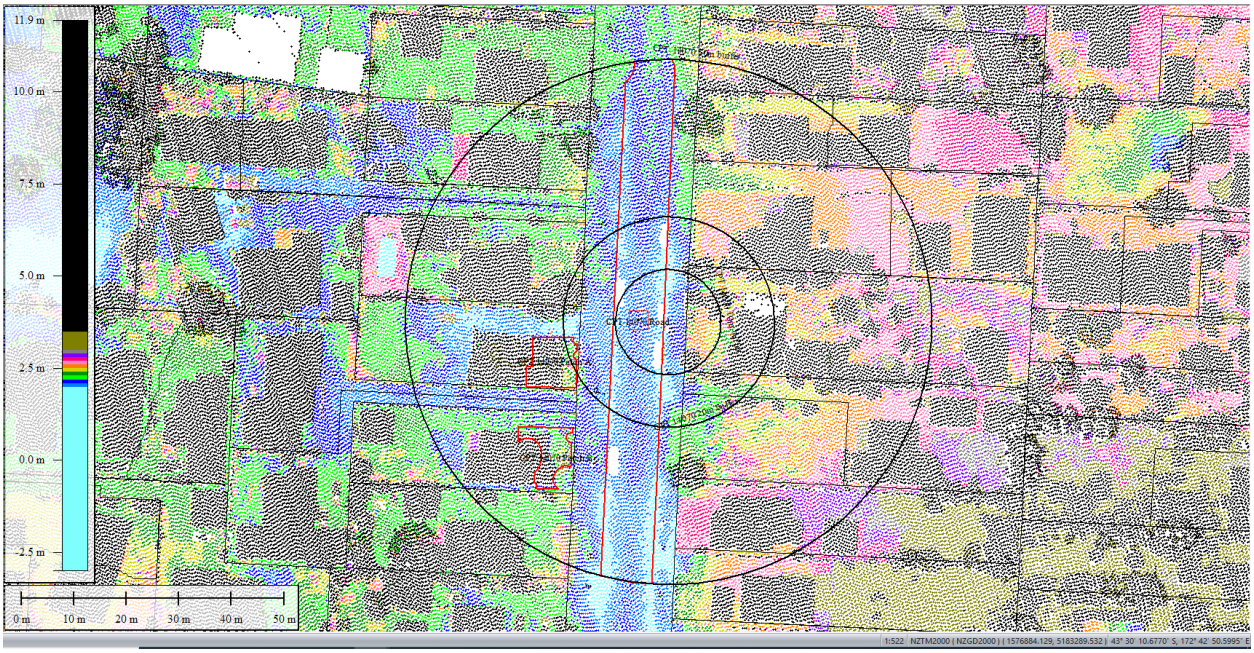

Figure 80: Ground surface elevation averaged over 50-m buffer for Road for Oct 2015 LiDAR survey (el. 2.080m).

Figure 81: Aerial photograph showing the ejecta outline at the site for Feb-11 EQ.

Figure 82: Aerial photograph acquired on 16 Jun 2011 showing the ejecta outline at the site for Jun-11 EQ.

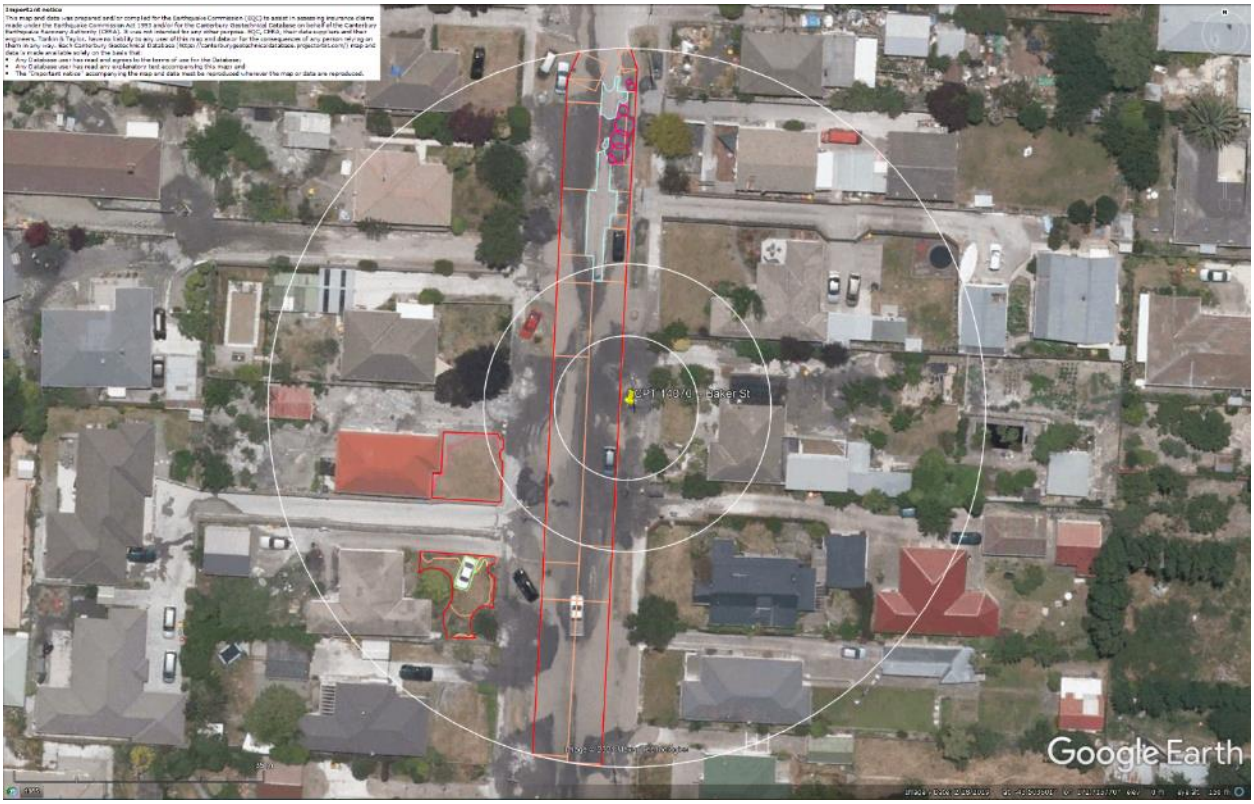

Figure 83: Aerial photograph showing the ejecta outline at the site for Dec-11 EQ.

Contents of this figure cannot be shared as doing so is restricted by a Non-Disclosure Agreement.

Figure 84: LDAT property inspection drawing for Patch A (inspection date: Jun 2011).

Figure 85: Ground photographs for Patch A (photograph date: Jun 2011).

Contents of this figure cannot be shared as doing so is restricted by a Non-Disclosure Agreement.

Figure 86: LDAT property inspection drawing for Patch B (inspection date: Feb 2012).

Figure 87: Ground photographs for Patch B (photograph date: Feb 2012).

Figure 88: Ground photographs showing the remnants of ejecta on the street (photograph date: Jun 2011).

Figure 89: Ground photographs showing ejecta in the backyard of a property in the NW quadrant of the 50-m buffer (124 Baker St). The backyard is outside the 50-m buffer and has more ejecta than the yards within the 50-m buffer as per the aerial photograph for the Feb-11 EQ. The maximum height of ejecta in this backyard was measured as 200 mm (photograph date: Jun 2011).

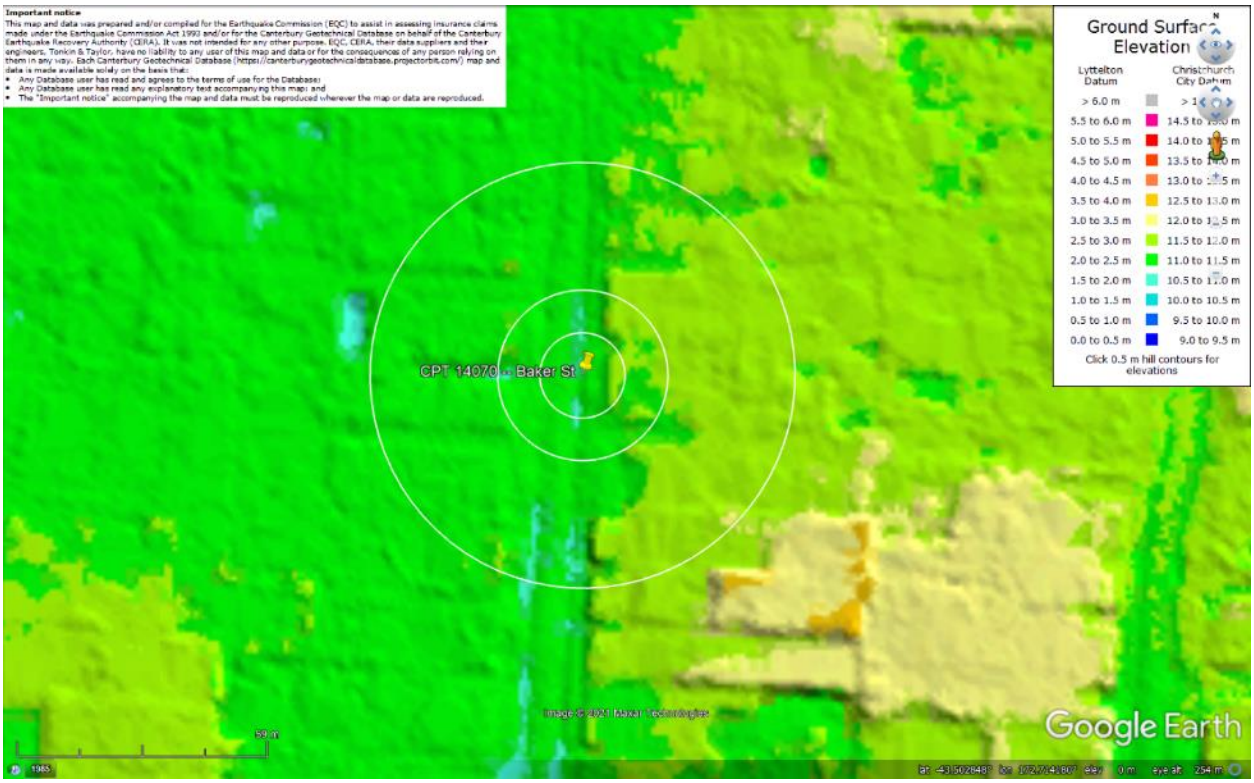

Figure 90: Ground surface elevation at the site according to the Sep 2011 LiDAR survey. The properties in the eastern half of the site are slightly elevated relative to the road (up to ~0.5 m).

Figure 91: PGA for Sep-10 EQ (st. dev. = 0.275-0.300 ln units).

Figure 92: PGA for Feb-11 EQ (st. dev. = 0.300-0.325 ln units).

Figure 93: PGA for Jun-11 EQ (st. dev. = 0.275-0.325 ln units).

Figure 94: PGA for Dec-11 EQ (st. dev. = 0.350-0.375 ln units).

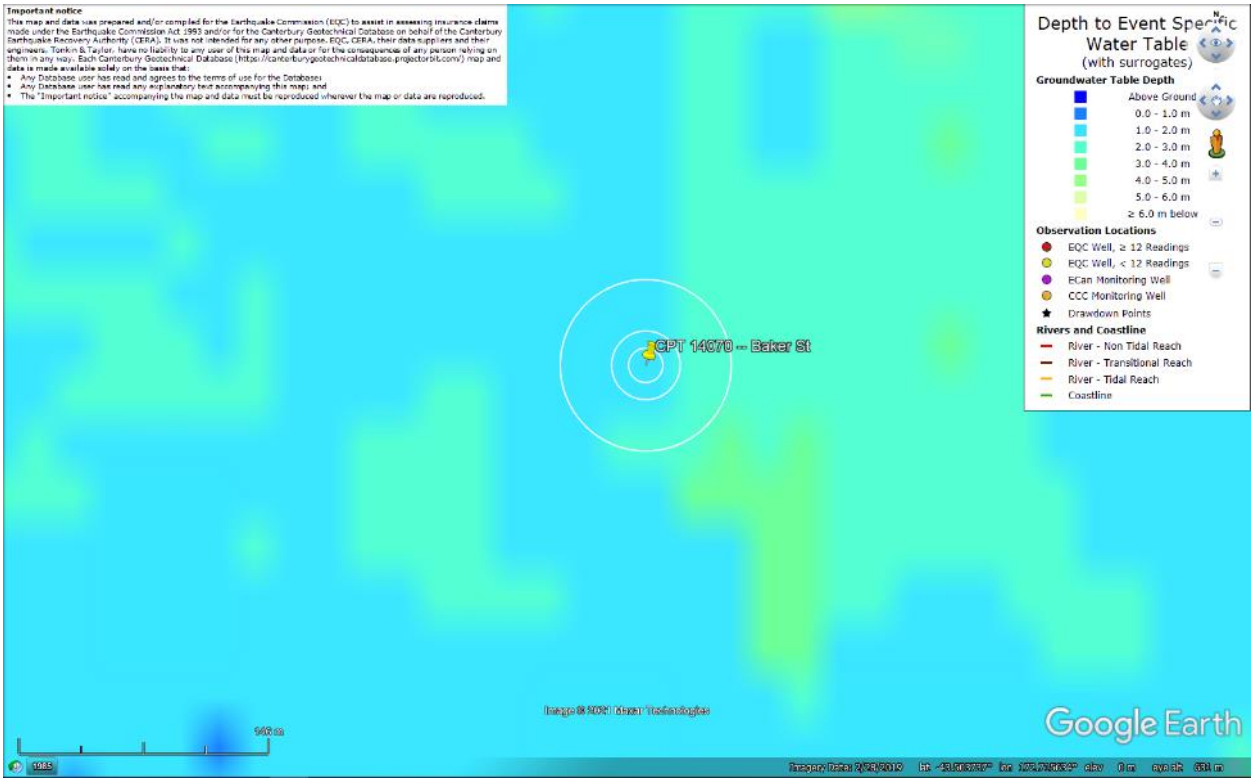

Figure 95: Depth to groundwater table for Sep-10 EQ.

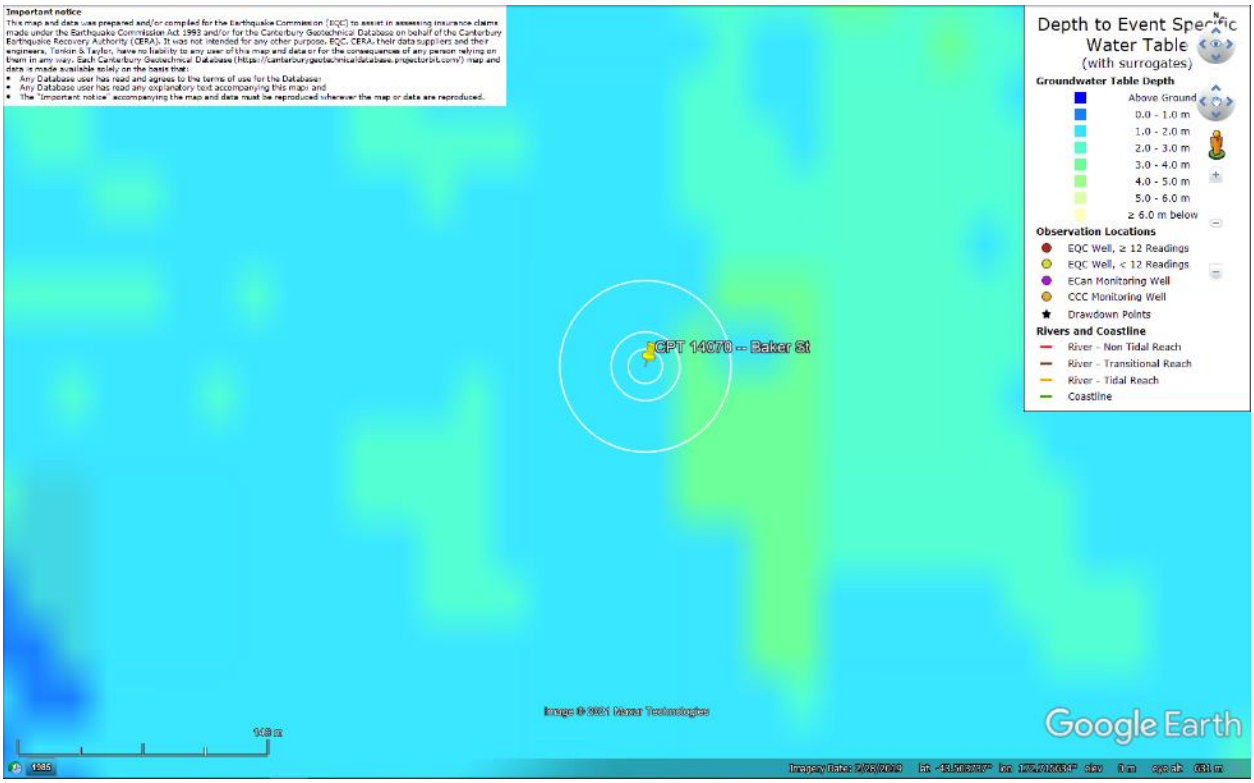

Figure 96: Depth to groundwater table for Feb-11 EQ.

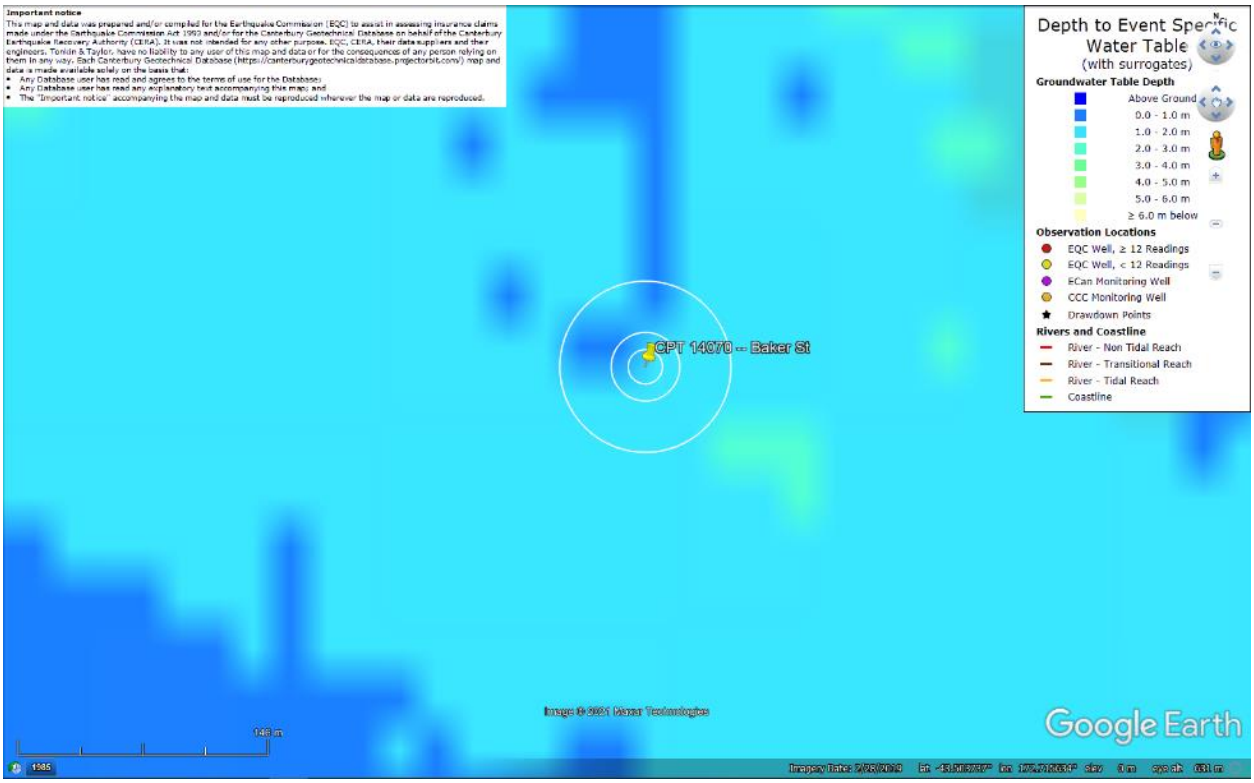

Figure 97: Depth to groundwater table for Jun-11 EQ.

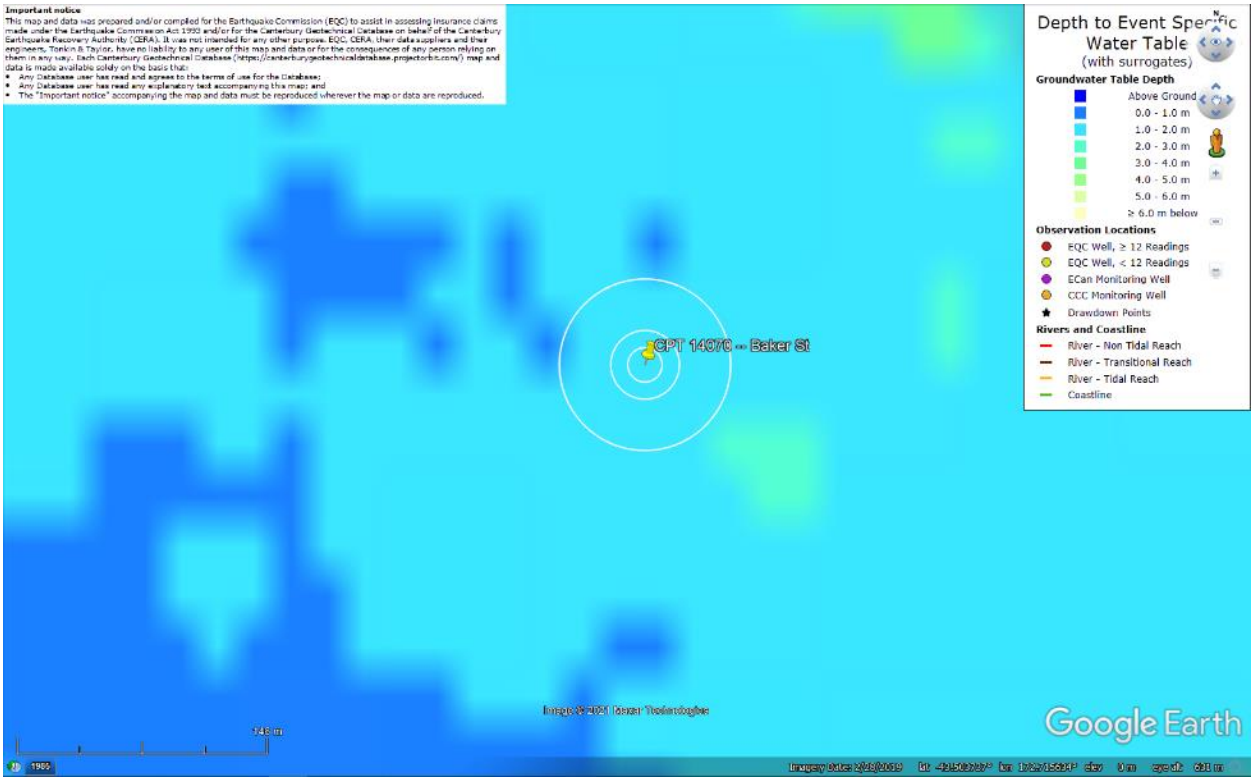

Figure 98: Depth to groundwater table for Dec-11 EQ.

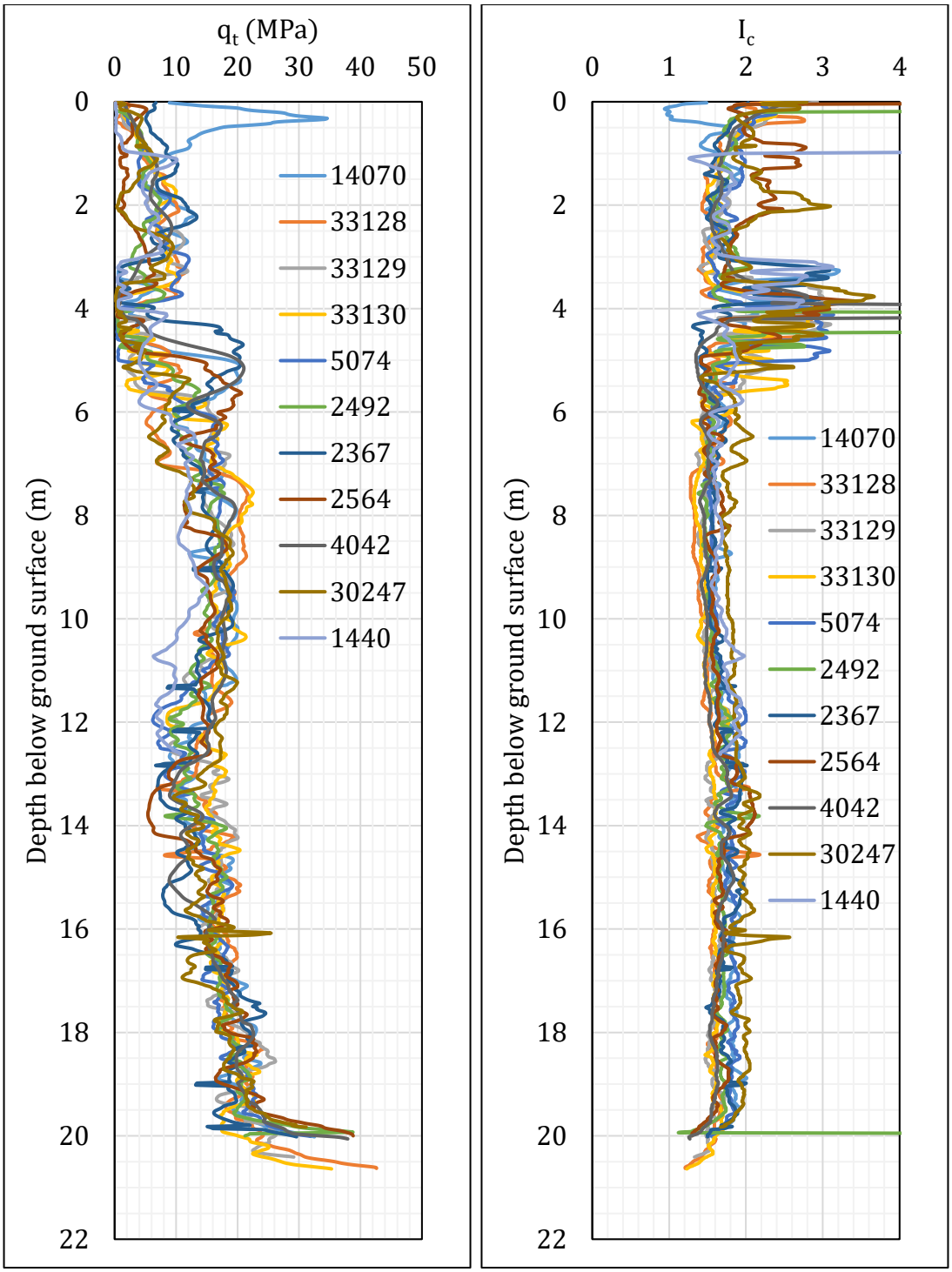

Figure 99: q_t and I_c profiles.

Note 6: The selection of CPTs for the area considered for settlement assessment (Figure 1) is based on the proximity of the CPTs to the considered areas. In accordance with that, the following table shows CPTs that were used for the volumetric settlement analysis in *Cliq v.3.0.3.2*, a CPT soil liquefaction software developed by GeoLogismiki. (The average volumetric settlements were reported in Table 8.)

Table 12: CPT profiles used in volumetric settlement analysis for areas selected for settlement assessment.

CPT ID No.	Patch A	Patch B	Road (10- and 20-m buffers)	Road (50-m buffer)
14070	✓		✓	✓
33128				
33129				
33130				
5074				
2492				
2367				✓
2564		✓		
4042	✓	✓		✓
30247				
1440				✓

Note: CPT 2564 was used to calculate the volumetric settlement for CPT 1440 for a depth range from 12.6 m to 20 m.

Table 13: CPT-based results.

		CPT ID									
EQ Event	Parameter	14070	33128	33129	33130	5074	2492	2367	2564	4042	30247
Sep-10	S_{V1D} (mm)	12	29	31	16	16	34	41	35	37	13
	LSN	3	5	5	3	2	7	5	7	6	3
	LPI	0	1	1	0	0	1	1	1	1	0
	LPI_{ish}	0	0	0	0	0	0	0	0	0	0
	$D_{FS<1}$ (m)	undet.	5.99	4.87	5.38	undet.	undet.	undet.	4.17	4.22	undet.
Feb-11	S_{V1D} (mm)	99	128	122	115	88	175	180	174	144	57
	LSN	15	19	18	17	13	30	22	29	21	14
	LPI	10	14	12	10	9	19	15	17	12	7
	LPI_{ish}	6	8	8	6	3	14	10	13	9	6
	$D_{FS<1}$ (m)	2.94	2.31	2.01	2.01	2.27	2.01	2.58	2.01	2.58	2.12
Jun-11	S_{V1D} (mm)	37	55	61	36	33	84	73	87	73	30
	LSN	8	9	10	6	5	20	10	25	13	9
	LPI	2	4	4	2	2	5	2	5	4	2
	LPI_{ish}	0	0	0	0	1	3	1	3	2	1
	$D_{FS<1}$ (m)	3.42	4.56	4.45	4.38	5.01	2.31	3.56	1.5	2.84	2.12
Dec-11	S_{V1D} (mm)	76	95	98	72	70	144	147	146	127	48
	LSN	14	15	17	12	11	31	19	34	22	13
	LPI	6	9	8	6	5	13	9	13	9	5
	LPI_{ish}	2	5	5	1	1	9	2	12	7	4
	$D_{FS<1}$ (m)	3.42	2.36	1.75	2.26	5.01	1.51	2.62	1.51	1.54	2.12

Notes: $D_{FS<1}$ = Depth to the first liquefiable layer ($FS_L<1$) that is at least 200-mm thick, as determined by the Boulanger and Idriss (2016) liquefaction-triggering procedure ($P_L=50\%$, $C_{FC}=0.13$, and $I_{c,cutoff}=2.6$), and exported from *Cliq v.3.0.3.2*; undet. = the specified soil layer was not detected.

Table 13 (continued): CPT-based results.

		CPT ID	
EQ Event	Parameter	1440	$\Delta_{12.6m-20m}$
Sep-10	S_{V1D} (mm)	42	22
	LSN	7	1
	LPI	1	0
	LPI_{ish}	0	--
	$D_{FS<1}$ (m)	3.52	--
Feb-11	S_{V1D} (mm)	179	81
	LSN	31	6
	LPI	23	5
	LPI_{ish}	14	--
	$D_{FS<1}$ (m)	2.02	--
Jun-11	S_{V1D} (mm)	96	38
	LSN	19	2
	LPI	5	0
	LPI_{ish}	0	--
	$D_{FS<1}$ (m)	3.52	--
Dec-11	S_{V1D} (mm)	162	70
	LSN	32	5
	LPI	16	3
	LPI_{ish}	10	--
	$D_{FS<1}$ (m)	1.62	--

Notes: $D_{FS<1}$ = Depth to the first liquefiable layer ($FS_L<1$) that is at least 200-mm thick, as determined by the Boulanger and Idriss (2016) liquefaction-triggering procedure (P_L=50%, C_{FC}=0.13, and $I_{c,cutoff}$ =2.6), and exported from *Cliq v.3.0.3.2*; undet. = the specified soil layer was not detected; $\Delta_{12.6m-20m}$ indicates the amount of S_{V1D}, LSN, and LPI to be added to CPT 1440 due to its penetration depth <20 m.

Note 7: Based on the borehole log (BH 2917, Figure 1), the groundwater table is at a depth of 2.6 m below the ground surface. The soil profile consists of (1) gravelly, GW, fill to a depth of 2.0 m, (2) fine to medium sand, SW, of the Christchurch formation to a depth of 3.5 m, (3) silt, ML, of the Christchurch formation to a depth of 3.7 m, (4) fine to medium sand, SP, of the Christchurch formation to a depth of 15.95 m (the end of the borehole). Based on the borehole log BH 3640 (~120 m to the NW from the center of the site), the SP layer of the Christchurch formation extends to a depth of 20 m. In addition, the borehole log BH 28355 (Figure 1) indicates that the groundwater table is at a depth of 1.15 m below the ground surface.

Note 8: The ejecta-induced free-field settlement provided in Table 11 is an areal average settlement due to ejecta, which is based on the total settlement assessment area, A_T (provided in Table 9 and repeated in Table 14). However, the considered area was not always covered completely with ejecta; thus, it is important to provide the localized ejecta-induced settlement, too. The localized settlement due to ejecta is estimated using photographic evidence only as

$$S_{E,P\_localized} = \frac{V_E}{A_E}$$

where V_E is the total volume of ejecta within A_T and A_E is the total coverage area of ejecta within A_T. Please note that the areal ejecta-induced settlement provided in Table 14 as S_{E,P_areal} is the same as $S_{E,P}$ in Table 11, which was estimated as

$$S_{E,P\_areal} = S_{E,P} = \frac{V_E}{A_T}$$

where V_E is the total volume of ejecta within A_T and A_T is the total settlement assessment area.

Table 14a: Areal and localized ejecta-induced settlement estimates for Patch A (20-m and 50-m buffers) based on photographic evidence.

Earthquake Event	A_T (m^2)	A_E (m^2)	V_E (m^3)	S_{E,P_areal} (mm)	$S_{E,P\_localized}$ (mm)
Sep-10	81.9	0	0	0	0
Feb-11	81.9	80.9	2.8-4.4	45±10	45±10
Jun-11	81.9	4.6	0.1-0.2	5±5	40±10
Dec-11	81.9	12.2	0.5-0.7	10±5	50±10

Notes: S_{E,P_areal} = $S_{E,P}$ reported in Table 11 = areal ejecta-induced settlement; $S_{E,P\_localized}$ = localized ejecta-induced settlement; A_T = total settlement assessment area; V_E = total volume of ejecta within A_T; A_E = total area of ejecta within A_T; The estimates of both areal and localized ejecta-induced settlement are rounded to the nearest 5; Final plus/minus values are also rounded to the nearest 5.

Table 14b: Areal and localized ejecta-induced settlement estimates for Patch B (50-m buffer) based on photographic evidence.

Earthquake Event	A_T (m^2)	A_E (m^2)	V_E (m^3)	S_{E,P_areal} (mm)	$S_{E,P\_localized}$ (mm)
Sep-10	68.5	0	0	0	0
Feb-11	68.5	41.0	2.3-3.2	40±5	65±10
Jun-11	68.5	2.8	0.08-0.1	<5	40±10
Dec-11	59.6	24.5	0.7-1.2	15±5	40±10

Notes: S_{E,P_areal} = $S_{E,P}$ reported in Table 11 = areal ejecta-induced settlement; $S_{E,P\_localized}$ = localized ejecta-induced settlement; A_T = total settlement assessment area; V_E = total volume of ejecta within A_T; A_E = total area of ejecta within A_T; The estimates of both areal and localized ejecta-induced settlement are rounded to the nearest 5; Final plus/minus values are also rounded to the nearest 5.

Table 14c: Areal and localized ejecta-induced settlement estimates for Road (20-m buffer) based on photographic evidence.

Earthquake Event	A_T (m^2)	A_E (m^2)	V_E (m^3)	S_{E,P_areal} (mm)	$S_{E,P\_localized}$ (mm)
Sep-10	363	0	0	0	0
Feb-11	363	363	42.7-75.0	165±45	165±45
Jun-11	363	363	35.0-42.0	105±10	105±10
Dec-11	363	363	36.2-49.7	120±20	120±20

Notes: S_{E,P_areal} = $S_{E,P}$ reported in Table 11 = areal ejecta-induced settlement; $S_{E,P\_localized}$ = localized ejecta-induced settlement; A_T = total settlement assessment area; V_E = total volume of ejecta within A_T; A_E = total area of ejecta within A_T; The estimates of both areal and localized ejecta-induced settlement are rounded to the nearest 5; Final plus/minus values are also rounded to the nearest 5.

Table 14d: Areal and localized ejecta-induced settlement estimates for Road (50-m buffer) based on photographic evidence.

Earthquake Event	A_T (m^2)	A_E (m^2)	V_E (m^3)	S_{E,P_areal} (mm)	$S_{E,P\_localized}$ (mm)
Sep-10	937	0	0	0	0
Feb-11	937	937	104-163	145±30	145±30
Jun-11	937	937	73.8-91.9	90±10	90±10
Dec-11	937	930	79.3-105	100±15	100±15

Notes: S_{E,P_areal} = $S_{E,P}$ reported in Table 11 = areal ejecta-induced settlement; $S_{E,P\_localized}$ = localized ejecta-induced settlement; A_T = total settlement assessment area; V_E = total volume of ejecta within A_T; A_E = total area of ejecta within A_T; The estimates of both areal and localized ejecta-induced settlement are rounded to the nearest 5; Final plus/minus values are also rounded to the nearest 5.

Summary 2:

- **The best estimate of the localized ejecta-induced free-field ground settlement at the Baker St site for the SEP 2010, FEB 2011, JUN 2011, and DEC 2011 earthquake is 0 mm, 45±10 mm, 40±10 mm, and 50±10 mm, respectively.**
- **The best estimate of the localized ejecta-induced settlement of the road at the Baker St site for the SEP 2010, FEB 2011, JUN 2011, and DEC 2011 earthquake is 0 mm, 165±45 mm, 105±10 mm, and 120±20 mm, respectively.**